CLIMATE IMPACT OF LAND-USE CHANGE IN THE NORTHEASTERN UNITED STATES: MEASURING ALBEDO AND CARBON SEQUESTRATION IN WILLOW AND FOREST BIOENERGY SYSTEMS

A Dissertation

Presented to the Faculty of the Graduate School

of Cornell University

In Partial Fulfillment of the Requirements for the Degree of

Doctor of Philosophy

by

Charlotte R. Levy

December 2019

QUANTIFYING THE CLIMATE IMPACT OF LAND-USE CHANGE IN THE NORTHEASTERN UNITED STATES: MEASURING ALBEDO AND CARBON SEQUESTRATION IN WILLOW AND FOREST BIOENERGY SYSTEMS

Charlotte R. Levy, Ph. D.

Cornell University 2019

In order to strategically implement climate mitigation projects, policy-makers need an accurate accounting of the complete climate impacts from biogeochemical and biogeophysical climate forcings. Particularly, the inclusion of land-use driven biogeophysical effects such as albedo are often neglected in carbon accounting that considers both life-cycle analyses and averted emissions. In this thesis we quantify the climate impact of albedo in the context of land-use change for climate mitigation projects such as production of bioenergy and afforestation. We provide a new methodology for measuring local albedo, describe its impact present and future, and examine the net impact of land-use change in the context of albedo. In **Chapter 1**, we outline a novel technique for measuring surface albedo at varying scales by utilizing a standard unmanned aerial vehicle (UAV) quadcopter. We compare summer measurements over a deciduous forest and short-rotation coppiced willow field to standard tower and satellite measurements. We conclude that UAV are an affordable and flexible tool for measuring albedo at the land surface. **Chapter 2** quantified the impact of albedo in land-conversion from cropfield to four different biofuel crops. We determined that albedo presented a small to substantial warming impact in all cases. We further examined the effect of anticipated future snow-loss on this forcing, and found that under moderate warming scenarios, snow-loss would be sufficient to reverse the albedo impact for some biofuel conversions within the next 100 years. In **Chapter 3** we identified the net impact of three reforestation and two willow biofuel scenarios accounting for albedo and carbon emissions. We concluded that albedo substantially altered net impact, particularly in forest systems.

BIOGRAPHICAL SKETCH

Charlotte Levy is a Boston native and a third-generation bird enthusiast. Her early fascination with wild landscapes developed as an undergraduate, conducting research in everything from spring ephemerals to avian behavior. While at Skidmore she studied at Kansas State University as an NSF REU student with Dr. Mark Ungerer, at the Rocky Mountain Biological Station as an independent research student with Dr. John Harte, and at the Centre Ecologique de Libanona in Madagascar as part of the School for International Training. While in Saratoga Springs, Levy became closely involved with city efforts to mitigate greenhouse gas emissions, conducting a municipal greenhouse gases inventory and co-writing two city ordinances to reduce vehicle idling and improve pedestrian and cyclist access within the city. She developed a passion for science in service of sound, evidence-based policy that she has brought to all her work since.

She received a Bachelor's of Arts in Biology from Skidmore College in 2013, graduating Summa Cum Laude and Phi Beta Kappa with Departmental Honors. Following graduation, she served for a year as a MassLift Americorps service member with North County Land Trust. There she worked with local communities to develop cross-cutting land conservation projects that served long-term recreational, conservation, and economic goals.

She joined the Goodale and Fahey labs at Cornell University in 2014. There she served as President of the Advancing Science & Policy (ASAP) and the Biogeochemistry, Environmental Science, and Sustainability (BESS) graduate associations. In 2018 she received the Katherine S McCarter award from the Ecological Society of America.

DEDICATION

In awe and admiration of family.

The ones who raised and inspired me, took me birding and splashing in muddy creeks.

The ones who'd send postcards from the other side of the world and call at any hour.

The ones who've mentored me, shared their passion, and always been ready to jam.

The ones who've always been there with a hug, a helping hand, a hot cup of tea.

To so many people – I love you and I'm grateful to know you.

This is for you

ACKNOWLEDGMENTS

With so much gratitude to my committee, Christy Goodale, Tim Fahey, and Natalie Mahowald; I will always be filled with awe and admiration for your knowledge and generosity. Thank you to my collaborators, contributors, and so many others who have been so generous with their time and wisdom. Thank you especially to Elizabeth Burakowski and Andrew Richardson for joining me in putting my first chapter out in the world. Thank you to Carl Bernacchi, David Weinstein, and Ryan Bright for contributing data and knowledge of their study systems. Thank you to Erika Mudrak, for her insightful stats consultations. Thank you so much to the organizations that have provided funding and support along the way: to the Atkinson Center Academic Venture Fund, to the CSBC IGERT Small Grant, to the Cornell Sigma Xi, and to the Andrew R Mellon Fund.

To Susan and Bhavya, for their constant support and good advice, and to the entire Goodale lab, past and present, for their energy and excellent sense of humor. To everyone in EEB – each and everyone of you has brightened my life with your talent, brilliance, and astonishing spirit. You truly are a community in million. Thank you to everyone in Ithaca who has hiked with me, traveled with me, supported me, and joined me for dinner. I love you all. Thank you to Zoe for the pumpkin bread, Adam for the dog pictures, Julia for the plants, and Nick for those good jokes.

To Melissa for being my perfect foil and to Caleb for insisting that I needed a real foil. To my parents, Karen & Nathaniel, who have the most curious and creative minds I know, and who have always supported me in all my dreams and mischief.

To Mike, who makes me tea and homemade bread when I need it most. Here's to our life together.

TABLE OF CONTENTS

Chapter 1

Chapter 2

Chapter 3

CHAPTER ONE: Novel Measurements of Fine-Scale Albedo: Using a Commercial Quadcopter to Measure Radiation Fluxes

Abstract

Remote sensing of radiative indices must balance spatially and temporally coarse satellite measurements with finer-scale, but geographically limited, in-situ surface measurements. Instruments mounted upon an Unmanned Aerial Vehicle (UAV) can provide small-scale, mobile remote measurements that fill this resolution gap. Here we present and validate a novel method of obtaining albedo values using an unmodified quadcopter at a deciduous northern hardwood forest. We validate this method by comparing simultaneous albedo estimates by UAV and a fixed tower at the same site. We found that UAV provided stable albedo measurements across multiple flights, with results that were well within the range of tower-estimated albedo at similar forested sites. Our results indicate that in-situ albedo measurements (tower and UAV) capture more site-to-site variation in albedo than satellite measurements. Overall, we show that UAVs produce reliable, consistent albedo measurements that can capture crucial surface heterogeneity, clearly distinguishing between different land uses. Future application of this approach can provide detailed measurements of albedo and potentially other vegetation indices to enhance global research and modeling efforts.

1. Introduction

Over the past few decades, the simultaneous rise of remote sensing technologies and earth system models has generated a broad, cross-disciplinary need for radiometric datasets with both global extent and fine-scale parameterization. Radiometric indices are used to estimate global primary productivity, vegetative cover, energy fluxes, and many more

properties essential to understanding present and future climate and ecosystem functioning [1,2]. An uneven or too sparse global distribution of sites will bias estimates and cause these ecosystem properties to be poorly represented by global climate models [3,4]. At the same time, local disturbances (forest fires, drought, plowing, thinning, snow aging) [5–7] can have outsize effects on regional and global climate [5,8–11], yet be poorly captured by coarse global measurements or too underrepresented to be well modeled by earth system models [12,13]. To understand current and future trends in ecosystem functioning and climatic change, we must be able to capture both global extent and fine-scale variation in remotely-sensed, radiometric datasets [6,14–20].

Patterns at the global scale are generally derived from broadband satellite products [3,16,21,22], that are far-reaching but coarse-scaled. The most commonly used albedo dataset, the MODIS data products, are scaled as 500 m sinusoidal grid resolutions, limiting their ability to register small-scale land use and management strategies [4,23,24]. Development of a well-validated LANDSAT albedo product is ongoing and will provide a 30 m product at 16-day intervals, significantly improving the spatial resolution of the remotely-sensed albedo measurements; however, fine-scale in-situ estimates will still be needed to continue to validate this product [7,25,26]. In-situ measurements can corroborate satellite data but have their own limitations. Fixed towers are immobile, few in number, and have physical limitations on maximum height that limit their spatial range. Thus, scattered point measurements from towers may not accurately represent variation across larger landscapes [3,24]. Portable spectroradiometers have been used to quantify radiation fluxes in fields and the understory, and are generally very effective for evaluating effects of snow depth [27], snow age, grain size, and layer structure [28,29]. However these tools are limited in their application above canopy [27]. Airborne high-resolution hyperspectral sensors mounted on

planes or helicopters have permitted quantification of radiation fluxes across broader regions, but tend to be extremely costly and logistically complex. They can capture only single time point measurements along the flight path and are subject to technical issues caused by the scattering of light by aerosols and water vapor at higher altitudes between the sensor and the land surface [27].

Unmanned aerial vehicles (UAVs) can increase both the flexibility and affordability of fine-scale measurements, providing an essential bridge between ground-truthing and global satellite data [30,31]. UAVs can move freely over tree canopies, allowing measurement over entire forest stands rather than just single points. UAVs can adjust to a range of canopy heights, giving them more flexibility to achieve optimal observation heights [24]. UAV flights are more affordable than piloted airborne missions; moreover, in the United States recent adjustments to Federal Aviation Administration regulations have made UAV technology more accessible for researchers [32]. Several caveats must be considered: flights are limited in range and flight time by the strength of the radio signal, the battery life, the payload, and the angle of view of the observer. Standards for accommodating any position or height instability must still be developed. Finally, adaptation of UAVs for measurement of radiative indices requiring both incoming and reflected radiation measurements has been technically difficult to make by UAVs due to issues of payload weight and balance. Albedo is the ratio between down-welling shortwave broadband solar radiation and reflected, up-welling shortwave broadband solar radiation; it is typically measured using paired (one upward facing, one downward facing) pyranometers. However, standard UAVs are generally designed to lift objects with a center of gravity beneath the vehicle, such that mounting an upward-facing pyranometer on top or on an extended boom off of an UAV requires extensive customization and technical adjustment to ensure flight stability. In addition, the weight of two sensors imposes a significant energy cost, greatly reducing flight time. Two previous studies measuring albedo via UAV (fixed-wing

craft over the Indian Ocean [33], fixed-wing craft over Greenland [34]) have required custom modifications not swiftly replicable by most research labs. The simple method of measuring albedo proposed here allows use of unmodified quadcopters such as have been widely adopted by many labs for other forms of aerial imaging while minimizing payload and maximizing flight time.

Here we employ a novel measurement method to investigate albedo over a mixed hardwood forest in central New York. UAV measurements were tested for consistency across flights and for comparability to conventional forest albedo measurements made by tower and satellite. We verify the validity of our technique through side-by-side tower and UAV comparison over a field of shrub willow. Finally, we examine albedo across three land uses and seven flights, comparing within flight variability to variability across land uses. In testing this novel method, which minimizes UAV payload and permits use of uncustomized quadcopters, we hope to expand the capacity for scientists to validate satellite estimates using fine-scale radiometric measurements.

2. Materials and Methods

2.1. A Novel Method of Measuring Albedo by UAV

In the method presented here, albedo was calculated as the ratio between reflected shortwave radiation, as measured from a downward-facing pyranometer mounted under a UAV, and incoming shortwave radiation, as measured from a separate upward-facing pyranometer mounted to a pole in an immediately adjacent open area (Figure 1). The UAV-mounted downward-facing pyranometer was a Kipp and Zonen CMP3 pyranometer (spectral range: 300–2800 nm). It was secured underneath a four-rotor Spyder 850 (Sky Hero, Pearland, TX, USA) UAV and leveled using a motorized Gaui Crane gimbal (Figure 2).

The UAV was only modified to the extent of having the carbon-fiber support legs

lengthened, to provide additional clearance for the pyranometer during take-off and landing. The UAV pyranometer was paired with an upward-facing Kipp and Zonen CMP6 pyranometer (spectral range: 285–2800 nm) mounted on a pneumatic telescoping pole (Total Mast Solutions, CP56-08) and secured to a portable tripod. The pyranometer was fixed on a 30 cm leveled boom, oriented to the south, at a height of 9.09 m [35]. To obtain reference albedo measurements for validation flights, a second Kipp and Zonen CMP6 pyranometer was fixed and leveled below the first, to determine reflected radiation from beneath the tower. All instruments had a sensitivity of 5 to 20 μV/W/m², a response time of 18 sec or less (95%), and an effective half field of view of 81°. The thirty-second averages of up-welling and down-welling shortwave radiation from both pyranometers were recorded by an attached Kipp and Zonen METEON datalogger. The internal clocks of the two dataloggers were synchronized by a common laptop computer an hour prior to the experiment start. For each individual flight, the sum of all reflected radiation values was divided by the sum of incoming radiation values to get a flux-weighted albedo value for that flight. The viewing area of the pyranometer was calculated as the area from which 99% of sensor input came. This area was calculated based on Kipp and Zonen (2016) recommendations:

$$\text{Footprint diameter} = 2 * \text{height} * \tan(\text{effective half field of view}) \quad (1)$$

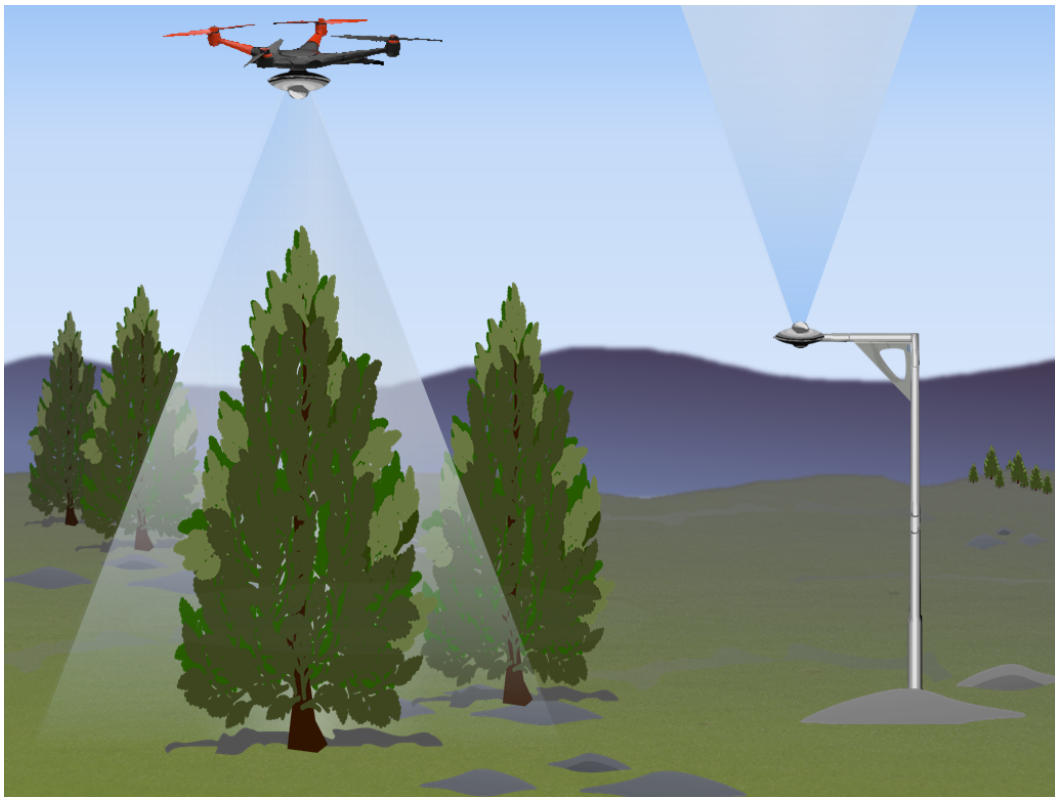

Figure 1. Diagram of flight design depicting the UAV with downward-facing pyranometer (**left**) and the fixed pole with the upward-facing pyranometer (**right**).

Figure 2. Preparation of the UAV for flight. The gimbal (**A**) is visible underneath the UAV, equipped with the downward-facing pyranometer secured beneath (**B**).

2.2. Experimental Design and Study Area

Albedo measurements consisted of targeted forest measurements by UAV (Section 2.2.1), along with comparative measurements of similar forests by tower and satellite (Section 2.2.2), validating measurements over a local willow field by UAV and tower (Section 2.2.3), and a final comparison of UAV measurements of forest, field, and coniferous forest (Section 2.2.4). The targeted forest measurements demonstrated the internal consistency of UAV measurements, while tower and satellite measurements showed the comparability of UAV albedo to ground and satellite measurements at similar sites. Validation flights compared simultaneous UAV and tower albedo. Finally, the comparison of deciduous, coniferous, and willow sites contrasted the variability across flights with variability across land uses.

Targeted UAV surveys over mixed hardwood forest took place in Tully, NY, USA at a closed-canopy mixed northern hardwood forest stand (Figure 3b; Table 1). Comparative tower and satellite-based measurements from other mixed hardwood sites were obtained from three sites with existing long-term tower albedo measurements, in Bartlett, NH; Durham, NH; and Petersham, MA (Figure 3a; Table 1). All three sites represented a temperate climate and mixed northern hardwood forest land cover. Albedo at each comparative site was obtained from a fixed-point tower and from MODIS satellite data. Validation UAV flights took place in Geneva, NY, USA over a cropped willow field (July 2017), where low height of vegetation allowed both tools to be used simultaneously (Figure 3c; Table 1). Finally, additional UAV flights at a Norway spruce monoculture stand (July 2017) were combined with 2017 forest and willow data for a comparison of different land uses (Table 1).

Table 1. The locations, typical July temperatures and precipitation, and dominant vegetation of the five study sites.

Objective	Site	Lat (°)	Lon (°)	Canopy Height (avg, m)	Dominant Land Cover
Targeted Flights *UAV, Satellite*	Tully, NY *Mixed Forest*	42.733	−76.081	23	*Acer saccharum, Fagus grandifolia*
Comparative *Tower, Satellite*	Durham, NH † *Mixed Forest*	43.111	−70.955	17	*Quercus rubra, Pinus strobus, Acer rubrum, Carya ovata, Quercus alba*
Comparative *Tower, Satellite*	Bartlett, NH ‡ *Mixed Forest*	44.065	−71.289	21	*F. grandifolia, Picea rubens, A. rubrum, Abies balsamea, Tsuga canadensis, A. saccharum, Betula alleghaniensis*
Comparative, *Tower, Satellite*	Petersham, MA § *Mixed Forest*	42.535	−72.190	16	*Q. rubra, P. strobus, A. rubrum, T. canadensis*
Validation, *UAV/Tower*	Geneva, NY *Cropped Willow*	42.883	−77.004	3	*Salix* spp.
Land Use Flight, *UAV*	Tully, NY *Spruce Stand*	42.733	−76.081	23	*Picea abies*

† [27]; ‡ [36]; § [37].

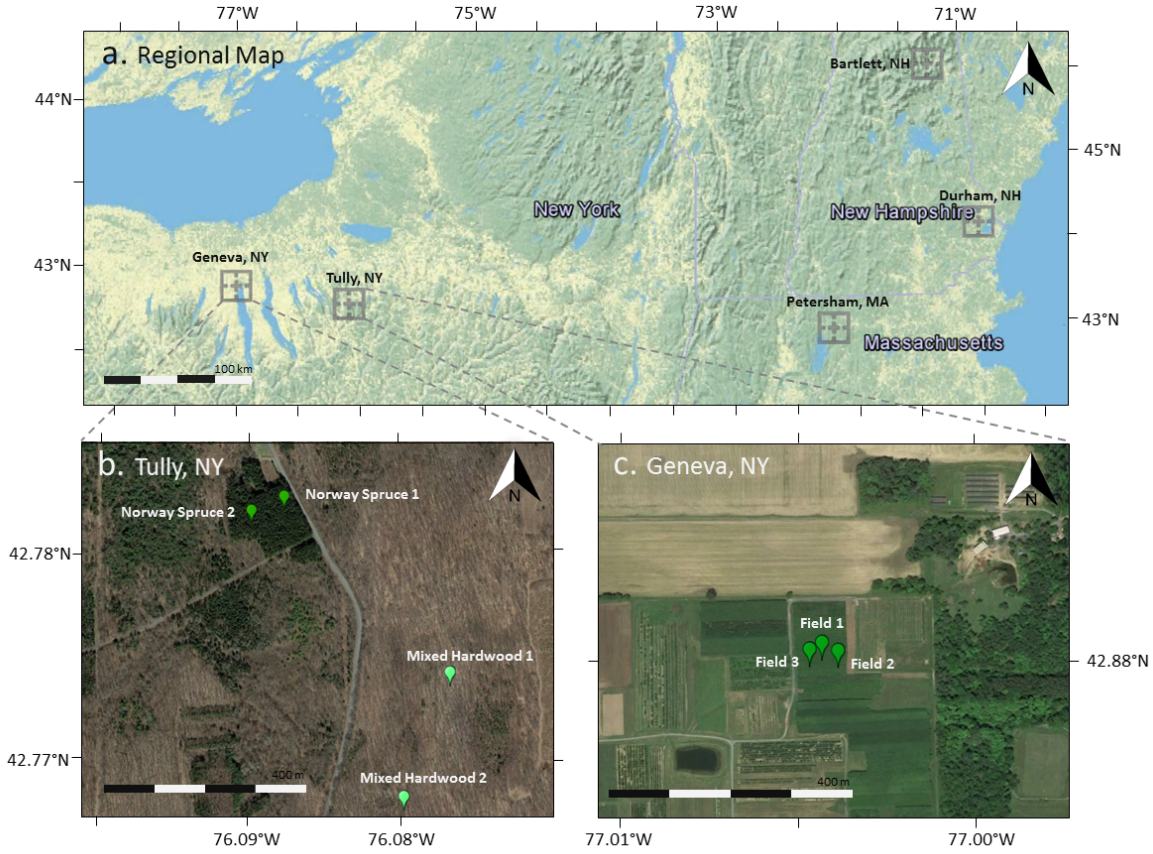

Figure 3. Inset A depicts a regional map of the sites measured in this study. Inset B highlights sites of UAV flights in Tully, NY. Inset C highlights sites of UAV flights in Geneva, NY. Inset A is sourced from 2018 NOAA Imagery. Insets B and C are sourced from Google Earth satellite imagery, April and July 1995 respectively.

2.2.1. Targeted UAV Measurements over Mixed Hardwood Forest

The UAV made five flights at Tully, NY over deciduous hardwood forest, one at local solar noon, two flights one and two hours prior to local solar noon, and two flights one and two hours after local solar noon on 27 July 2016 (Supplementary Table S1). In each flight, the UAV followed a pre-programmed course to the designated coordinates and altitude in approximately one minute. The UAV then held its position until the battery was nearly exhausted, approximately ten minutes, before returning to the staging area. Conditions on 27 July 2016 were clear, with minimal cloud cover moving in around local solar noon, and local air quality index less than 50 for both particulate matter and ozone [38].

2.2.2. Comparative Tower and Satellite Measurements over Mixed Hardwood Forest

Tower albedo measurements for the three other mixed hardwood forest sites used here were made in July 2014 and 2015 between 20 July and 24 July. Only measurements taken between 2.5 h prior to and 2.5 h post solar noon were used, to better match UAV data. Readings at Durham were taken every 30 s, Bartlett readings were taken every 5 s, and Petersham measurements were taken every 1 s. Half-hour averages of these measurements were used. For each individual day, the sum of all half-hourly reflected radiation values was divided by the sum of incoming radiation values to get a flux-weighted albedo value for the day.

Durham, NH, USA albedo was measured by a Kipp and Zonen CMA6 (effective half field of view = 81°) placed on a 4.5 m leveling boom extended from 25 m up a 30 m tower [27]. Albedo at Bartlett, NH, USA was collected using two Kipp and Zonen CMP3 pyranometers (effective half field of view = 81°) placed 23.8 m and 25 m up a 30 m tower, facing downwards on a 3 m leveling boom and upwards on a 1 m boom respectively [36]. Albedo values at Petersham, MA, USA were taken using a CNR-4 Kipp & Zonen 4-channel net radiometer mounted on a 3 m boom extending south from a 40 m tower (Effective Field of

View 81°) [39,40].

Satellite albedo measurements for Tully mixed hardwood forest and the three comparative forest sites were extracted from the MODIS bidirectional reflectance distribution function albedo product (MCD43A3: MODIS/Terra and Aqua Albedo Daily L3 Global 500 m SIN Grid V006) [41], for DOY 201–215, from 2014, 2015, and 2016. Pixels marked as low-quality in the MODIS quality control data were removed from the analysis. Due to these conditions, only data from 2015 and 2016 was available for Bartlett, NH and Durham, NH. Satellite albedo at the UAV flight site at Tully were extracted from four pixels, a square half kilometer each (Supplementary Table S2). Satellite albedo for the tower sites were pulled from single pixels (Supplementary Table S3). Satellite shortwave albedo at solar noon were converted from black-sky and white-sky albedo to blue-sky using a standard conversion formula [42,43]. Aerosol optical depth (AOD; unitless) was assumed to be 0.2, although a realistic range of environmental depths from 0.1–0.5 was also examined to test sensitivity (Supplementary Table S4). The sensitivity analysis showed that the low and high estimates were not significantly different from 0.2 for any of the examined satellite datasets, and so the 0.2 AOD value was used for the final comparison [44].

2.2.3. Validation Measurements Comparing Simultaneous UAV and Tower Data

Validation flights were conducted on 31 July 2017 over a cropped willow field in Geneva, NY to compare UAV-measured albedo to tower-based measurements. Fixed tower data was collected from a mounted Kipp and Zonen CMA6 albedometer fixed at 8 m on a 30 cm boom. The UAV was first positioned one meter due west of the mounted albedometer, maintaining a height of 8 m (Supplementary Table S1). This first flight took place 30 min prior to local solar noon; two subsequent flights took place 15 min prior, and 30 min post local solar noon. For the second and third flight the UAV was positioned at the same height, 24 m west and 29 m east of the tower, which remained fixed at the center point. All flights took

place on a clear day with the local air quality index less than 50 for ozone and below 100 for particulate matter (unitless) [38]. Partial cloud cover appeared towards the end of the third validation flight.

2.2.4. UAV Measurements Comparing Albedo across Multiple Scenarios of Land Use

Follow-up flights took place a year later, on 30 July 2017. First and second flights on 30 July were made at Tully, NY over a Norway spruce (*Picea abies*) plantation, over two neighboring locations within the same spruce plantation, at 0.5 and 1 h post local solar noon, respectively. A second and third flight revisited the same deciduous hardwood forest site as was measured above, as well as a second deciduous hardwood site within the same forest block, at 1.5 h post solar noon and 2 h post local solar noon. 30 July 2017 was completely clear with no clouds; local air quality index was less than 50 for both particulate matter and ozone [38]. Finally, willow albedo data as collected above was used alongside the spruce and deciduous forest data to compare albedo over three different land uses.

2.3. Data Processing and Analysis

Outliers were removed where measured incoming solar radiation was less than 60% of predicted solar insolation.

$$\text{Predicted Solar Insolation} = \text{Solar Constant} * \cos\left(\frac{\text{Zenith Angle} * \pi}{180}\right) \quad (2)$$

This removed values representing 18%, 48%, 57%, and 46% of the original data, at Tully, Durham, Bartlett, and Petersham, respectively (the multiple day measurements at the last three sites resulted in there having been more clouded days to remove). We also examined albedo at solar noon, as solar noon measurements are more comparable to solar noon-approximated satellite values. For both UAV and tower data, albedo at solar noon was defined as all measurements within one hour of solar noon at that site on the day of the measurement.

Data were analyzed in R version 3.2.1 [45]. We conducted a Type II ANOVA [46] and the Tukey HSD test from stats v3.4.1., to compare site level differences across both in-situ and satellite measurements; Anova residuals were normally distributed. We used the R *t*-test from stats v3.4.1. to conduct a Student *t*-test to compare in-situ and satellite measurements; albedo was transformed with a negative reciprocal 7th power transformation.

3. Results

3.1. Targeted UAV Measurements over Mixed Hardwood Forest

We examined the temporal consistency of albedo estimates across flights and years in a series of flights over a mixed hardwood forest in Tully, NY. The series of five flights spaced hourly around local solar noon measured a summer forest albedo of 0.145 ± 0.005 SD, $n = 5$, and ranged from 0.140 to 0.146. The mixed hardwood albedo at solar noon, 0.145, was the same as the mean and was consistent with albedo values recorded over the course of the day.

3.2. Comparative Tower and Satellite Measurements over Mixed Hardwood Forest

UAV albedo values were compared to tower measurements from three similar mixed northern hardwood forests (Figure 4).

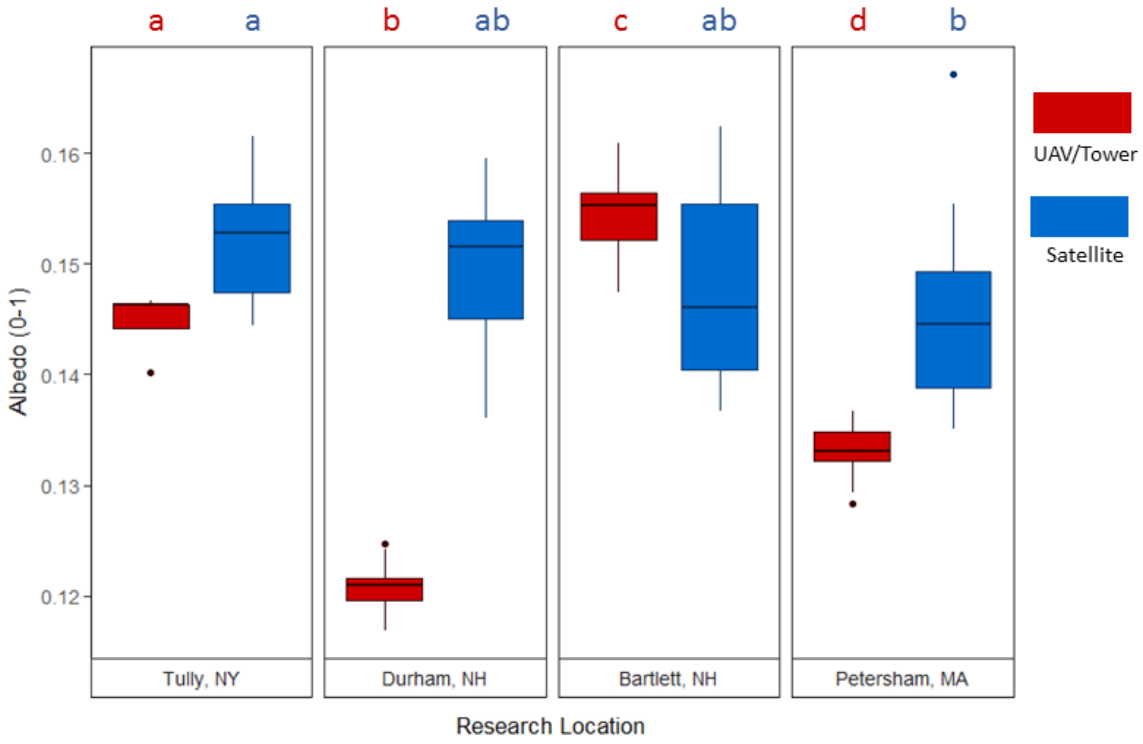

Figure 4. Boxplots showing albedo over mixed temperate forest as measured by UAV (red) and MODIS satellite data (blue) in (a) Tully, NY and by fixed towers (red, 0.145 ± 0.003 SD, *n* = 5) and MODIS satellite data (blue, 0.152 ± 0.005 SD, *n* = 70) at (b) Durham (red, 0.121 ± 0.015 SD, *n* = 12; blue, 0.151 ± 0.006 SD, *n* = 23), (c) Bartlett (red, 0.155 ± 0.008 SD, *n* = 13; blue, 0.148 ± 0.008 SD, *n* = 18), and (d) Petersham (red, 0.133 ± 0.009 SD, *n* = 12; blue, 0.145 ± 0.008 SD, *n* = 18). Box and whisker plots show medians, data quartiles, and outliers. Letters over tower and satellites represent significant differences within UAV and tower measurements at Tully, Durham, Bartlett, and Petersham (calculated by ANOVA, Tukey HSD), and within satellite measurements at each of the same (calculated by ANOVA, Tukey HSD).

The average summer albedo at the Durham, NH tower was lower than UAV measurements by 0.02, while albedo at the Bartlett tower was higher by 0.02. Albedo at the

Petersham, MA tower was lower by 0.01. While differences between each of the four sites were small, they were statistically significant, showing clear across-site heterogeneity (Type II Anova, df = 3, F value = 271, $p < 0.001$). At all sites, albedo at solar noon was within 0.01 units of the five hour albedo, and was not significantly different from the full albedo. Overall, all sites fell within the needed accuracy of 0.02–0.05 albedo units of each other. In comparison, satellite albedo data varied little across sites, with only Tully and Petersham showing a significant difference of less than 0.01 units, showing very little across site heterogeneity.

We then compared the in-situ UAV and tower measurements to albedo measurements made by satellite. At the Tully site, MODIS average albedo was slightly higher than in-situ, UAV-measured albedo (Student t-test: df = 8.05, $t = -6.34$, $p < 0.001$). In Durham, satellite albedo was also significantly greater than in-situ, tower-measured albedo values (Student t-test: df = −15.3, $t = 23.1$, $p < 0.001$). Likewise, Petersham satellite albedo was significantly greater than the in-situ measurements by tower (Student t-test: df = 21.2, $t = -6.03$, $p < 0.001$). However, at Bartlett, the average albedo value measured by satellite was significantly less than the average tower albedo (Student t-test: df = 18.0, $t = -4.60$, $p < 0.001$). Both UAV showed similar consistency (0.01 albedo units lower) with satellite measurements as tower measurements had with respective satellite measurements (Durham: 0.03 lower, Bartlett: 0.01 higher, Petersham: 0.01 higher). Overall, the coefficient of variation across all summer UAV albedo measurements made over mixed hardwood forest at Tully (2.1%) was similar to the variability observed at the in-situ estimates made by towers (Durham: 1.9%, Bartlett: 2.7%, Petersham: 1.9%).

3.3. Validation Measurements comparing Simultaneous UAV and Tower Data

We compared albedo measurements taken by tower and UAV approaches, over the same field of willow biofuels. Initial side by side flights by both methods produced closely

matched albedo estimates (Figure 5).

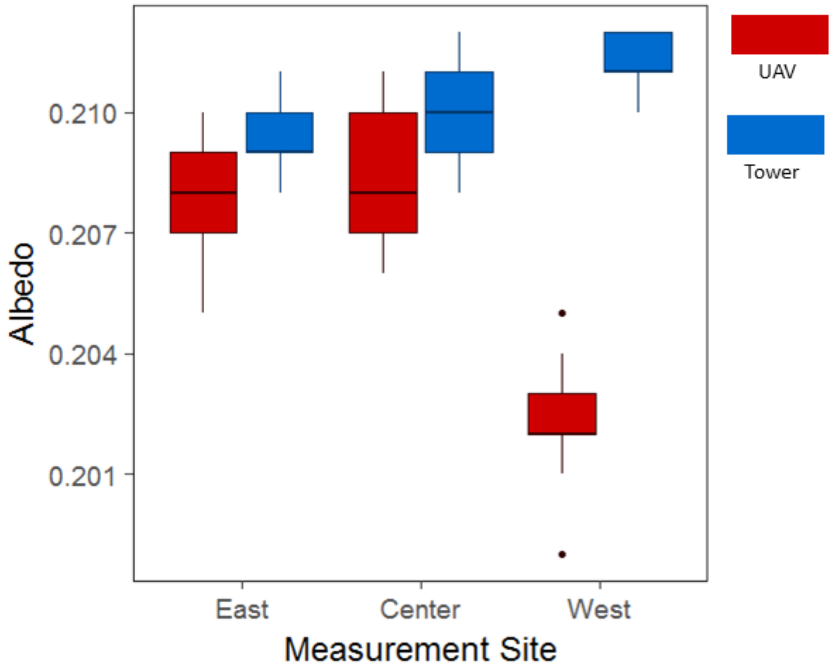

Figure 5. Albedo was measured by UAV over a willow biofuel field at three sites: immediately adjacent to a fixed tower (0.208 ± 0.001 SD, *n* = 19), 24 meters east of the tower (0.208 ± 0.002 SD, *n* = 23), and 24 m west of the tower (0.202 ± 0.002 SD, *n* = 21). Tower measurements were taken simultaneously with each flight from a fixed location at center (0.209 ± 0.001 SD, *n* = 19; 0.210 ± 0.001 SD, *n* = 23; 0.211 ± 0.001 SD, *n* = 21). UAV measurements are depicted in red, while paired, simultaneous fixed tower measurements are depicted in blue. Box and whisker plots show medians, data quartiles, and outliers. Measurements were repeated over the same willow field, using the UAV in flights 24 m west and then 29 m east of the tower. All UAV-derived willow albedo measurements were well within ±0.01 of each other, but there was slightly greater correspondence between the side-by-side measurements and measurements made over willow a distance from the tower. UAV albedo tended to have greater variability than tower albedo, regardless of the sub-site, although overall variance was low.

3.4. UAV Measurements Demonstrating Albedo across Multiple Scenarios of Land Use

Three land use types were examined in parallel: surveys of monoculture of Norway spruce (Figure 6) measured an albedo of 0.0743 and 0.0824. Two flights resurveyed the same forest site and an adjacent point, as described above, with albedo of 0.149 and 0.154. Three flights over a cropped willow field, as described above, were measured at 0.208, 0.208, and 0.202 albedo. The variation across sites was an order of magnitude less than the variation across the different land uses.

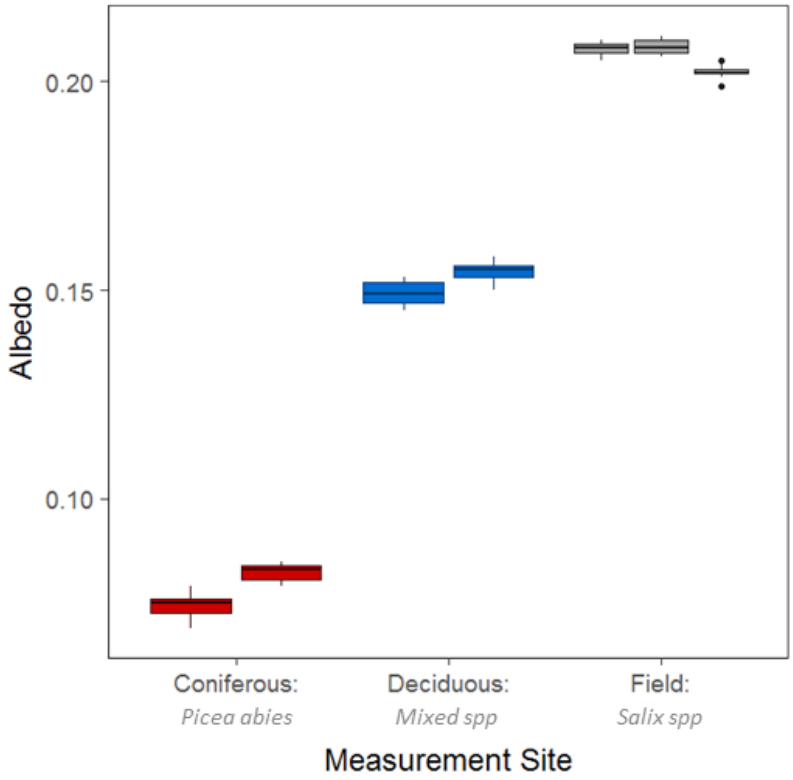

Figure 6. Albedo measured by UAV for three different land use types: two adjacent coniferous forest sites at Tully, NY (0.074 ± 0.002, *n* = 24; 0.082 ± 0.002, *n* = 23) (red), two adjacent mixed northern hardwood forest sites at Tully, NY (0.149 ± 0.002, *n* = 22; 0.154 ± 0.002, *n* = 23) (blue), and three adjacent cropped willow sites at Geneva, NY (0.208 ± 0.001, *n* = 19; 0.208 ± 0.002, *n* = 23; 0.202 ± 0.002, *n* = 21) (gray). Error bars represent the variance, reported as standard error, within each flight.

4. Discussion

Evaluation of earth system models requires surface albedo estimates with an absolute accuracy of between 0.02-0.05 units of albedo [24,42,47]. In this study, UAV flights over a mixed northern hardwood forest produced measurements within 0.01 units of each other across five flights and five hours. This albedo fell well within the range of site variation in albedo for fixed tower measurements of mixed forest albedo in Bartlett, NH; Durham, NH; and Petersham, MA, differing by no more than 0.02 units despite small cross-site differences in field of view, topography, and species composition. The tight grouping of UAV and tower estimates over a common, well–surveyed land use type supports the idea that this methodology will be able to provide accurate albedo measurements over land use types that have been poorly surveyed by conventional methods. Measurements made over a Norway spruce monoculture and cropped willow field show that the UAV easily distinguishes between land use types across multiple flights. These flights demonstrate how UAV may be used to sample sites that are not well captured by either satellite or tower measurements due to their small footprint or high rate of turnover for harvesting.

Although ground measurements (UAV and tower) were tightly grouped within a small range of albedo, each site was significantly different from the others, indicating site to site variation likely caused by species, land use, and topographic differences. This variability was poorly captured by satellite measurements, which were more tightly grouped and generally not significantly different from each other. Due to this, satellite data poorly estimated variation on the ground; UAV and tower data were generally lower than satellite data by 6 to 16%, although Bartlett forest reported 9% higher albedo than the satellite. UAV data did not differ from tower data in this way. This finding provides additional support for the use of ground measurements, such as can be obtained by UAV, to validate satellite measurements and refine model predictions. Satellites have a larger and differently distributed field of view which may

be confounded by different land use types at the pixel boundaries [4,24]. UAV can capture albedo with greater precision, and with the flexibility to take fine-scale measurements across the entire landscape.

Certain caveats of this method should be considered; uneven cloud cover means that a homogenous down-welling flux of incoming solar radiation cannot be assumed over the UAV's entire flight path. All flights in this study had to be recorded on days with no to very minimal cloud cover. UAVs must be flown such that unaided line of site is maintained, which can limit the range and altitude possible for flights over high canopy (Supplementary Table S5). Finally, continuous albedo measurements over the course of an entire day would be dependent either on the capacity to make many serial flights over the time horizon desired.

Satellites are often insufficient to capture the fine-scale landscape heterogeneity caused by local variation in canopy density, vegetative community, terrain, and other local scale properties [4,24,42]. Fine-scale point measurements, however, often lack the range needed to assess these properties on a global scale [3]. It is our belief that using UAVs to measure albedo will improve our ability to determine sources of variability in albedo measurements. Payload mass reduction through a split upwards and downward-facing sensor widens the range of UAVs available for these types of measurements and maximizes flight time (Table 2). The method described here provides a simple method of albedo assessment accessible to the typical researcher.

Table 2. Payload capacity and expected payload for common UAVs and commercially available albedo equipment.

UAV	Payload Capacity (g)	Payload	Mass (g)
DJI Phantom 3	300	CMP3	300
Sky Hero Spyder 700	1600	Datalogger	200
Freefly Systems ALTA	6800	Gimbal *	200–600
DJI Spreading Wings S900 Professional Hexacopter	8200		

* Based on MK HiSight SLR1 and Gaui Crane Gimbal.

5. Conclusions

UAVs offer an opportunity to make flexible, efficient radiation measurements at many locations and scales. Here, we validated a method of measuring albedo by UAV while minimizing payload and technical requirements. We found that UAVs provided stable albedo measurements across multiple flights over a mixed hardwood forest, with results that were well within the range of tower-estimated albedo at similar forested sites. Simultaneous albedo estimates by UAV and a fixed tower at the same site showed that the two methods produced near identical results. Finally, we demonstrated that in-situ albedo measurements (tower and UAV) capture more site-to-site variation in albedo than satellite measurements. Overall, we show that UAVs produce reliable, consistent albedo measurements that can capture crucial surface heterogeneity, clearly distinguishing between different land uses.

References

1. Latifi, H.; Galos, B. Remote sensing-supported vegetation parameters for regional climate models: A brief review. IForest 2010, 3, 98–101, doi:10.3832/ifor0543-003.

2. Pfeifer, M.; Disney, M.; Quaife, T.; Marchant, R. Terrestrial ecosystems from space: A review of earth observation products for macroecology applications. Glob. Ecol. Biogeogr. 2012, 21, 603–624, doi:10.1111/j.1466-8238.2011.00712.x.

3. Pan, S.; Tian, H.; Dangal, S. R. S.; Ouyang, Z.; Tao, B.; Ren, W.; Lu, C.; Running, S. Modeling and monitoring terrestrial primary production in a changing global environment: Toward a multiscale synthesis of observation and simulation. Adv. Meteorol. 2014, 2014, doi:10.1155/2014/965936.

4. Cescatti, A.; Marcolla, B.; Santhana Vannan, S. K.; Pan, J. Y.; Roman, M. O.; Yang, X.; Ciais, P.; Cook, R. B.; Law, B. E.; Matteucci, G.; Migliavacca, M.; Moors, E.; Richardson, A. D.; Seufert, G.; Schaaf, C. Intercomparison of MODIS albedo retrievals and in situ measurements across the global FLUXNET network. Remote Sens. Environ. 2012, 121, 323–334, doi:10.1016/j.rse.2012.02.019.

5. Randerson, J. T.; Liu, H.; Flanner, M. G.; Chambers, S. D.; Jin, Y.; Hess, P. G.; Pfister, G.; Mack, M. C.; Treseder, K. K.; Welp, L. R.; Chapin, F. S.; Harden, J. W.; Goulden, M. L.; Lyons, E.; Neff, J. C.; Schuur, E. a G.; Zender, C. S. The impact of boreal forest fire on climate warming. Science (80-.). 2006, 314, 1130–1132, doi:10.1126/science.1132075.

6. Otto, J.; Berveiller, D.; Bréon, F. M.; Delpierre, N.; Geppert, G.; Granier, A.; Jans, W.; Knohl, A.; Kuusk, A.; Longdoz, B.; Moors, E.; Mund, M.; Pinty, B.; Schelhaas, M. J.; Luyssaert, S. Forest summer albedo is sensitive to species and thinning: How should we account for this in Earth system models? Biogeosciences 2014, 11, 2411–2427, doi:10.5194/bg-11-2411-2014.

7. Wang, Z.; Erb, A. M.; Schaaf, C. B.; Sun, Q.; Liu, Y.; Yang, Y.; Shuai, Y.; Casey, K. A.;

Román, M. O. Early spring post-fire snow albedo dynamics in high latitude boreal forests using Landsat-8 OLI data. Remote Sens. Environ. 2016, 185, 71–83, doi:10.1016/j.rse.2016.02.059.

8. Jackson, R. B.; Randerson, J. T.; Canadell, J. G.; Anderson, R. G.; Avissar, R.; Baldocchi, D. D.; Bonan, G. B.; Caldeira, K.; Diffenbaugh, N. S.; Field, C. B.; Hungate, B. a; Jobbágy, E. G.; Kueppers, L. M.; Nosetto, M. D.; Pataki, D. E. Protecting climate with forests. Environ. Res. Lett. 2008, 3, 1–5, doi:10.1088/1748-9326/3/4/044006.

9. Kirschbaum, M. U. F.; Whitehead, D.; Dean, S. M.; Beets, P. N.; Shepherd, J. D.; Ausseil, A.-G. E. Implications of albedo changes following afforestation on the benefits of forests as carbon sinks. Biogeosciences 2011, 8, 3687–3696, doi:10.5194/bg-8-3687-2011.

10. Betts, R.; Falloon, P. D.; Goldewijk, K. K.; Ramankutty, N. Biogeophysical effects of land use on climate: Model simulations of radiative forcing and large-scale temperature change. Agric. For. Meteorol. 2007, 142, 216–233, doi:10.1016/j.agrformet.2006.08.021.

11. Betts, R. Offset of the potential carbon sink from boreal forestation by decreases in surface albedo. Lett. to Nat. 2000, 408, 187–190, doi:10.1038/35041545.

12. Wang, Z.; Zeng, X. Evaluation of snow albedo in land models for weather and climate studies. J. Appl. Meteorol. Climatol. 2010, 49, 363–380, doi:10.1175/2009JAMC2134.1.

13. Flanner, M. G.; Zender, C. S. Linking snowpack microphysics and albedo evolution. J. Geophys. Res. 2006, 111, 2156–2202, doi:10.1029/2005JD006834.

14. Bonan, G. B. Forests and climate change: forcings, feedbacks, and the climate benefits of forests. Science (80-.). 2008, 320, 1444–1449, doi:10.1126/science.1155121.

15. Bright, R. M. Metrics for biogeophysical climate forcings from land use and land cover changes (LULCC) and their inclusion in Life Cycle Assessment (LCA): A critical review. Environ. Sci. Technol. 2015, 49, 3291–3303, doi:10.1021/es505465t.

16. Zhao, K.; Jackson, R. B. Biophysical forcings of land-use changes from potential forestry

activities in North America. Ecol. Monogr. 2014, 84, 329–353, doi:10.1890/12-1705.1.

17. Chen, L.; Dirmeyer, P. A. Adapting observationally based metrics of biogeophysical feedbacks from land cover/land use change to climate modeling. Environ. Res. Lett. 2016, 11, doi:10.1088/1748-9326/11/3/034002.

18. Burakowski, E.; Tawfik, A.; Ouimette, A.; Lepine, L.; Novick, K.; Ollinger, S.; Zarzycki, C.; Bonan, G. The role of surface roughness, albedo, and Bowen ratio on ecosystem energy balance in the Eastern United States. Agric. For. Meteorol. 2018, 249, 367–376, doi:10.1016/j.agrformet.2017.11.030.

19. Lee, X.; Goulden, M. L.; Hollinger, D. Y.; Barr, A.; Black, T. A.; Bohrer, G.; Bracho, R.; Drake, B.; Goldstein, A.; Gu, L.; Katul, G.; Kolb, T.; Law, B. E.; Margolis, H.; Meyers, T.; Monson, R.; Munger, W.; Oren, R.; Paw U, K. T.; Richardson, A. D.; Schmid, H. P.; Staebler, R.; Wofsy, S.; Zhao, L. Observed increase in local cooling effect of deforestation at higher latitudes. Nat. Lett. 2011, 479, 384–387, doi:10.1038/nature10588.

20. Lutz, D. A.; Burakowski, E. A.; Murphy, M. B.; Borsuk, M. E.; Niemiec, R. M.; Howarth, R. B. Tradeoffs between three forest ecosystem services across the state of New Hampshire, USA: timber, carbon, and albedo. Ecol. Appl. 2016, 26, 146–161.

21. Barnes, C. A.; Roy, D. P. Radiative forcing over the conterminous United States due to contemporary land cover land use albedo change. Geophys. Res. Lett. 2008, 35, 1–6, doi:10.1029/2008GL033567.

22. Montenegro, A.; Eby, M.; Mu, Q.; Mulligan, M.; Weaver, A. J.; Wiebe, E. C.; Zhao, M. The net carbon drawdown of small scale afforestation from satellite observations. Glob. Planet. Change 2009, 69, 195–204, doi:10.1016/j.gloplacha.2009.08.005.

23. Campagnolo, M. L.; Sun, Q.; Liu, Y.; Schaaf, C.; Wang, Z.; Román, M. O. Estimating the effective spatial resolution of the operational BRDF, albedo, and nadir reflectance products from MODIS and VIIRS. Remote Sens. Environ. 2016, 175, 52–64,

doi:10.1016/j.rse.2015.12.033.

24. Roman, M. O.; Schaaf, C.; Woodcock, C. E.; Strahler, A. H.; Yang, X.; Braswell, R. H.; Curtis, P. S.; Davis, K. J.; Dragoni, D.; Goulden, M. L.; Gu, L.; Hollinger, D. Y.; Kolb, T. E.; Meyers, T. P.; Munger, J. W.; Privette, J. L.; Richardson, A. D.; Wilson, T. B.; Wofsy, S. C. The MODIS (Collection V005) BRDF/albedo product: Assessment of spatial representativeness over forested landscapes. Remote Sens. Environ. 2009, 113, 2476–2498, doi:10.1016/j.rse.2009.07.009.

25. Franch, B.; Vermote, E. F.; Claverie, M. Intercomparison of Landsat albedo retrieval techniques and evaluation against in situ measurements across the US SURFRAD network. Remote Sens. Environ. 2014, 152, 627–637, doi:10.1016/j.rse.2014.07.019.

26. Roy, D. P.; Zhang, H. K.; Ju, J.; Gomez-Dans, J. L.; Lewis, P. E.; Schaaf, C.; Sun, Q.; Li, J.; Huang, H.; Kovalskyy, V. A general method to normalize Landsat reflectance data to nadir BRDF adjusted reflectance. Remote Sens. Environ. 2016, 176, 255–271, doi:10.1016/j.rse.2016.01.023.

27. Burakowski, E. a.; Ollinger, S. V.; Lepine, L.; Schaaf, C.; Wang, Z.; Dibb, J. E.; Hollinger, D. Y.; Kim, J.; Erb, A.; Martin, M. Spatial scaling of reflectance and surface albedo over a mixed-use, temperate forest landscape during snow-covered periods. Remote Sens. Environ. 2015, 158, 465–477, doi:10.1016/j.rse.2014.11.023.

28. Adolph, A. C.; Albert, M. R.; Lazarcik, J.; Dibb, J. E.; Amante, J. M.; Price, A. Dominance of grain size impacts on seasonal snow albedo at open sites in New Hampshire. J. Geophys. Res. 2017, 122, 121–139, doi:10.1002/2016JD025362.

29. Warren, S. G.; Wiscombe, W. J. A Model for the Spectral Albedo of Snow. II: Snow Containing Atmospheric Aerosols. J. Atmos. Sci. 1980, 37, 2734–2745, doi:10.1175/1520-0469(1980)037<2734:AMFTSA>2.0.CO;2.

30. Anderson, K.; Gaston, K. J. Lightweight unmanned aerial vehicles will revolutionize

spatial ecology. Front. Ecol. Environ. 2013, 11, 138–146, doi:10.1890/120150.

31. Cruzan, M. B.; Weinstein, B. G.; Grasty, M. R.; Kohrn, B. F.; Hendrickson, E. C.; Arredondo, T. M.; Thompson, P. G. Small Unmanned Aerial Vehicles (Micro-UAVs, Drones) in Plant Ecology. Appl. Plant Sci. 2016, 4, 1600041, doi:10.3732/apps.1600041.

32. U.S. Department of Transportation Federal Aviation Administration (FAA). *Air Traffic Organization Policy, Order JO 7110.65V*; FAA: Washington, DC, USA, 2017.

33. Ramana, M. V; V, R.; D, K.; C, R. G.; E, C. C. Albedo, atmospheric solar absorption and heating rate measurements with stacked UAVs. Q. J. R. … 2007, 133, 937–948, doi:10.1002/qj.

34. Schneider, C.; Truffer, M.; Michael Shea, J.; Hubbard, A.; Ryan, J. C.; Box, J. E.; Brough, S.; Cameron, K.; Cook, J. M.; Cooper, M.; Doyle, S. H.; Edwards, A.; Holt, T.; Irvine-Fynn, T.; Jones, C.; Pitcher, L. H.; Rennermalm, A. K.; Smith, L. C.; Stibal, M.; Snooke, N. Derivation of High Spatial Resolution Albedo from UAV Digital Imagery: Application over the Greenland Ice Sheet. 2017, 5, 1–13, doi:10.3389/feart.2017.00040.

35. Weiser, U.; Olefs, M.; Schöner, W.; Weyss, G.; Hynek, B. Correction of broadband snow albedo measurements affected by unknown slope and sensor tilts. Cryosph. 2016, 10, 775–790, doi:10.5194/tc-10-775-2016.

36. Jenkins, J. P.; Richardson, A. D.; Braswell, B. H.; Ollinger, S. V.; Hollinger, D. Y.; Smith, M. L. Refining light-use efficiency calculations for a deciduous forest canopy using simultaneous tower-based carbon flux and radiometric measurements. Agric. For. Meteorol. 2007, 143, 64–79, doi:10.1016/j.agrformet.2006.11.008.

37. Wang, Z.; Schaaf, C.; Strahler, A. H.; Chopping, M. J.; Román, M. O.; Shuai, Y.; Woodcock, C. E.; Hollinger, D. Y.; Fitzjarrald, D. R. Evaluation of MODIS albedo product (MCD43A) over grassland, agriculture and forest surface types during dormant and snow-covered periods. Remote Sens. Environ. 2014, 140, 60–77, doi:10.1016/j.rse.2013.08.025.

38. Environmental Protection Agency AirNow Available online: https://www.airnow.gov/index.cfm?action=airnow.mapsarchivecalendar (accessed on Oct 25, 2016).

39. Richardson, A. D. Radiometric and Meteorological Data from Harvard Forest Barn Tower Since 2011 Available online: http://harvardforest.fas.harvard.edu:8080/exist/apps/datasets/showData.html?id=hf249 (accessed on Oct 25, 2016).

40. Aubrecht, D. M.; Helliker, B. R.; Goulden, M. L.; Roberts, D. A.; Still, C. J.; Richardson, A. D. Continuous, long-term, high-frequency thermal imaging of vegetation: Uncertainties and recommended best practices. Agric. For. Meteorol. 2016, 228–229, 315–326, doi:10.1016/j.agrformet.2016.07.017.

41. Schaaf, C. MCD43A3 MODIS/Terra + Aqua BRDF/Albedo Daily L3 Global-500 m V006; NASA: Washington, DC, USA, 2015.

42. Lucht, W.; Hyman, A. H.; Strahler, A. H.; Barnsley, M. J.; Hobson, P.; Muller, J. P. A comparison of satellite-derived spectral albedos to ground-based broadband albedo measurements modeled to satellite spatial scale for a semidesert landscape. Remote Sens. Environ. 2000, 74, 85–98, doi:10.1016/S0034-4257(00)00125-5.

43. Lewis, P.; Barnsley, M. Influence of the sky radiance distribution on various formulations of the earth surface albedo. Proc. Conf. Phys. Meas. Signatures Remote Sens. 1994, 707–715.

44. NASA, USGS. Application for Extracting and Exploring Analysis Ready Samples (AρρEEARS). 2016. https://lpdaacsvc.cr.usgs.gov/appeears/help.

44. R Development Core Team, R. R: A Language and Environment for Statistical Computing. R Found. Stat. Comput. 2011, 1, 409.

46. Fox, J.; Weisberg, S. An {R} Companion to Applied Regression, Second Edition; Sage Group: Thousand Oaks, CA, 2011;

47. Liu, J.; Schaaf, C.; Strahler, A.; Jiao, Z.; Shuai, Y.; Zhang, Q.; Roman, M.; Augustine, J. A.; Dutton, E. G. Validation of moderate resolution imaging spectroradiometer (MODIS) albedo retrieval algorithm: Dependence of albedo on solar zenith angle. J. Geophys. Res

Supplementary Information

Suppl. Table 1. Dates, times, and locations of described UAV flights

Date	Site	Land Use	Times (EDT)	Latitude (˚)	Longitude (˚)	Altitude above Ground Canopy (m)	
7/27/2016	**Tully, NY**	Mixed Hardwood	11:10-12:10	42.77728	-76.08168	83	60
7/27/2016	**Tully, NY**	Mixed Hardwood	12:18-12:28	42.77728	-76.08168	83	60
7/27/2016	**Tully, NY**	Mixed Hardwood	13:04-13:14	42.77728	-76.08168	83	60
7/27/2016	**Tully, NY**	Mixed Hardwood	14:10-14:20	42.77728	-76.08168	83	60
7/27/2016	**Tully, NY**	Mixed Hardwood	15:08-15:18	42.77728	-76.08168	83	60
7/30/2017	**Tully, NY**	Mixed Hardwood	13:40-13:52	42.77613	-76.08541	31	8
7/30/2017	**Tully, NY**	Mixed Hardwood	14:00-14:11	42.77605	-76.08573	31	8
7/30/2017	**Tully, NY**	Spruce Plantation	14:36-14:46	42.77728	-76.08168	24	1
7/30/2017	**Tully, NY**	Spruce Plantation	15:09-15:20	42.77112	-76.08297	37	14
7/31/2017	**Geneva, NY**	Cropped Willow	12:43-12:52	42.88322	-77.00353	8	5
7/31/2017	**Geneva, NY**	Cropped Willow	13:02-13:13	42.88310	-77.00320	9	6
7/31/2017	**Geneva, NY**	Cropped Willow	13:29-13:40	42.88312	-77.00378	8	5

Suppl. Table 2 Latitude and Longitude of the northwest corner of each of the 500*500m satellite pixels retrieved for comparison to UAV estimates of albedo at Tully, NY. Satellite data retrieved using the LPDAAC APPEEARS tool and latitude and longitude of MODIS pixels retrieved using the MODLAND Pixel Calculator.

Latitude	Longitude
42.77729	-76.08656
42.77729	-76.08044
42.77282	-76.08656
42.77282	-76.08044

Suppl. Table 3. Latitude and Longitude of the northwest corner of each of the 500*500m satellite pixels retrieved for comparison to tower estimates of albedo at Petersham, MA; Bartlett, NH; and Durham, NH.

Tower site	Latitude	Longitude
Petersham, MA USA	42.53919	-72.17566
Bartlett, NH USA	44.06875	-71.29669
Durham, NH USA	43.11042	-70.95806

Suppl. Table 4. Blue sky albedo estimates for sites in Tully, NY; Durham, NH; Bartlett, NH; and Petersham, MA. Estimates were created with high (0.5), low (0.1) and typical (0.2) estimates for optical depth to examine the sensitivity of the results to the assumption of 0.2.

Site	OD	Mean	SE
Tully	Low	0.152	0.001
Tully	Med	0.152	0.001
Tully	High	0.151	0.001
Bartlett	Low	0.148	0.002
Bartlett	Med	0.148	0.002
Bartlett	High	0.147	0.002
Durham	Low	0.151	0.001
Durham	Med	0.151	0.001
Durham	High	0.149	0.001
Petersham	Low	0.146	0.002
Petersham	Med	0.146	0.002
Petersham	High	0.145	0.002

Suppl. Table 5. Current FAA requirements for UAV research within the United States

Requirement	Approximate Cost	Location	Expiration
Craft Registration	Registration Fee: $5	Form available online	3 years
Pilot Cert. Exam	Exam Fee: $150	One of 700 national test centers	2 years
Pilot Certification	No Cost	Form available online Includes security screening	2 years
Pilot Requirements/Restrictions			
• **Be at least 16 years old** • **Be able to read, speak, write, and understand English (exceptions may be made if the person is unable to meet one of these requirements for a medical reason)** • **Be in a physical and mental condition to safely operate a small UAV** • **Pass the aeronautical knowledge exam at an FAA-approved testing center (above)** • **Undergo Transportation Safety Administration (TSA) security screening (above)**			
Equipment Requirements/ Restrictions			
• **Unmanned aircraft must weigh less than 25 kgs, including payload, at takeoff** • **The remote pilot in command must conduct a preflight check of the small UAV to ensure that it is in a condition for safe operation**			
Operational Requirements/Restrictions			
• **Unmanned aircraft must weigh less than 25 kgs, including payload, at takeoff** • **Fly in Class G airspace*** • **Keep the unmanned aircraft within visual line-of-sight; vision must be unaided except by corrective lenses*** • **Fly at or below 122 m*** • **Fly during daylight or civil twilight*** • **Fly at or under 161 km h^{-1}*** • **Yield right of way to manned aircraft*** • **Do not fly directly over people*** • **Do not fly from a moving vehicle, unless in a sparsely populated area*** • **Minimum weather visibility of 4.8 km from operator** • **Maintain line of sight with UAV at all times** • **No careless or reckless operations** • **No carriage of hazardous materials**			

*These rules are subject to waiver.

CHAPTER TWO: Contemporary and Future Climate Impacts of Biofuels and Reforestation in the Northeastern US

Abstract

Climate mitigation projects such as reforestation or planting of bioenergy crops have potential for widespread application in former cropland in the northeastern United States. However, changes in albedo from these land use projects, have the potential to cause large negative feedbacks due to differences in reflection and retention of shortwave radiation at the planet surface. These differences in reflectivity are driven both by growing season canopy and leaf properties, but also substantially by dormant season albedo and sensitivity to snow cover. We collected seasonal albedo data and albedo~snow response trends from four land-use types, including the first report of albedo from short-rotation willow crop. Using as a reference row-crop agriculture in Ithaca, NY, we found that albedo changes for all four land-use conversions led to a warming impact on climate, between 27.3 kg CO_2 m^2 (forest) and 0.3 kg CO_2 m^{-2} (switchgrass). However, a more complete analysis of the long-term impact of albedo forcing required us to account for how loss of snow due to regional climate warming would impact albedo. We used an ensemble of global climate models to project snow loss over the next hundred years for four Representative Concentration Pathways (RCP) together with a projection of empirically measured rates of local snow loss from the past thirty years. We found that a 20% loss of snow cover sufficed to turn a positive (warming) forcing into a negative (cooling) forcing for switchgrass and elephantgrass. In order to effectively address climate change, mitigation projects need to incorporate the substantial climate forcing from albedo. We not only found substantial differences across land use types in the magnitude of this climate forcing, but also additionally that both the magnitude and the direction of this forcing was affected by predicted snow loss.

1. Introduction

Land-use and land-cover change can impact global climate by altering the reflectivity, or albedo, of the Earth's surface, altering the fraction of incoming shortwave solar radiation absorbed by the earth's climate system. Albedo varies considerably within and among land cover types (Bonan, 2008; Bright, 2015; Zhao and Jackson, 2014). Thus, land conversion (e.g. deforestation, urbanization, crop rotation) can significantly alter the planetary energy balance and impact global temperature (Betts et al., 2007; Jackson et al., 2008; Kirschbaum et al., 2011; Randerson et al., 2006). In the past few decades numerous researchers have demonstrated that albedo changes can have global consequences on climate (Bala et al., 2007; Betts, 2007; Marland et al., 2003). A study examining reforestation in Switzerland found that the climate impact of albedo could offset the impact of carbon sequestration in these forests by 11-109% depending on forest composition, altitude, and snow cover. Conversely, a study of future land-use change in relatively snow-free Massachusetts projected that albedo change would increase global warming potential by 10 kg CO_2-equivalents ha^{-1} $year^{-1}$, or 8% of the total expected climate forcing of increasing deforestation and urbanization (Reinmann et al., 2016). A model-based comparison of potential uses for temperate croplands around the world found albedo to almost completely offset carbon uptake by 2100 (Schaeffer et al., 2007). As differences in albedo can have non-negligible consequences on global climate, climate mitigation projects should consider the albedo impact of land-cover and land-use change (Bonan, 2008; Bright, 2015; Zhao and Jackson, 2014).

On the scale of a century, positive feedbacks between a warming climate and surface albedo will impact the likely effectiveness of mitigation projects by affecting high-reflectivity snow cover. In particular, warmer temperatures will likely decrease winter snowfall and the duration of the snow season (Qu and Hall, 2014; Thackeray and Fletcher, 2016); this reduction

in snow cover can greatly decrease albedo and further warm the climate. Snow cover can more than double the average winter albedo of a wide range of land-use types, both forested and non-forested (Bonan, 2008; Jin et al., 2002). Greater snow depth increases albedo by covering darker understory vegetation (Sturm et al., 2005) and crop residues (Kaye and Quemada, 2017). A shorter snow season will decrease the overall average annual albedo (Bright, 2015). Even with persistent snow cover, frequent thawing and refreezing, or warmer overall air temperatures, will increase snow grain size and lower wintertime albedo (Adolph et al., 2017),

Snow cover is also a major driver of differences in albedo across otherwise similar land-cover types. A satellite survey of albedo across four land-use types suggested that snow cover could more than triple the wintertime albedo of crop or grassland, nearly double that of broadleaf deciduous forested land, and more than double that of evergreen forested land (Zhao and Jackson, 2014). Differences in typical snow depth among different vegetation types (Liston and Hiemstra, 2011; Sturm et al., 2005), as well as differential capacity of vegetation to catch and hold snow blowing across the landscape (Sturm et al., 2005, 2001) can influence these effects. Past studies have consistently shown that the impact of albedo associated with land-use change is highly dependent on snow cover, as changing vegetation cover may obscure or expose the snow-covered ground. Anticipated snow cover loss has also been shown to shorten optimal forest harvest rotation length for climate mitigation in New Hampshire (Lutz et al., 2016) where a large decrease in snowfall would increase the optimal rotation length by 40 years due to the anticipated decrease in albedo; with greater snow cover albedo effects compensated for by more frequent cutting. A study in Norway found that reforestation projects should make use of deciduous broadleaf, rather than coniferous stands due in part to the snow-masking effects of coniferous evergreen forests in the wintertime (Bright et al., 2014). Thus, when considering the impacts of albedo on land-use change for climate

mitigation, the long-term effects of snow loss must be considered as well.

The northeastern United States contains millions of hectacres classified as "marginal agricultural land" that may present an ideal opportunity for conversion to forest or biofuels production (Hobbs, 2007). This land is 1) considered unprofitable for conventional agriculture due to its steep grade, wet condition, or poor soil, 2) not currently in use for grazing or haying, and 3) being maintained against natural forest regeneration by periodic mowing (Stoof et al., 2015). Recent estimates suggest as much as 10,150 km^2, or 7.2% of New York State are classified as marginal agricultural land based on this definition (Shortall, 2013). In the broader Northeast (New England, NJ, PA, and NY), as much as 24,300 km^2, or 4.4% of the land area, consists of marginal agricultural land. Often, this land is being maintained in reserve for future use, should crop prices rise or new agricultural opportunities become available (Richards et al., 2014). This marginal land can present a significant opportunity for land managers interested in climate mitigation.

One potential use for marginal land in the Northeast is reforestation. Forests may be managed for income from forest products and in many northeastern regions abandoned fields will naturally revert to forest with little or no direct interference (Cramer et al., 2008). However, forests can have low surface reflectivity compared to most cropland; summertime albedo is 0.13-0.19 for broadleaf deciduous forest, 0.08-0.15 for evergreen coniferous forest (Hollinger et al., 2010) compared with 0.16-0.25 for cropland. Thus, conversion of fields to forest often exerts a warming influence on the climate through decreased growing-season albedo (Betts and Ball, 1997; Betts, 2000; Bonan, 2008; Bonan et al., 1992; Chapin et al., 2008; Syktus and McAlpine, 2016; Zhao and Jackson, 2014). Moreover, this warming impact is significantly larger in winter because of snow cover; evergreen forests remain dark year round (Bonan et al., 1992; Li et al., 2015), while deciduous forests expose either bright snow

or dark bare ground following leaf-fall (Hollinger et al., 2010; Li et al., 2015). A further complication is the sometimes prolonged retention of fresh snow on conifer forest canopies (Hedstrom and Pomeroy, 1998).

Alternatively, marginal land could be converted to the production of second-generation biofuels; these energy crops are able to tolerate low quality sites, allowing production on sites not suitable for food crops. Biomass produced by these crops can be used for energy generation (direct firing, gasification) thereby replacing fossil fuels (Keoleian and Volk, 2005). Herbaceous biofuels are already widely grown, and include perennial C_4 grasses such as elephantgrass (*Miscanthus giganteus*) and switchgrass (*Panicum virgatum*). These crops have relatively high summer albedo (Miller et al., 2016). In addition, as they are harvested annually, little biomass remains on the ground during the winter months; thus, these crops can have high winter albedo in areas with consistent snow cover. Another option for land conversion is coppiced willow (*Salix sp.*), a cellulosic biofuel. Willow is especially well-suited to wet, rocky, and low-fertility fields common in the Northeast and is typically harvested every three years. Willow has only recently been studied in the context of albedo (Levy et al., 2018); the present study is the first to report seasonal albedo variation for this land cover type(Cherubini et al., 2012).

We evaluated the relative climate impact of albedo change from four land-use conversion scenarios, from maize croplands (baseline) into either mixed hardwood-conifer forest or one of three biofuels (willow, elephantgrass, and switchgrass), in Ithaca, NY. We examined the impact of each of these four proposed conversion scenarios first for contemporary snow depth and then with snow depth as projected into 2100 by modeled scenarios for local snow loss. Under current conditions, we predicted that conversion from cropland to biofuels would exert a small cooling impact on climate due to the high growing

season albedo of perennial biofuel crops compared to annual crops, while conversion to forests would have a warming impact due to the lower reflectivity of mixed deciduous-evergreen forests, across seasons. We also predicted that as snow cover diminishes under future climate warming scenarios, winter albedo will decrease more for biofuels than forest, causing the cooling impact of biofuels to disappear and the warming impact of forests to be reduced.

2. Methods

Analytical Process

Effects of land cover change on albedo and climate were assessed using both contemporary snow cover and projected snow cover at the year 2100, considering both land-cover differences in snow-free albedo and the role of current differences and projected changes in snow cover. For the contemporary assessments, we determined the monthly snow-free albedo for each of the four conversion options. The baseline land-use was assumed to be a maize cropland, while the four potential land-use scenarios were conversion to: 1) willow, a woody biofuel, 2) mixed deciduous/conifer forest, 3) elephantgrass, and 4) switchgrass, both herbaceous perennial biofuels. Snow-free albedo values for each land-use type were determined from our direct field measurements for willow and literature values for the other land covers. Albedo values from all sources were then paired with respective local snow depth data, to determine the relationship between snow depth and albedo. The albedo-snow depth relationships were then used to adjust all land-use scenarios to contemporary snow conditions in the common location of Ithaca, NY. The impact on climate of land-use-driven differences in albedo were quantified as the projected radiative forcing and global warming potential (GWP) for each land-use change scenario relative to baseline land-use (Ch.2 Figure 1).

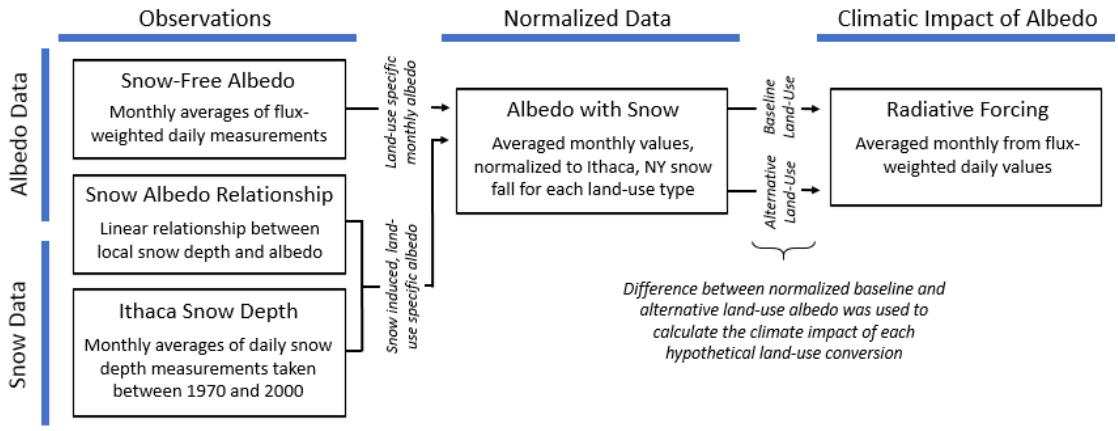

Ch.2 Figure 1. Roadmap of observations, normalization, and calculation of climatic impact of land-use conversion scenarios.

Future snow was established by obtaining snow depth predictions from an ensemble of global climate models for each of four Representative Concentration Pathways (2.6, 4.5, 6.0, 8.5) (Intergovernmental Panel on Climate Change, 2014). Additionally, we examined a snow-depth scenario based on future projections of local historical snow depth trends (hereafter described as the empirical scenario), and an extreme snow depth pathway based on no winter snowfall (hereafter described as the total snow-loss scenario). Future monthly albedo was calculated from the snow-free albedo and the relationship between snow depth and albedo for each land cover. The projected radiative forcing and GWP in 2100 under each climate pathway and land use were calculated, using equations described below.

Study Site and Region

Conversion of crop marginal land for alternative uses has the potential to impact much of the global temperate zone, and the northeastern United States in particular; however, for this study albedo measurements were normalized to a reference site in Ithaca, NY (42.4° N, 76.5° W). This region has been a focal site for research into lignocellulosic biofuels, particularly coppiced short-rotation willow (Heller et al., 2003), which has not previously

been examined from the perspective of albedo and land-use change (Cherubini et al., 2012). In addition, research into the potential for marginal croplands to be converted to lignocellulosic fuel-types has been of particular interest in New York State (Stoof et al., 2015). Finally, the Ithaca region has a long-term record of consistent snow depth data through the Northeast Regional Climate Center. Winter snow depth in Ithaca averaged 6.61 cm (November- April; 1970-2000). The highest monthly average during this interval was 13.7 cm.

Ch.2 Table 1. Background information for each land-use type describing sites and methods by which albedo information was collected.

Data Type	**Location**	**Species/ Cultivar**	**Method**	**Lat, Lon**	**Mean Annual Temperature (°C)**
Baseline) Crop	University of Illinois Champaign & Pana, IL	*Zea mays*	CNR 1 & CNR 2, Kipp & Zonen	40.0, -88.2 40.1, -88.2	10.5, 11.6
1) Willow Woody Biofuel	Cornell University Geneva, NY	*Salix sp. mixed cultivars*	CMA6, Kipp & Zonen	42.8, -76.1	8.6
2) Mixed forest	Harvard Forest Petersham, MA	*Q. rubra, P. strobus, A. rubrum, T. canadensis*	CNR 4, Kipp & Zonen	42.5, -72.2	8.0
3) Elephantgrass Herbaceous Biofuel	University of Illinois Champaign & Pana, IL	*Miscanthus sp.*	CNR 1 & CNR 2, Kipp & Zonen	40.0, -88.2 40.1, -88.2	10.5, 11.6
4) Switchgrass Herbaceous Biofuel	University of Illinois Champaign & Pana, IL	*Panicum sp.*	CNR 1 & CNR 2, Kipp & Zonen	40.0, -88.2 40.1, -88.2	10.5, 11.6

a. Sources for overall site descriptions: (Fabio et al., 2016; Levy et al., 2018; Miller et al., 2016; Richardson, 2015)

b. Sources for climate normal and growing degree day descriptions: (Your Weather Service, 2019) (USA National Phenology Network, 2019)

c. Sources for snow fall averages: (National Oceanic Atmospheric Administration and National Operational Hydrologic Remote Sensing Center, n.d.) (Angel, 2018) (National Climactic Data Center et al., 2019) (Hellstrom, 2015)

Snow-Free Albedo and Measurement of Albedo

Monthly albedo averages for each land-use type were obtained from published values and our measurements of willow biofuels (Table 1). Baseline crop (maize) data were obtained from University of Illinois research sites in Pana and Champaign, IL (Miller et al., 2016). We collected willow albedo data at the New York State Agricultural Experiment Station in Geneva, NY, as described below. Temperate forest data were obtained from long-term field studies at Harvard Forest, Petersham, MA. Temperate forest was composed of approximately 70% deciduous and 30% coniferous tree cover. Finally, herbaceous biofuel albedo data (elephantgrass; switchgrass) were obtained at the University of Illinois Energy Farm and South Farms/SoyFACE research facilities in Champaign and Pana, Illinois (Miller et al., 2016).

Willow albedo data were collected at a research site in Geneva, NY using a paired set of pyranometers on a telescoping pneumatic pole (Kipp and Zonen, CMA6; Total Mast Solutions, CP56-08) (Table 1). Incoming and reflected shortwave radiation measurements ($SW_{\downarrow}$ and $SW_{\uparrow}$) were recorded on a Meteon datalogger (Kipp and Zonen) every 2 minutes throughout the day. Measurements were taken periodically between 2016 and 2018. The sensor was placed at 9.09 m on a 30 cm leveled boom oriented to the south. Albedo of baseline crop, forest, and herbaceous biofuels were recorded using tower-mounted net radiometers (Table 1) as described in (Miller et al., 2016; Richardson, 2015).

For all datasets, individual measurements of $SW_{\downarrow}$ and $SW_{\uparrow}$ over the course of each day were averaged and reported as daily flux-weighted averages:

$$Albedo_{daily}(l,d) = \frac{\sum_{t} SW\uparrow(l,d,t)}{\sum_{t} SW\downarrow(l,d,t)} \qquad (1)$$

where l indicates the land use, *d* indicates the day of measurement, and *t* indicates the individual measurement over the course of the day. Individual time points with $SW_{\downarrow}$ was at least 60% of the maximum $SW_{\downarrow}$ at the surface as predicted by the latitude, time of year, and insolation angle ($SW^{\downarrow}_{max}$. To ensure that flux-weighted averages would not be skewed by unequal distribution of individual time points, values for $Albedo_{daily}$ were only used where individual observations covered 90% of possible measurements over the course of the day; where observations covered more than 99% of possible measurements prior to solar noon; where observations covered more than 99% of measurements following solar noon; and where days had at least one data point within an hour of solar noon. All datasets were analyzed identically. This process removed 43% (crop), 58% (willow), 41% (forest), 32% (elephantgrass), and 44% (switchgrass) of measurement days. Two additional winter days (1/18/2016 and 1/20/2018) were removed from the willow albedo dataset as anomalously high afternoon albedo values suggested that late in the day snowfall occurred that was not captured by morning snowfall measurements. The final number of data points for $Albedo_{daily}$ ranged from 889 days (baseline crop) to 91 days (willow) (Suppl. Table 1; Figure 3).

Monthly albedo values were estimated as the average of all available datapoints across that month; where annual values were reported, these reflected the unweighted average by month. Variance was reported correspondingly as standard deviation; the standard deviation of the unweighted annual average was calculated using the delta method and reported using the deltavar function in the emdbook package in R. ANOVA was performed on the unaveraged datapoints using the aov function in the R stats package.

Relationships between Snow Depth and Albedo

Relationships between snow depth and albedo for each land use were determined from on-site measurements of both albedo and snow depth for each of the five land-use types

(Table 2), up to a maximum of 76.5 cm depth, chosen because the maximum measured in Ithaca, NY between 1970 and 1999. Snow-free albedo during winter months was also included. Ithaca snow data were obtained from 1970-1999 monthly snow depth averages measured at the Game Farm Road site, Ithaca, NY (42.449, -76.449) (NOAA Northeast Regional Climate Center at Cornell University, 2017). Snow fall at the Geneva sites were collected from a long-term temperature monitoring station within the same field as measurements were taken, in Geneva, NY (42.883, -77.000). Snow depth of the forested system were obtained from a long-term monitoring site at Prospect Hill, Petersham, NY (42.542, -72.180). The Illinois measurements took place at Pana, IL (39.372, -89.024) and Champaign-Urbana, IL (40.083, -88.238). Linear regressions were performed using the linear model function from R; this function was also used to report adjusted R squared values and significance of fit (R Development Core Team, 2017).

Recent Snow Depth and Projected Future Change

Projections of how changing snow cover interacts with land-use change and albedo to influence GWP were developed for the standard site at Ithaca, NY. A 30-year monthly average snow depth was determined from historic data measured in Ithaca, NY between 1970 and 2000. Predicted future changes in Ithaca snow depth were taken from a model ensemble of eleven global climate models (Suppl. Figure 1; Suppl. Table 2). Model runs were curated by the Climate Model Intercomparison Project , CMIP5 (Van Den Hurk et al., 2016). Annual change in snow depth over time for each month was taken from the ensemble average from 2000-2095, for each of four representative concentration pathways (RCPs). The RCP scenarios are based on four possible trajectories of greenhouse gas concentrations developed by the Intergovernmental Panel on Climate Change (Stocker, 2013). The 2.6 RCP projects about 1°C of warming by 2100, RCP 4.5 projects 1.8 °C, RCP 6.0 projects 2.2°C, and RCP 8.0 projects 3.7 °C of warming. The final predicted snow depth for each RCP scenario was

calculated by normalizing the current day albedo to the observed monthly historical averages adjusting the snow depth over time based on monthly predicted snow loss for each month and RCP (Table 3). Linear regressions were performed using the linear model function from R; this function was also used to report adjusted R squared values and significance of fit (R Development Core Team, 2017).

Ch.2 Table 2. Models included in the ensemble of global climate models, as provided by the Climate Model Intercomparison Project, CMIP5 (Van Den Hurk et al., 2016). The representative concentration pathways (RCP) scenarios available for each, as provided by the IPCC, are described alongside the model abbreviation.

Models	**RCP Available**
BCC	2.6, 4.5, 6.0, 8.5
NASAGISS-H	2.6, 4.5, 6.0, 8.5
NASAGISS-R	2.6, 4.5, 6.0, 8.5
NorESM	2.6, 4.5, 6.0, 8.5
BCC-1	4.5, 6.0, 8.5
CNRM-CM5	4.5, 8.5
CanESM2	2.6, 8.5
CMCC-CMS	4.5, 8.5
CMCC-CM	4.5, 8.5
NCARCCSM4	2.6, 4.5, 6.0, 8.5
CESMCAM	2.6, 4.5, 6.0, 8.5

Radiative Forcing and Carbon Dioxide Equivalents

The climate impact of changing albedo was expressed as radiative forcing$\left(W\,m^{-2}\right)$ and as the 100-year GWP $\left(kg\,CO_2\,eq\right)$. The radiative forcing of surface albedo at the top of the atmosphere ($RF^{TOA}_{\Delta a_s}; W\,m^{-2}$was calculated from the monthly average difference between baseline (maize cropland) and albedo for alternative land covers ($\Delta a_s; unitless$, monthly incoming shortwave radiation incident at the land surface ($R^{\downarrow}_{SWs}; W\,m^{-2}$), and the upward

atmospheric transmittance ($T_{SW}^{\uparrow}$; $W\,m^{-2}$) (Equation 1) (Bright, 2015; Bright et al., 2015):

$$RF_{\Delta a_s}^{TOA}(t)/W\,m^{-2} = \sum_{m=1}^{m=12} \Delta a_s(t,m) R_{SWs}^{\downarrow}(t,m) T_{SW}^{\uparrow} \left(\frac{1}{12}\right)\left(\frac{A_{local}}{A_{earth}}\right)$$

(2)

where A_{Earth} represents the total surface area of the Earth, and A_{Local} represents an arbitrary km^2 block, t represents the year, and m represents the month. Monthly $R_{SWs}^{\downarrow}$ for the latitude and longitude of the study was obtained from the NASA Langley Research Center (LaRC) POWER Project (NASA Earth Science's Applied Sciences Program, n.d.). $T_{SW}^{\uparrow}$ represents the two-way atmospheric transmittance factor, which is the fraction of shortwave radiation reflected from the ground that reaches the top of the atmosphere again. This parameter is typically assumed within the literature to be equal to 0.854 (unitless) across seasons and locations (Cherubini, Bright and Strømman, 2012; Bright and Kvaleväg, 2013; Lenton & Vaughan, 2009; Munoz, Campra and Fernandez-Alba, 2011). In this study, we also examined the results of calculations made using manually calculated $T_{SW}^{\uparrow}$ obtained by calculating the monthly ratio between solar radiation at the surface $R_{SWs}^{\downarrow}$ and solar radiation at the top of the atmosphere $R_{SWtoa}^{\downarrow}$. Calculations were made monthly and normalized for forcing per square kilometer land conversion. Radiative forcing of albedo at the top of the atmosphere was then used to calculate the GWP of the transition. An explicit treatment of the normalizing CO_2 forcing was used, as shown below:

$$GWP_{\Delta a_s}(100\ years)/kg\ of\ CO_2 - (m^2)^{-1} = \frac{\int_{t=0}^{t=100} RF_{\Delta a_s}^{TOA}(t)}{k_{CO_2} \int_{t=0}^{t=100} y_{CO_2}(t)}$$

(3)

where k_{CO_2} is the radiative efficiency (W m^{-2} kg^{-1}) of CO_2 equivalents in the atmosphere at 389 ppm, y_{CO_2} is the impulse-response function (Joos et al., 2013).

3. Results

Monthly Albedo by Land Cover Scenario without Snow Cover

We first considered the snow-free albedo of each land cover type (Figure 3). As expected, during the growing season, mixed deciduous-evergreen forest albedo was lower than baseline cropland (maize) albedo. Elephantgrass and switchgrass had the highest growing season albedos. During the growing season willow was slightly more reflective than the baseline crop, more similar to herbaceous biofuels than the temperate forest (May-September snow-free albedo: *Crop:* 0.187 ± 0.026; *Willow:* 0.198± 0.017; *Forest:* 0.134 ± 0.005; *Elephantgrass:* 0.227 ± 0.018; *Switchgrass:* 0.203 ± 0.016). During the dormant season in the absence of snow, the highest albedo was observed in the elephantgrass, switchgrass, and forest cases. Willow and maize albedo followed expected seasonal patterns (lower values in winter and higher values in summer), but albedo for mixed forest, elephantgrass, and switchgrass sites was higher than the same as summer values. (October-April, snow-free albedo: *Crop:* 0.174 ± 0.038; *Willow:* 0.170 ± 0.017; *Forest:* 0.166 ± 0.026; *Elephantgrass:* 0.217 ± 0.054; *Switchgrass:* 0.239 ± 0.026). Forest had remained the lowest snow-free albedo among land uses across dormant, growing season, and annual averages; switchgrass and elephantgrass remained the highest snow-free albedo across the same.

Relationships between Snow Depth and Albedo

For all five land-use types, albedo increased significantly with increasing snow depth (Figure 2). However, the slopes of these relationships varied significantly among cover types, with the steepest increase in the maize cropfield, followed by willow. Switchgrass and elephantgrass exhibited significantly lower slopes, and mixed forest the lowest. With 20 cm of

snow depth the maize cropland typically reflected about 80% of SW↓. By contrast, the forest reflected about 19% of incoming solar radiation with 20 cm of snow depth, only slightly higher than the snow-free average of 15%. These striking differences in responsiveness to snow depth resulted in greatly different winter albedos, with January albedo of crop and forest differing by almost 40%.

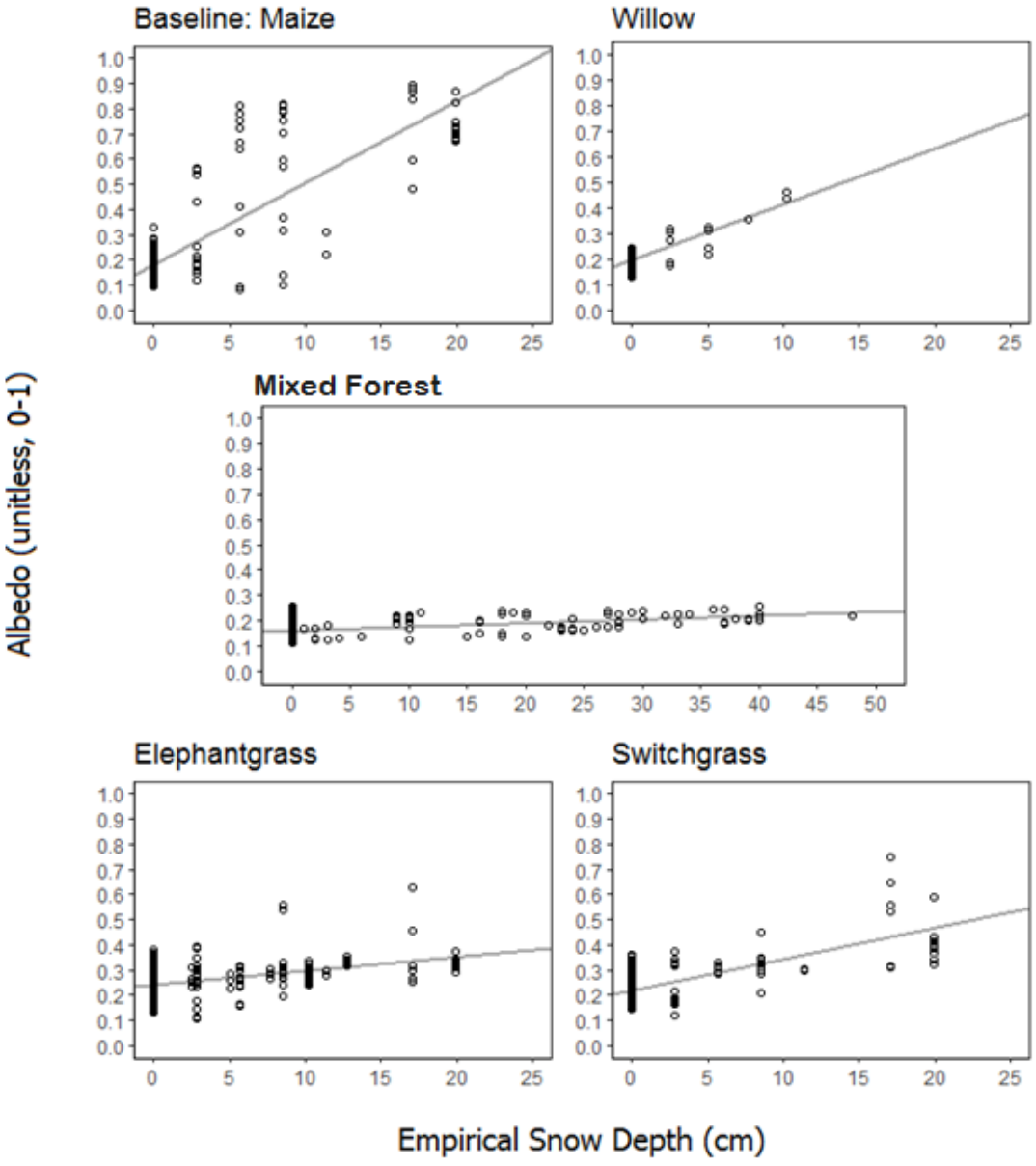

Ch.2 Figure 2. The relationship between snow depth (cm) and measured albedo for each

land cover type. Data are represented by open circles and are fitted to a linear regression (black line). Baseline Maize: $y=0.033x + 0.182$; $p<0.001$; adj R2: 0.672; n=800. Willow: $y=0.022x + 0.193$; $p<0.001$; adj R2: 0.609; n=800. Mixed Forest: $y=0.001x + 0.166$; $p<0.001$; adj R2: 0.163; n=222. Elephantgrass: $y=0.005x + 0.242$; $p<0.001$; adj R2: 0.155; n=887. Switchgrass: $y=0.013x + 0.216$; $p<0.001$; adj R2: 0.376; n=793.

Estimated Monthly Albedo by Land Cover Scenario, Inclusive of Snow Cover

Monthly albedo including snow cover was estimated for each land-use type by normalizing to typical Ithaca monthly snow depth (1970-2017). That is, the measured responsiveness of albedo for each land-use type to snow depth (Figure 3) was used to calculate the consequent increase in albedo. Including snow albedo, the baseline cropfield was much brighter than forest, and slightly brighter on an annual basis than any of the biofuels. This pattern was driven by the large response of crop albedo to snow; small increases in snow depth effectively obscured the ground and drastically increased wintertime albedo in this land-use type (Figure 3). Mixed deciduous-evergreen forest had the lowest year-round albedo (0.17 ± SD 0.01), driven both by the low snow-free albedo and especially by the weak response of albedo to variation in snow depth. The steep response of maize field albedo to snow-depth meant that annual crop albedo (0.28 ± SD 0.02) slightly exceeded willow (0.25 ± SD 0.01), elephantgrass (0.26 ± SD 0.01), and switchgrass (0.27 ± SD 0.01) albedo (anova: F-value: 180.8; $p<0.0001$, significant for all comparisons).

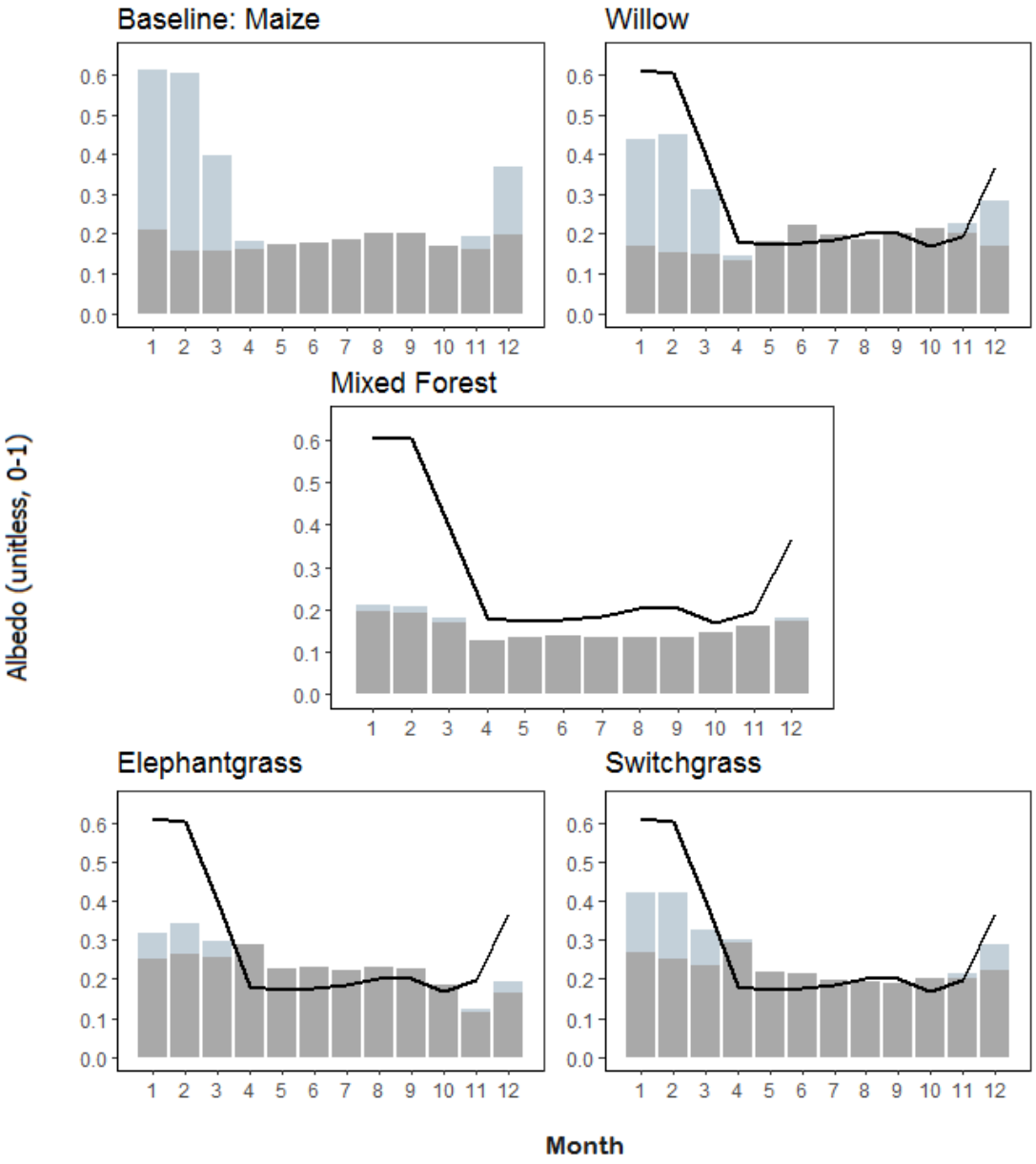

Ch.2 Figure 3. Monthly albedo for each of five land-use types based on measured snow-free albedo without snow (dark grey) and estimated snow albedo (light grey) where 1 represents January and 12 represents December. Albedo of the baseline cropland with snow (panel A) is superimposed (black line) on the four alternative land-use types.

Albedo-Driven Climate Impacts of Land-Use Change in Contemporary Snow Conditions.

In contemporary snowpack conditions, land-use conversion from cropland to mixed forest had the greatest albedo-driven warming potential **(**16.4 kg CO_2 m^{-2}). Converting cropland to willow had the next greatest warming potential **(**3.00 kg CO_2 m^{-2}), followed by elephantgrass **(**1.48 kg CO_2 m^{-2}) and switchgrass **(**0.49 kg CO_2 m^{-2}) (Figure 4). The main driver behind these positive forcings was the higher snow- driven albedo in cropland compared to alternative land covers. In the summer, maize cropland was slightly less reflective than any of the biofuel crops (Figure 3), causing a small summer cooling from converting maize crops to biofuels. Effects of land-use change on annual GWP did not always coincide with land-use change effects on annual mean albedo, because GWP calculations (Equation 1) weight differences in monthly albedo by the amount of incoming solar radiation. For example, elephantgrass was less reflective than willow on an annual basis, but the conversion from maize crop to elephantgrass had a lower annual climate warming than the conversion from crop to willow because elephantgrass was slightly brighter than willow in summer months when the greatest amount of solar radiation is received. When the conventional Ta of 0.854 is applied, much higher winter values are observed (Suppl. Fig. 4b)

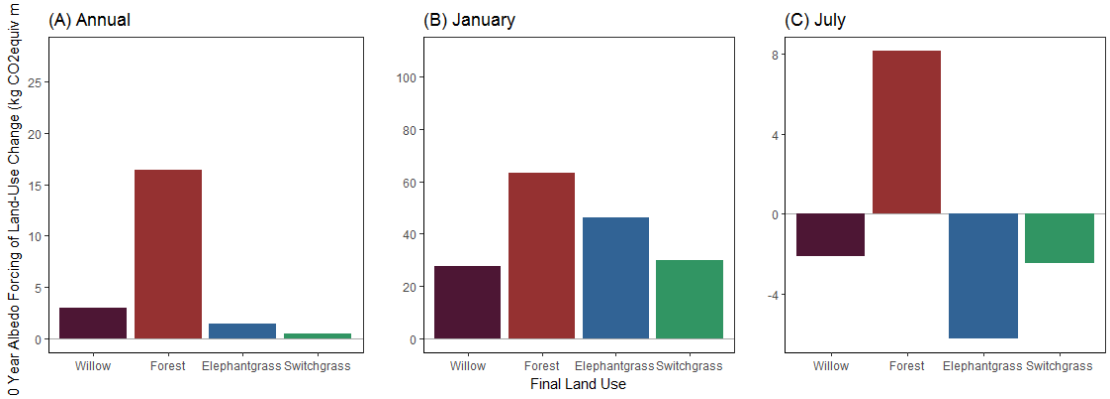

Ch.2 Figure 4. The 100-year climate impact of albedo in carbon dioxide equivalents per square meter of maize cropland converted to each of four potential alternative land-uses for Ithaca, NY; (A) annual mean; (B) in January; and (C) in July.

Predicted Model Ensemble and Empirical Trends in Snow Loss

Modeled snow loss trends were significant for every winter month except in the least severe pathway, RCP 2.6. CMIP5 climate model ensemble averages showed little change to snow depth between 2000 and 2100 for the region containing Ithaca, NY under the RCP 2.6 scenario; only one month showed a significant trend (Suppl. Table 2). Under the RCP 4.5, 6.0, and 8.5 scenarios, all non-summer months showed significant and progressively greater decreases in snow depth. Under RCP 6.0, the greatest losses occurred during peak snowfall months with smaller losses recorded for the end of the dormant season. The RCP 8.5 scenario resulted in a projected annual snow loss of only 4 cm over the next century, with the fastest loss, 12 cm per century, in February and March; this would result in near total loss of snow cover during these months. Rates of snow-loss between 9 and 2 cm per century were reported for the remaining dormant season months.

Analysis of empirical snow depth data in Ithaca, NY from 1970-2000 showed an average rate of snow loss that fell between RCP 4.5 and 6.0 scenarios; however, the empirical data showed substantial month to month variation. While the annual mean empirical snow loss averaged only 2.5 cm per century, a much faster rate of snow loss was noted at 18 cm per century (Adj. R^2=0.040, p<0.001). Records for 1970-2000 also indicate a small, non-significant increase in snow depth in March (Adj. R^2=0.001, p=0.108), Empirical snow loss trends were significant for January, February, April, and December, the months with the greatest average snowfall; however, the trends over time were weak, again indicating high year to year variability (Jan: Adj R^2=0.040, p<0.001; Feb: Adj R^2=0.006, p=0.004; Apr: Adj R^2=0.003, p=0.023; Dec: Adj R^2=0.015, p<0.001).

Effect of Snow Loss on Albedo and Climate Forcing

As snow is lost under future warming conditions, the albedo of all five land uses is projected to decrease in accordance with the importance of current snow-driven albedo and the

responsiveness of albedo for each land-use to changes in snow depth (Figure 3; Figure 5). Between 2000 and 2100, estimated albedo for the baseline crop and the willow biofuel decreased the most, while albedo of the mixed forest decreased very little.

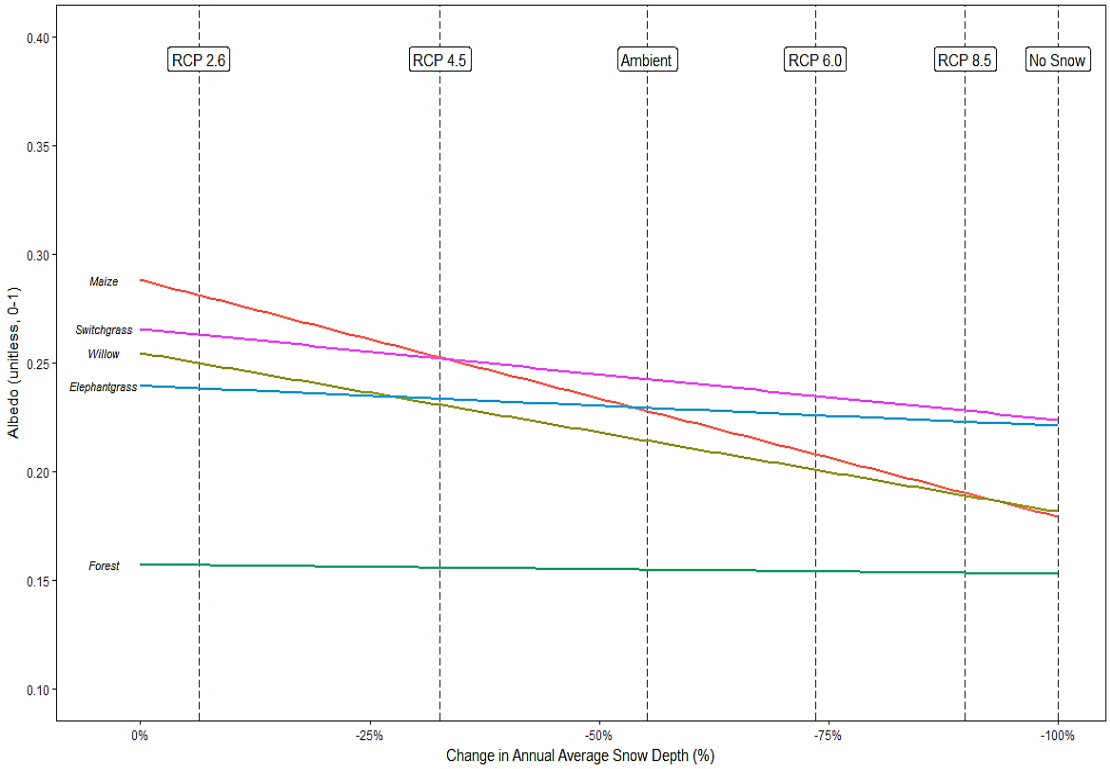

Ch.2 Figure 5. Projected decreases in albedo for five land uses resulting from reduction in snow depth for the reference site in Ithaca, NY; snow loss ranges from 0 to 100% under five climate scenarios. Solid lines show the annual mean albedo of each land cover type as it changes with diminishing snow depth. Vertical, dotted lines provide a reference to indicate the amount of snow cover loss anticipated by 2100 under each RCP scenario (2.6, 4.5, 6.0, 8.5), by extrapolating empirical trends, and under the extreme, no-snow scenario. Snow loss at 0% is based on contemporary snowfall in Ithaca, NY.

We next considered the carbon-equivalent climate forcing from albedo changes after 100 years of warming (Figure 6). Estimating albedo changes from extrapolated empirical

trends in snow depth over the next century, switchgrass and elephantgrass both shifted from a warming to a cooling impact (-2.22, -2.18 kg CO_2 m^{-2}) as did willow (1.55 kg CO_2 m^{-2}). Conversion to forest remained warming, but the impact was greatly reduced (12.22 kg CO_2 m^{-2}) showed the least percent difference in global warming impact from loss of snow between 2000 and 2100.

More extreme snow loss could result in some land-conversion scenarios actually cooling the climate. Under the most severe warming scenario (RCP 8.5), conversion from the baseline maize crop to willow resulted in a cooling impact by 2100. In contrast, conversion of cropland to elephantgrass resulted in a cooling impact under all but the mildest warming scenario (RCP 2.5); converting cropland to switchgrass resulted in a cooling impact under all scenarios by 2100. Although conversion to forest or willow never became a cooling impact, loss of snow did lessen the warming impact of both these conversions.

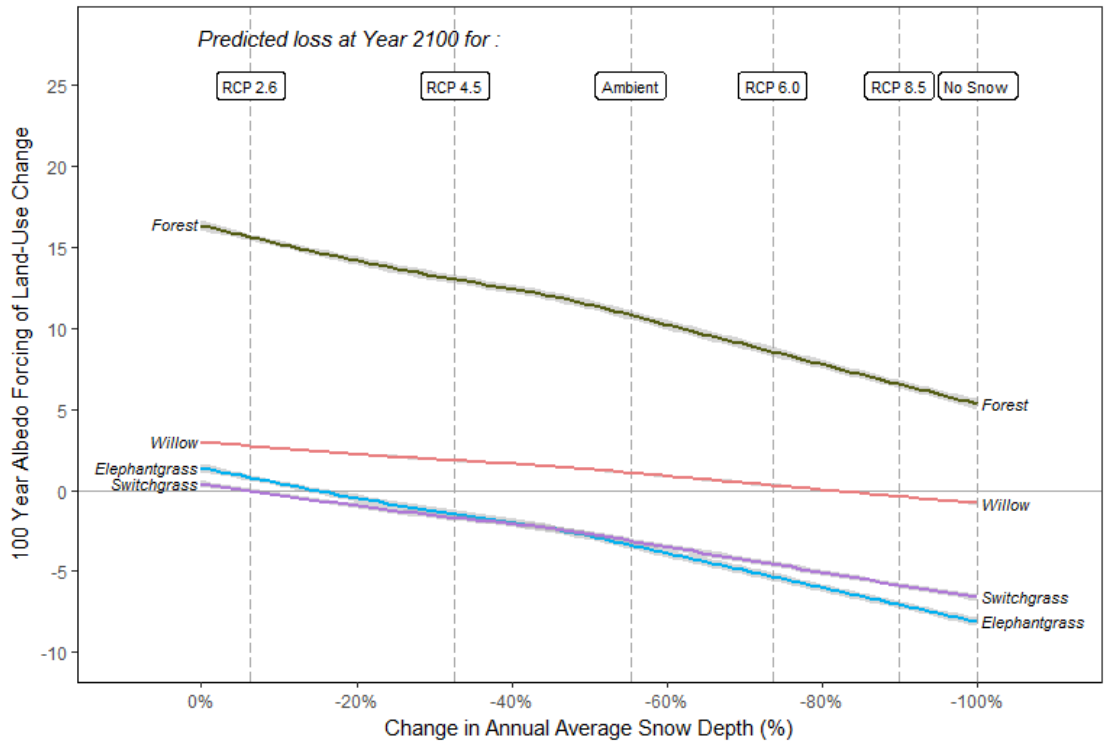

Ch.2 Figure 6. Projected future change in global warming impact of five land-use conversions in relation to changes in snow depth between 0% and 100% loss. Solid lines show the climate forcing of each land cover type as it changes with diminishing snow cover. Vertical, dotted lines reflect the amount of snow cover loss anticipated after 100 years of warming under each climate warming projection. Projections are based on four model ensemble RCP scenarios, an empirical warming scenario, and the extreme, no snow scenario.

4. Discussion

To better understand the potential climate forcing associated with biofuel production and other land-use conversions in northeastern North America, we summarized observations of albedo from five land-use types: baseline maize, mixed temperate forest, two herbaceous biofuels, and short-rotation willow. The last has not previously been reported in the literature; our seasonal albedo measurements will be the first to address this important land-cover type.

Our research also posed the question of how changing future snow depth would affect albedo and consequent climate impacts. Understanding how albedo of different land cover types varies within and across plant types as well as during the season is essential for predicting the consequences of land use change on global climate.

Albedo across Seasons: The Climate Impact of Four Land-use Conversion Scenarios

Phenological and structural differences across vegetation types lead to distinctly different seasonal albedo patterns across land uses. The dense, structurally complex canopy of forests leads to low growing-season albedo, while cropland has brighter, less structurally complex vegetation (Hollinger et al., 2010; Miller et al., 2016). Canopy differences across evergreen conifer and deciduous broadleaf forest types can also influence albedo, with conifer forests typically being 5% less reflective. The low reflectivity of growing season forests compared to the relatively high reflectivity of croplands is well known in the literature and was substantiated here. While willow had the second largest warming impact from albedo, it was much closer to the herbaceous biofuels and crop baseline, than to the forest stands in growing season climate forcing. The density of willow growth and brightness of the leaves itself may result in less light penetration into the canopy than in the herbaceous biofuels or cropland, as has been shown for complex forest canopies (Otto *et al*., 2014). However, willow leaves individually appeared to be more highly reflective than typical broadleaf leaves, and the upright, minimally branched structure of the growing willow stems resulted in an overall highly reflective land cover type.

These differences in albedo due to vegetative growth form and leaf traits can lead to substantial climate effects. A study comparing simulated albedo at different latitudes showed a similar climate forcing for conversion of cropland in the eastern US to temperate coniferous evergreen forest (26 kg CO_2 m^{-2}) (Betts, 2000), similar to the change of 16.4 kg CO_2 m^2 we estimated for conversion to mixed deciduous-evergreen forest (Figure 3). Conversely,

deforestation and conversion to elephantgrass in Wisconsin resulted in an albedo emissions equivalent of -24.5 kg CO_2 m^{-2} over 100 years (Bright, 2015; Jørgensen et al., 2014) in comparison to this study's -14.9 kg CO_2 m^{-2} (forest to crop: -16.4 kg CO_2 m^{-2}, crop to elephantgrass: 1.48 kg CO_2 m^{-2}). Conversion from mixed pasture and cropland to switchgrass generated 4.2 kg CO_2 m^{-2}, where our study found a negligible emissions equivalent of 0.49 kg CO_2 m^{-2} (Cai et al., 2016). Conversion from mixed pasture and cropland to elephantgrass generated 5.4 kg CO_2 m^{-2}, where our study generated 1.48 kg CO_2 m^{-2} (Cai et al., 2016). These differences may indicate the importance of the reference baseline; in this study we used cropland as a baseline, rather than field. Although field data co-associated with snowfall was not available, snow-free values obtained in the literature suggested that an old field site in North Carolina could be higher by 0.02-0.07 in the winter, and as much as 0.01 in the summer time (Juang *et al*., 2007).

During the dormant season, the loss of leaf cover and the structure of remnant, unharvested material has the largest impact on albedo. Seasonal loss (or retention) of forest canopy is a major driver of albedo differences. In conifer forests the dense vegetation obscures snow covered ground and can lead to low year-round albedo; in deciduous broadleaf forests the ground is revealed by fall leaf fall. However, the standing boles and branches of the dormant trees still absorb a substantial amount of energy, such that even deciduous forests have low dormant season albedo. In contrast, crops such as herbaceous biofuels and maize are harvested by winter and only remnant stubble obscures highly reflective snow covering these fields. Again, willow represented an intermediate case. While standing biomass in the willow fields continued to partially obscure the ground following leaf fall, the unbranching upright posture and narrowness of dormant season albedo allowed significant winter sunlight to penetrate through the upright willow stems compared to the deciduous forest (Figure 7). This was demonstrated by the high responsiveness of willow to snowfall, showing that snow was

visible through the standing stems. This high responsiveness also suggested that dark woody stems and basal stool of the willow were being concealed by increasing depth of high-albedo snow cover, similar to effects observed in arctic shrublands (Liston and Hiemstra, 2011; Sturm et al., 2005).

We found that studies that focused only on growing season differences had very different results from our full-year albedo response. A study of the conversion of maize crops to switchgrass in the midwestern USA was expected to have an emissions equivalent of 6.9 kg CO_2 m^{-2}, while our full-year study anticipated less than a kg of CO_2 m^{-2} (Bright, 2015; Georgescu et al., 2011). One possible reason for this is that the study by Georgescu *et al* assumed winter albedo to be constant across land-use types and thus calculated no wintertime radiative forcing. However, our study found that the largest differences in albedo occur over the winter when snow is on the ground, as the different land uses respond differently to snow depth. Previous studies have shown the sensitivity of albedo and climate forcing to snow cover using geographic or altitudinal variation in snow fall. Global satellite imagery of forests and cropland have shown greater wintertime than summertime differences in albedo, likely driven primarily by snow depth and cover (Cai et al., 2016; Zhao and Jackson, 2014). Similarly, Schwaab et al. (2015) made use of a montane landscape to show that high albedo radiative forcing corresponded to areas of high snow cover.

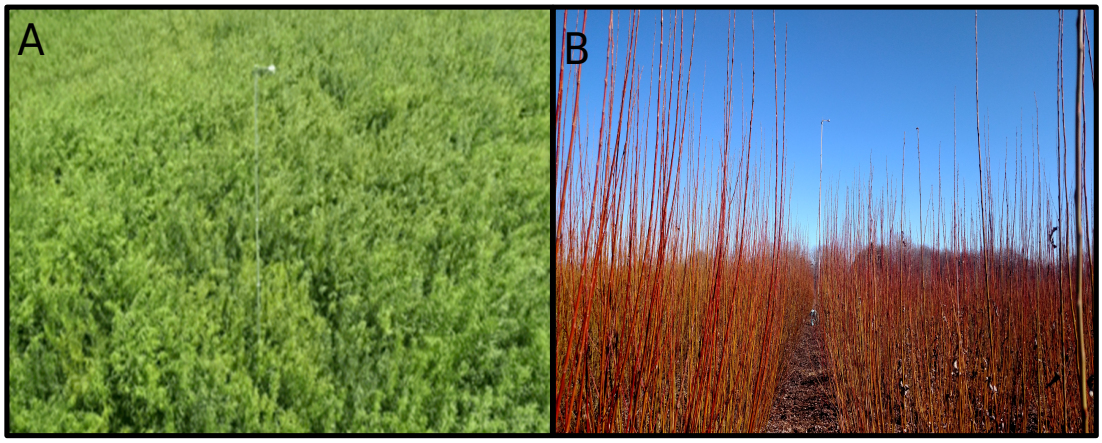

Ch.2 Figure 7. Our study sites in Geneva, NY depicting a one-year old short-rotation coppiced willow field both during the growing season (A) and during the dormant season prior to snowfall (B).

Understanding albedo differences across the entire growing and dormant season is essential to accurately assessing the overall climate impact. Using an annual albedo average, rather than the monthly average, has been shown to decrease the measured climate impact by 62% (Bright, 2015). Not all months are equal in evaluating albedo. When calculating climate forcing, the growing season is weighted more heavily, due to the higher influx of $SW^{\downarrow}_{max}$ during these months. However, the dormant season, as demonstrated in this study, may reveal the largest overall differences in albedo across land-use types, driven by the different response rates of land-use albedo to increasing snow depth. Any change to wintertime snow depth will in turn change the magnitude of dormant season albedo differences. For this reason, this study also examined the long-term impacts of warning and snow loss on the albedo impact of land-use change.

Winter snowfall: dormant season albedo as a major driver of climate forcing from land-use change

Snow cover has been frequently identified as the most important driver of surface albedo after land use (Schwaab et al., 2015; Zhao and Jackson, 2014). Here, we were able to use ground albedo measurements to isolate the interactive effects of snow depth and land use (Figure 3). A significant wintertime increase in albedo with increasing snow depth was observed for all land-use types. We propose a combination of drivers as controls for this general relationship. First, as described above, increasing snow depth covers progressively more of the uneven terrain and biomass on the ground surface. Second, a decline in snow depth might be associated with aging of the snowpack. As snow ages it accrues debris

(decreasing albedo) and freezes and refreezes (increasing grain size and reducing albedo) (Adolph et al., 2017; Flanner and Zender, 2006). Finally, at low snow depth, patchy snow cover becomes more common leading to lower average albedo due to exposure of the darker ground surface (Pielke and Avissar, 1990).

A key consideration for the evaluation of these results is the ability to separate datapoints with and without snowfall. Without snow on the ground, albedo was expected to be lower in the winter because of darker bare ground, and higher in the summer when foliage reflected more of the incoming short-wave radiation. This pattern was clear in the willow and maize datasets but did not emerge for forest, elephantgrass, and switchgrass sites. This suggested that days with snow cover may have been misreported as snow-free, driving winter snow-free albedo unrealistically high. It is possible that locally sited snow depth measurements did not account for the snow-trapping effects of standing vegetation such as that found in the forest; however, willow would then have been expected to show similar impacts. Alternatively, snow depth datasets at these three sites may not have accounted for the impact of trace snow on the soil surface which could also drive up winter albedo.

Over the next century, northeastern U.S. sites similar to Ithaca, New York could lose as much as 90% of snow cover under the RCP 8.5 scenario. Empirical measurements from Ithaca suggest that a simple linear extrapolation of its historical rate of reduction in snow would project 55% loss by 2100, even as RCP projections predict much faster warming rates. Projections of empirical change in snow cover yielded reductions in albedo of 1% (forest) to 21% (maize). For comparison, total loss of snow would cause an increase in albedo of 2 to 38% (forest and maize). While the incremental impact of snow loss on albedo is significant, especially for crops and biofuels, this suggests that by 2100 snow loss could be great enough that its effects on albedo would have begun to plateau, as some months cease to experience frequent snowfalls. Loss of snow has the capacity to fundamentally alter both the magnitude

and direction of the albedo impact on climate and should be taken into account when developing long-term strategies for climate mitigation.

Interpretation for Policy and Climate Mitigation Strategies

The albedo driven offset to carbon sequestration from these studies and as reported in this paper is comparable to the potential climate forcing from greenhouse gases. The conversion of a hectare of cropland to mixed forest might be expected to sequester 500-600 Mg CO_2 ha^{-1} over 100 years (Curtis et al., 2002; Gahagan et al., 2015) (Chapter 3); thus the albedo forcing of ~280 Mg CO_2 ha^{-1} would offset 47-56% of the carbon forcing. A study comparing unforested and coniferous evergreen forest in Switzerland found a range of albedo offset between 11 and 109%, with the range driven largely by snow cover. The offset was found to only exceed 50% if the snow cover lasted over 120 days $year^{-1}$. At the Ithaca, NY location in this study, the days with snow cover over the 1970-1999 period averaged 75 days $year^{-1}$. Satellite studies based in the temperate United States suggested an offset on the lower end of that range, between 12 and 40%. However, these were based on coarse definitions of what constituted the temperate US, and relied on satellite interpretation of grid cell contents (Betts, 2000; Thompson et al., 2009).

If policies are developed to incentivize land management for climate change mitigation, quantitative projections of albedo forcings will be needed. Local and regional climate mitigation projects, such as the Regional Greenhouse Gas Initiative (Raciti et al., 2012) provide motivation for such afforestation and bioenergy projects. Radiative forcings from albedo are region-specific due to their sensitivity to site and snow cover conditions (Bright et al., 2011; Cherubini et al., 2012). Here, we seek to assist land managers in the northeast who seek to incorporate albedo into their climate mitigation strategy by providing the first regional albedo estimates of land use change for biofuels, and the first ever estimates for short-rotation willow. Further, our projections of the albedo~snow cover relationship may

allow managers to determine how these estimates would differ for their local climate and conditions. Finally, a tool to determine the long-term impacts of snow loss will help when deciding on long-term strategies that may become locked in by conservation restrictions or land use agreements even as snow disappears.

5. Conclusion

Albedo exerts a climate forcing that can substantially offset carbon sequestration and have vital importance for planned climate mitigation projects making use of biological carbon sequestration and bioenergy. This study addressed four potential land conversion scenarios, including the previously untested case of conversion to short-rotation willow. Previous research had only speculated on whether coppiced willow albedo would more closely resemble forest or crop albedo (Bright et al., 2012; Levy et al., 2018). We found that willow was similar to herbaceous biofuels in magnitude of albedo and climate impact, but with a seasonal pattern that more closely remembered forest. Willow response to snowfall was closer to herbaceous biofuels than to forest. Dormant season albedo has been shown to have an outsized impact on annual averages, and thus climate forcing from land use change. Few attempts have been made previously to examine feedbacks between snow loss and climate forcing from albedo. We found that loss of snow could dramatically change both the magnitude and relative impact of the four land-conversion scenarios. Snow loss even changed the sign of this forcing, as conversion to willow, switchgrass, and elephantgrass were all found to result in climate cooling when snow was completely removed; both herbaceous biofuels were cooling under RCP pathway predicted snow loss.

Both contemporary and projected climate forcings were substantial in comparison with carbon balance effects of land-use changes. Albedo driven offsets to anticipated carbon sequestration/emission avoidance from reforestation and biofuel use will be substantial and should be considered in decisions or large-scale land-use policies. Further, that these offsets

may diminish or even reverse over the next century will affect albedo is incorporated into state and regional climate goals.

References

Adolph, A.C., Albert, M.R., Lazarcik, J., Dibb, J.E., Amante, J.M., Price, A., 2017. Dominance of grain size impacts on seasonal snow albedo at open sites in New Hampshire. Journal of Geophysical Research 122, 121–139. doi:10.1002/2016JD025362

Angel, J., 2018. Climate Observations for Champaign-Urbana, IL [WWW Document]. State Climatologist Office for Illinois.

Bala, G., Caldeira, K., Wickett, M., Phillips, T.J., Lobell, D.B., Delire, C., Mirin, A., 2007. Combined climate and carbon-cycle effects of large-scale deforestation. Proceedings of the National Academy of Sciences 104, 6550–6555. doi:10.1073/pnas.0608998104

Betts, A.K., Ball, J.H., 1997. Albedo over the boreal forest. Journal of Geophysical Research 102, 901–909.

Betts, R., 2007. Implications of land ecosystem-atmosphere interactions for strategies for climate change adaptation and mitigation. Tellus, Series B: Chemical and Physical Meteorology 59, 602–615. doi:10.1111/j.1600-0889.2007.00284.x

Betts, R., 2000. Offset of the potential carbon sink from boreal forestation by decreases in surface albedo. Letters to Nature 408, 187–190. doi:10.1038/35041545

Betts, R., Falloon, P.D., Goldewijk, K.K., Ramankutty, N., 2007. Biogeophysical effects of land use on climate: Model simulations of radiative forcing and large-scale temperature change. Agricultural and Forest Meteorology 142, 216–233. doi:10.1016/j.agrformet.2006.08.021

Bonan, G.B., 2008. Forests and climate change: forcings, feedbacks, and the climate benefits of forests. Science 320, 1444–1449. doi:10.1126/science.1155121

Bonan, G.B., Pollard, D., Thompson, S.L., 1992. Effects of Boreal Forest Vegetation on Global Climate. Nature 359, 716–718. doi:Doi 10.1038/359716a0

Bright, R.M., 2015. Metrics for biogeophysical climate forcings from land use and land cover changes and their inclusion in life cycle assessment: A critical review. Environmental Science and Technology 49, 3291–3303. doi:10.1021/es505465t

Bright, R.M., Antón-Fernández, C., Astrup, R., Cherubini, F., Kvalevåg, M., Strømman, A.H., 2014. Climate change implications of shifting forest management strategy in a boreal forest ecosystem of Norway. Global Change Biology 20, 607–621. doi:10.1111/gcb.12451

Bright, R.M., Cherubini, F., Strømman, A.H., 2012. Climate impacts of bioenergy: Inclusion of carbon cycle and albedo dynamics in life cycle impact assessment. Environmental Impact Assessment Review 37, 2–11. doi:10.1016/j.eiar.2012.01.002

Bright, R.M., Kvaleväg, M.M., 2013. Technical Note: Evaluating a simple parameterization of radiative shortwave forcing from surface albedo change. Atmospheric Chemistry and Physics 13, 11169–11174. doi:10.5194/acp-13-11169-2013

Bright, R.M., Strømman, A.H., Peters, G.P., 2011. Radiative forcing impacts of boreal forest biofuels: A scenario study for Norway in light of albedo. Environmental Science and Technology 45, 7570–7580. doi:10.1021/es201746b

Bright, R.M., Zhao, K., Jackson, R.B., Cherubini, F., 2015. Quantifying surface albedo and other direct biogeophysical climate forcings of forestry activities. Global Change Biology 21, 3246–3266. doi:10.1111/gcb.12951

Burakowski, E., Tawfik, A., Ouimette, A., Lepine, L., Novick, K., Ollinger, S., Zarzycki, C., Bonan, G.B., 2018. The role of surface roughness, albedo, and Bowen ratio on ecosystem energy balance in the Eastern United States. Agricultural and Forest Meteorology 249, 367–376. doi:10.1016/j.agrformet.2017.11.030

Cai, H., Wang, J., Feng, Y., Wang, M., Qin, Z., Dunn, J.B., 2016. Consideration of land use change-induced surface albedo effects in life-cycle analysis of biofuels. Energy Environ. Sci. 9, 2855–2867. doi:10.1039/C6EE01728B

Chapin, F.S., Randerson, J.T., McGuire, A.D., Foley, J.A., Field, C.B., 2008. Changing feedbacks in the climate-biosphere system. Frontiers in Ecology and the Environment 6, 313–320. doi:10.1890/080005

Cherubini, F., Bright, R.M., Strømman, A.H., 2012. Site-specific global warming potentials of biogenic carbon dioxide for bioenergy: contributions from carbon fluxes and albedo dynamics. Environmental Research Letters 7, 1–11. doi:10.1088/1748-9326/7/4/045902

Cramer, V.A., Hobbs, R.J., Standish, R.J., 2008. What's new about old fields? Land abandonment and ecosystem assembly. Trends in Ecology and Evolution 23, 104–112. doi:10.1016/j.tree.2007.10.005

Curtis, P., Hanson, P.J., Bolstad, P., Barford, C., Randolph, J.C., Schmidt, H.P., Wilson, K.B., 2002. Biometric and eddy covariance based estimates of annual carbon storage in five eastern North American deciduous forests. Agricultural and Forest Meteorology 113, 3–19.

Fabio, E.S., Volk, T.A., Miller, R.O., Michelle, J., Gauch, H.G., Rees, K.E.N.C.J.V.A.N., Hangs, R.D., Beyhan, Y., 2016. Genotype 3 environment interaction analysis of North American shrub willow yield trials confirms superior performance of triploid hybrids. GCB Bioenergy 1–15. doi:10.1111/gcbb.12344

Flanner, M.G., Zender, C.S., 2006. Linking snowpack microphysics and albedo evolution. Journal of Geophysical Research 111, 2156–2202. doi:10.1029/2005JD006834

Gahagan, A., Giardina, C.P., King, J.S., Binkley, D., Pregitzer, K.S., Burton, A.J., 2015. Carbon fluxes, storage and harvest removals through 60years of stand development in red pine plantations and mixed hardwood stands in Northern Michigan, USA. Forest

Ecology and Management 337, 88–97. doi:10.1016/j.foreco.2014.10.037

Georgescu, M., Lobell, D.B., Field, C.B., 2011. Direct climate effects of perennial bioenergy crops in the United States. Proceedings of the National Academy of Sciences 108, 4307–4312. doi:10.1073/pnas.1008779108

Hedstrom, N., Pomeroy, J., 1998. Accumulation of intercepted snow in the boreal forest: measurements and modelling. Hydrological Processes 12, 1611–1625.

Heller, M.C., Keoleian, G.A., Volk, T.A., 2003. Life cycle assessment of a willow bioenergy cropping system. Biomass and Bioenergy 25, 147–165. doi:10.1016/S0961-9534(02)00190-3

Hellstrom, R., 2015. Snowpack in Hemlock, Hardwood, and Open Sites at Harvard Forest 2008-2014 [WWW Document]. Harvard Forest Data Archive.

Hobbs, R.J., 2007. Old Fields: Dynamics and Restoration of Abandoned Farmland. Society for Ecological Restoration International.

Hollinger, D.Y., Ollinger, S. V., Richardson, A.D., Meyers, T.P., Dail, D.B., Martin, M.E., Scott, N.A., Arkebauerk, T.J., Baldocchi, D.D., Clark, K.L., Curtis, P.S., Davis, K.J., Desai, A.R., Dragoni, D., Goulden, M.L., Gu, L., Katul, G.G., Pallardy, S.G., Pawu, K.T., Schmid, H.P., Stoy, P.C., Suyker, A.E., Verma, S.B., 2010. Albedo estimates for land surface models and support for a new paradigm based on foliage nitrogen concentration. Global Change Biology 16, 696–710. doi:10.1111/j.1365-2486.2009.02028.x

Intergovernmental Panel on Climate Change, 2014. Climate Change 2014: Impacts, Adaptation and Vulnerability - Contributions of the Working Group II to the Fifth Assessment Report. pp. 1–32. doi:10.1016/j.renene.2009.11.012

Jackson, R.B., Randerson, J.T., Canadell, J.G., Anderson, R.G., Avissar, R., Baldocchi, D.D., Bonan, G.B., Caldeira, K., Diffenbaugh, N.S., Field, C.B., Hungate, B. a, Jobbágy, E.G.,

Kueppers, L.M., Nosetto, M.D., Pataki, D.E., 2008. Protecting climate with forests. Environmental Research Letters 3, 1–5. doi:10.1088/1748-9326/3/4/044006

Jin, Y., Schaaf, C.B., Gao, F., Li, X., Strahler, A.H., Zeng, X., Dickinson, R.E., 2002. How does snow impact the albedo of vegetated land surfaces as analyzed with MODIS data? Geophysical Research Letters 29, 12-1-12–4. doi:10.1029/2001GL014132

Joos, F., Roth, R., Fuglestvedt, J.S., Peters, G.P., Enting, I.G., Von Bloh, W., Brovkin, V., Burke, E.J., Eby, M., Edwards, N.R., Friedrich, T., Frölicher, T.L., Halloran, P.R., Holden, P.B., Jones, C., Kleinen, T., Mackenzie, F.T., Matsumoto, K., Meinshausen, M., Plattner, G.K., Reisinger, A., Segschneider, J., Shaffer, G., Steinacher, M., Strassmann, K., Tanaka, K., Timmermann, A., Weaver, A.J., 2013. Carbon dioxide and climate impulse response functions for the computation of greenhouse gas metrics: A multi-model analysis. Atmospheric Chemistry and Physics 13, 2793–2825. doi:10.5194/acp-13-2793-2013

Jørgensen, S. V., Cherubini, F., Michelsen, O., 2014. Biogenic CO2 fluxes, changes in surface albedo and biodiversity impacts from establishment of a miscanthus plantation. Journal of Environmental Management 146, 346–354. doi:10.1016/j.jenvman.2014.06.033

Juang, J., Katul, G., Siqueira, M., Stoy, P., Novick, K. 2007. Separating the effects of albedo from eco-physiological changes on surface temperature along a successional chronosequence in the southeastern United States. Geophysical Research Letters. 34.

Kaye, J.P., Quemada, M., 2017. Using cover crops to mitigate and adapt to climate change. A review. Agronomy for Sustainable Development 37. doi:10.1007/s13593-016-0410-x

Keoleian, G.A., Volk, T. A., 2005. Renewable energy from willow biomass crops: Life cycle energy, environmental and economic performance. Critical Reviews in Plant Sciences 24, 385–406. doi:10.1080/07352680500316334

Kirschbaum, M.U.F., Whitehead, D., Dean, S.M., Beets, P.N., Shepherd, J.D., Ausseil, A.-

G.E., 2011. Implications of albedo changes following afforestation on the benefits of forests as carbon sinks. Biogeosciences 8, 3687–3696. doi:10.5194/bg-8-3687-2011

Levy, C., Burakowski, E., Richardson, A., 2018. Novel Measurements of Fine-Scale Albedo: Using a Commercial Quadcopter to Measure Radiation Fluxes. Remote Sensing 10, 1303. doi:10.3390/rs10081303

Li, Y., Zhao, M., Motesharrei, S., Mu, Q., Kalnay, E., Li, S., 2015. Local cooling and warming effects of forests based on satellite observations. Nature Communications 6, 1–8. doi:10.1038/ncomms7603

Liston, G.E., Hiemstra, C.A., 2011. Representing grass- and shrub-snow-atmosphere interactions in climate system models. Journal of Climate 24, 2061–2079. doi:10.1175/2010JCLI4028.1

Lutz, D.A., Burakowski, E.A., Murphy, M.B., Borsuk, M.E., Niemiec, R.M., Howarth, R.B., 2016. Tradeoffs between three forest ecosystem services across the state of New Hampshire, USA: timber, carbon, and albedo. Ecological Applications 26, 146–161.

Marland, G., Pielke, R. a., Apps, M., Avissar, R., Betts, R. a., Davis, K.J., Frumhoff, P.C., Jackson, S.T., Joyce, L. a., Kauppi, P., Katzenberger, J., MacDicken, K.G., Neilson, R.P., Niles, J.O., Niyogi, D.D.S., Norby, R.J., Pena, N., Sampson, N., Xue, Y., 2003. The climatic impacts of land surface change and carbon management, and the implications for climate-change mitigation policy. Climate Policy 3, 149–157. doi:10.1016/S1469-3062(03)00028-7

Miller, J.N., VanLoocke, A., Gomez-Casanovas, N., Bernacchi, C.J., 2016. Candidate perennial bioenergy grasses have a higher albedo than annual row crops. GCB Bioenergy 8, 818–825. doi:10.1111/gcbb.12291

NASA Earth Science's Applied Sciences Program, n.d. All Sky Surface Shortwave Downward Flux [WWW Document]. Prediction of Worldwide Energy Resources Project

Data Sets. URL https://power.larc.nasa.gov/data-access-viewer/%0A (accessed 5.1.18).

National Climactic Data Center, Administration;, National Oceanic and Atmosperic Administration, 2019. New York Snow Depth Data [WWW Document]. Daily US Snowfall and Snow Depth.

National Oceanic Atmospheric Administration, National Operational Hydrologic Remote Sensing Center, n.d. Snow Depth at Station PNAI2 [WWW Document]. Interactive Snow Information.

NOAA Northeast Regional Climate Center at Cornell University, 2017. Daily Snow Depth Data Set.

Pielke, R.A.I., Avissar, R., 1990. Influence of landscape structure on local and regional climate 4, 133–155.

Qu, X., Hall, A., 2014. On the persistent spread in snow-albedo feedback. Climate Dynamics 42, 69–81. doi:10.1007/s00382-013-1774-0

R Development Core Team, 2017. R: A language and environment for statistical computing.

Raciti, S.M., Fahey, T.J., Thomas, R.Q., Woodbury, P.B., Driscoll, C.T., Carranti, F.J., Foster, D.R., Gwyther, P.S., Hall, B.R., Hamburg, S.P., Jenkins, J.C., Neill, C., Peery, B.W., Quigley, E.E., Sherman, R., Vadeboncoeur, M.A., Weinstein, D.A., Wilson, G., 2012. Local-Scale Carbon Budgets and Mitigation Opportunities for the Northeastern United States. BioScience 62, 23–38. doi:10.1525/bio.2012.62.1.7

Randerson, J.T., Liu, H., Flanner, M.G., Chambers, S.D., Jin, Y., Hess, P.G., Pfister, G., Mack, M.C., Treseder, K.K., Welp, L.R., Chapin, F.S., Harden, J.W., Goulden, M.L., Lyons, E., Neff, J.C., Schuur, E. a G., Zender, C.S., 2006. The impact of boreal forest fire on climate warming. Science 314, 1130–1132. doi:10.1126/science.1132075

Reinmann, A.B., Hutyra, L.R., Trlica, A., Olofsson, P., 2016. Assessing the global warming potential of human settlement expansion in a mesic temperate landscape from 2005 to

2050. Science of the Total Environment 545–546, 512–524. doi:10.1016/j.scitotenv.2015.12.033

Richards, B.K., Stoof, C.R., Cary, I.J., Woodbury, P.B., 2014. Reporting on Marginal Lands for Bioenergy Feedstock Production: A Modest Proposal. Bioenergy Research 7, 1060–1062. doi:10.1007/s12155-014-9408-x

Richardson, A.D., 2015. Radiometric and Meteorological Data from Harvard Forest Barn Tower Since 2011 [WWW Document]. Harvard Forest Data Archive. URL http://harvardforest.fas.harvard.edu:8080/exist/apps/datasets/showData.html?id=hf249 (accessed 10.25.16).

Schaeffer, M., Eickhout, B., Hoogwijk, M., Strengers, B., van Vuuren, D., Leemans, R., Opsteegh, T., 2007. The albedo climate impacts of biomass and carbon plantations compared with the carbon dioxide impact, in: Human-Induced Climate Change: An Interdisciplinary Assessment. pp. 72–83. doi:10.1017/CBO9780511619472.008

Schwaab, J., Bavay, M., Davin, E., Hagedorn, F., Hüsler, F., Lehning, M., Schneebeli, M., Thürig, E., Bebi, P., 2015. Carbon storage versus albedo change: Radiative forcing of forest expansion in temperate mountainous regions of Switzerland. Biogeosciences 12, 467–487. doi:10.5194/bg-12-467-2015

Shortall, O.K., 2013. “Marginal land” for energy crops: Exploring definitions and embedded assumptions. Energy Policy 62, 19–27. doi:10.1016/j.enpol.2013.07.048

Stocker, T.F., 2013. IPCC AR5 WG1 Climate Change 2013: The Physical Science Basis. Working Group 1 (WG1) Contribution to the Intergovernmental Panel on Climate Change (IPCC) 5th Assessment Report (AR5).

Stoof, C.R., Richards, B.K., Woodbury, P.B., Fabio, E.S., Brumbach, A.R., Cherney, J., Das, S., Geohring, L., Hansen, J., Hornesky, J., Mayton, H., Mason, C., Ruestow, G., Smart, L.B., Volk, T.A., Steenhuis, T.S., 2015. Untapped Potential: Opportunities and

Challenges for Sustainable Bioenergy Production from Marginal Lands in the Northeast USA. Bioenergy Research 8, 482–501. doi:10.1007/s12155-014-9515-8

Sturm, M., Douglas, T., Racine, C., Liston, G.E., 2005. Changing snow and shrub conditions affect albedo with global implications. Journal of Geophysical Research 110, 1–13. doi:10.1029/2005JG000013

Sturm, M., McFadden, J.P., Liston, G.E., Stuart Chapin, F., Racine, C.H., Holmgren, J., 2001. Snow-shrub interactions in Arctic Tundra: A hypothesis with climatic implications. Journal of Climate 14, 336–344. doi:10.1175/1520-0442(2001)014<0336:SSIIAT>2.0.CO;2

Syktus, J.I., McAlpine, C.A., 2016. More than carbon sequestration: Biophysical climate benefits of restored savanna woodlands. Scientific Reports 6, 29194. doi:10.1038/srep29194

Thackeray, C.W., Fletcher, C.G., 2016. Snow albedo feedback: Current knowledge, importance, outstanding issues and future directions. Progress in Physical Geography 40, 392–408. doi:10.1177/0309133315620999

Thompson, M., Adams, D., Johnson, K.N., 2009. The Albedo Effect and Forest Carbon Offset Design. Journal of Forestry 107, 425–431.

USA National Phenology Network, 2019. 30 Year Average Temperature Accumulations - 50 Base Temperature.

Van Den Hurk, B., Kim, H., Krinner, G., Seneviratne, S.I., Derksen, C., Oki, T., Douville, H., Colin, J., Ducharne, A., Cheruy, F., Viovy, N., Puma, M.J., Wada, Y., Li, W., Jia, B., Alessandri, A., Lawrence, D.M., Weedon, G.P., Ellis, R., Hagemann, S., Mao, J., Flanner, M.G., Zampieri, M., Materia, S., Law, R.M., Sheffield, J., 2016. LS3MIP (v1.0) contribution to CMIP6: The Land Surface, Snow and Soil moisture Model Intercomparison Project - Aims, setup and expected outcome. Geoscientific Model

Development 9, 2809–2832. doi:10.5194/gmd-9-2809-2016

Your Weather Service, 2019. US Climate Data [WWW Document]. URL https://www.usclimatedata.com/climate/ (accessed 1.4.19).

Zhao, K., Jackson, R.B., 2014. Biophysical forcings of land-use changes from potential forestry activities in North America. Ecological Monographs 84, 329–353. doi:10.1890/12-1705.1

Supplementary Information

The examined model ensemble had unequal representation of each of the RCPs tested. Here we compared the slopes predicted from the full model and from a trimmed model where RCPs were represented evenly across each component model.

Suppl. Ch.2 Table 1. Measured, snow-free albedo for five land-use types with standard deviation and sample number.

Source	Month	Year	Mean	Standard Deviation	Total Days	Days with Snowfall
Forest	1	2012	0.178	0.037	18	0
Forest	1	2013	0.213	0.031	19	0
Forest	1	2014	0.191	0.033	19	14
Forest	2	2012	0.149	0.004	17	0
Forest	2	2013	0.195	0.034	14	4
Forest	2	2014	0.204	0.019	2	2
Forest	3	2012	0.145	0.032	18	0
Forest	3	2013	0.146	0.008	7	7
Forest	4	2012	0.131	0.001	9	0
Forest	4	2013	0.128	0.006	11	6
Forest	4	2014	0.13	0.013	11	5
Forest	12	2011	0.172	0.015	15	0
Forest	12	2012	0.179	0.041	10	0
Forest	12	2013	0.177	0.04	9	1
Elephantgrass	1	2011	0.282	0.072	40	30
Elephantgrass	2	2011	0.283	0.03	34	26
Elephantgrass	3	2011	0.246	0.03	26	0
Elephantgrass	3	2012	0.215	0.004	6	0
Elephantgrass	4	2011	0.297	0.044	22	0
Elephantgrass	5	2011	0.251	0.023	8	0
Elephantgrass	6	2011	0.244	0.009	6	0
Elephantgrass	6	2012	0.236	0.012	18	0
Elephantgrass	7	2011	0.212	0.028	6	0
Elephantgrass	7	2012	0.246	0	2	0
Elephantgrass	8	2011	0.264	0.003	6	0
Elephantgrass	9	2011	0.253	0.006	4	0
Elephantgrass	9	2012	0.238	0.006	4	0
Elephantgrass	10	2011	0.247	0.019	4	0

Elephantgrass	10	2012	0.229	0	2	0
Elephantgrass	11	2011	0.228	0	2	0
Elephantgrass	12	2011	0.232	0.02	22	0
Switchgrass	1	2011	0.334	0.033	18	14
Switchgrass	1	2012	0.25	0.016	15	3
Switchgrass	2	2011	0.357	0.123	10	6
Switchgrass	2	2012	0.239	0.013	13	0
Switchgrass	3	2011	0.265	0.013	12	0
Switchgrass	3	2012	0.215	0.016	20	0
Switchgrass	4	2011	0.293	0.035	17	0
Switchgrass	5	2011	0.227	0.018	19	0
Switchgrass	5	2012	0.213	0.006	26	0
Switchgrass	6	2011	0.212	0.019	18	0
Switchgrass	6	2012	0.215	0.008	24	0
Switchgrass	7	2011	0.203	0.026	26	0
Switchgrass	7	2012	0.196	0.011	26	0
Switchgrass	8	2011	0.203	0.014	29	0
Switchgrass	8	2012	0.185	0.008	27	0
Switchgrass	9	2011	0.196	0.013	19	0
Switchgrass	9	2012	0.18	0.018	15	0
Switchgrass	10	2011	0.208	0.01	22	0
Switchgrass	10	2012	0.187	0.012	11	0
Switchgrass	11	2011	0.202	0.008	13	0
Switchgrass	12	2011	0.226	0.026	12	0
Switchgrass	12	2012	0.177	0.025	3	3
Baseline: Maize	1	2011	0.52	0.243	18	14
Baseline: Maize	1	2012	0.2	0.046	15	3
Baseline: Maize	2	2011	0.328	0.315	10	6
Baseline: Maize	2	2012	0.164	0.018	13	0
Baseline: Maize	3	2011	0.152	0.021	12	0
Baseline: Maize	3	2012	0.16	0.024	23	0
Baseline: Maize	4	2011	0.161	0.026	17	0
Baseline: Maize	5	2011	0.178	0.019	19	0
Baseline: Maize	5	2012	0.166	0.033	26	0
Baseline: Maize	6	2011	0.174	0.032	18	0

Baseline: Maize	6	2012	0.176	0.014	24	0
Baseline: Maize	7	2011	0.197	0.028	26	0
Baseline: Maize	7	2012	0.171	0.012	26	0
Baseline: Maize	8	2011	0.224	0.016	29	0
Baseline: Maize	8	2012	0.178	0.009	27	0
Baseline: Maize	9	2011	0.215	0.028	19	0
Baseline: Maize	9	2012	0.192	0.024	20	0
Baseline: Maize	10	2011	0.178	0.014	22	0
Baseline: Maize	10	2012	0.148	0.017	11	0
Baseline: Maize	11	2011	0.161	0.017	13	0
Baseline: Maize	12	2011	0.185	0.017	12	0
Baseline: Maize	12	2012	0.172	0.057	3	3
Willow	1	2016	0.158	0.025	3	1
Willow	1	2018	0.246	0.083	5	2
Willow	2	2017	0.188	0.064	8	4
Willow	2	2018	0.271	0.053	4	3
Willow	3	2017	0.463	NA	1	1
Willow	3	2019	0.151	0.013	3	0
Willow	4	2017	0.133	0.007	2	0
Willow	4	2018	0.134	NA	1	0
Willow	5	2016	0.185	0.021	5	0
Willow	5	2017	0.201	0.008	6	0
Willow	5	2018	0.144	0.009	3	0
Willow	6	2016	0.203	0.006	7	0
Willow	6	2017	0.229	0.006	15	0
Willow	7	2017	0.197	0.003	5	0
Willow	8	2016	0.184	0.022	6	0
Willow	9	2016	0.182	NA	1	0
Willow	9	2017	0.222	0.008	2	0
Willow	10	2016	0.213	0.018	6	0
Willow	11	2016	0.226	0.074	10	1

Suppl. Ch.2 Figure 1. When only those models with representation in each RCP were considered, there was not a significant impact on the predicted monthly trend in snow depth over time (Paired t-test: t = 0.96378, df = 47, p-value = 0.3401). RCPs are indicated by color (2.6=yellow, 4.5, peach, 6.0=orange, 8.5=red) and the black line indicated the 1:1 line. Months with no snowfall are not depicted.

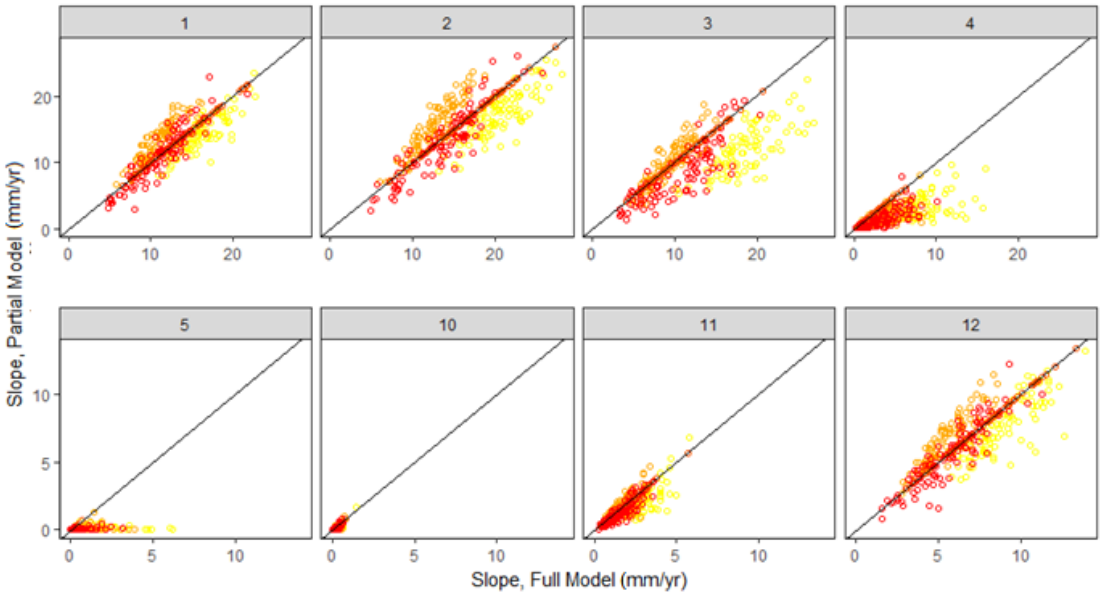

Suppl. Ch.2 Table 2. Slope and significance of the model ensemble predicted snow depth over time relationship, shown monthly for four RCP scenarios.

RCP	Month	Slope	R^2	P	RCP	Month	Slope	R^2	P
2.6	1	0	-0.009	NS	4.5	1	0	0.186	***
	2	0	-0.011	NS		2	0	0.132	***
	3	0	0.011	NS		3	0	0.114	***
	4	0	0.039	*		4	0	0.077	**
	5	0	-0.009	NS		5	0	0.027	NS
	6	0	-0.01	NS		6	0	0.018	NS
	7	0	0.001	NS		7	0	0.005	NS
	8	0	-0.009	NS		8	0	0.004	NS
	9	0	-0.008	NS		9	0	-0.007	NS
	10	0	-0.009	NS		10	0	0.118	***
	11	0	0.005	NS		11	0	0.082	**
	12	0	-0.009	NS		12	0	0.158	***
6	1	-0.001	0.279	***	8.5	1	-0.001	0.672	***
	2	-0.001	0.349	***		2	-0.001	0.647	***
	3	-0.001	0.377	***		3	-0.001	0.582	***
	4	0	0.299	***		4	-0.001	0.53	***
	5	0	0.123	***		5	0	0.314	***
	6	0	0.012	NS		6	0	0.043	*
	7	0	0.605	***		7	0	-0.006	NS
	8	0	-0.002	NS		8	0	0.036	*
	9	0	0.029	NS		9	0	0.1	**
	10	0	0.119	***		10	0	0.546	***
	11	0	0.314	***		11	0	0.571	***
	12	-0.001	0.406	***		12	-0.001	0.612	***

For this study, we required monthly albedo data paired with measurements of snow depth. These data were not available at directly overlapping study sites, hence this study used

disparate site location normalized to our primary study location. To validate this approach, we examined the overlap of albedo from the same land uses as measured between our maize field measurement (gray) and similar data from the far extreme of our target area (blue) (Figure 2). The comparison data used in Figure 2 was obtained from a maizefield located in Durham, NH (Burakowski et al., 2018). Days with snow cover were considered in this comparison.

Suppl. Ch.2 Figure 2. Overlap of measured albedo from maize fields located in 40 °N, 88 °W (gray) and maizefields located at 43°N 70°W (dark blue). We show that the measurements used in this study (gray).

We further examined the overlap between our forest measurements (gray) and limited forest data present at site (blue) (Figure 3). The comparison data from Figure 3 was obtained from drone flights over a deciduous forest located in Tully, NY; please see our previous paper for methodological details (Chapter 3) (Levy et al., 2018). Days with snow cover were not removed in this comparison.

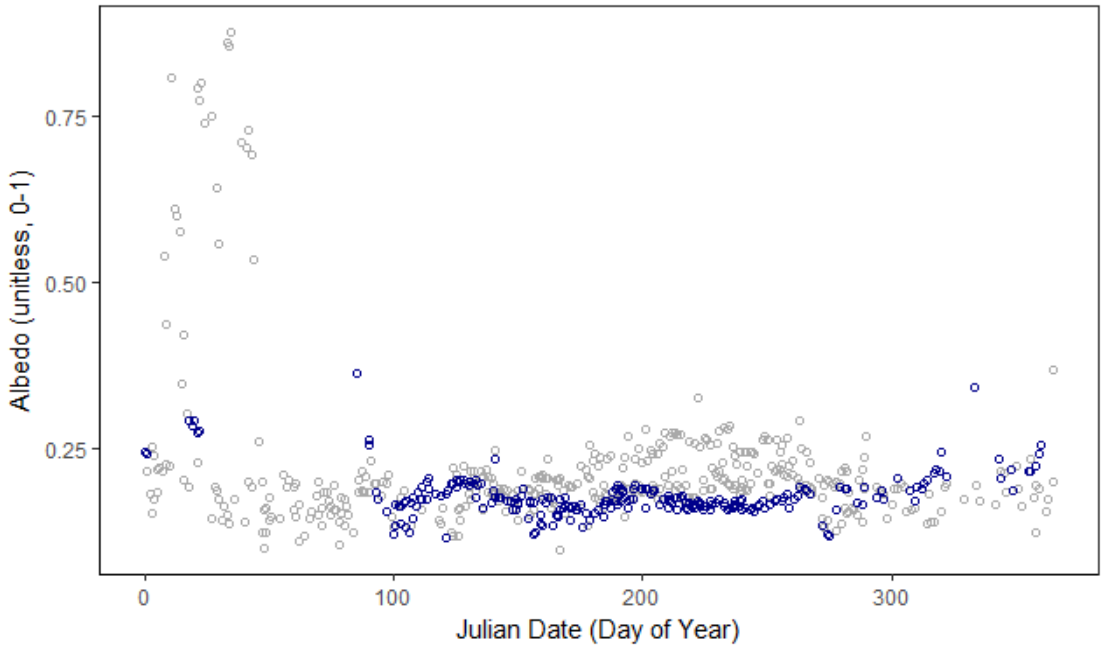

Suppl. Ch.2 Figure 3. Overlap of measured albedo from deciduous forest sites located in 43 °N, 76 °W and maizefields located at 42 °N, 72 °W.

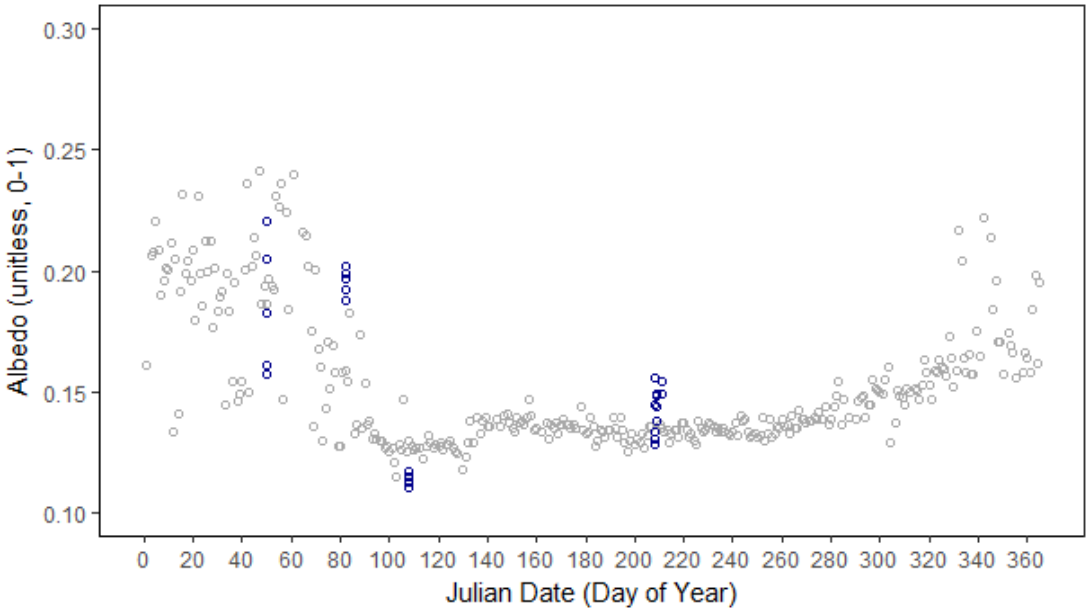

In each case, we found that measurements from different locations were generally in agreement with each other. However, the maizefield site in Illinois showed higher late summer albedo than the site located in New Hampshire. Forest comparison data was far more spotty, with early spring measurements showing a much lower albedo in Tully, NY than in Harvard, MA, potentially indicating a difference in forest structure. This discrepancy does not appear to be tied to leaf out date, as leaf out date at the Massachusetts sate appears to occur at day 130, or approximately May 10th.

Suppl. Ch.2 Table 3. Standard deviation of albedo (unitless) associated with predicted albedo due to uncertainty in the measured snow~albedo relationship and in the cumulative error from snow measurements, albedo measurements, and the snow~albedo relationship.

Site	Month	Snow ~ Albedo Relationship	Cumulative Error
Forest	1	0.097	0.225
Forest	2	0.102	0.251
Forest	3	0.103	0.139
Forest	4	0.045	0.011
Forest	5	0.009	0.007
Forest	6	0.000	0.005
Forest	7	0.000	0.005
Forest	8	0.000	0.004
Forest	9	0.000	0.005
Forest	10	0.020	0.007
Forest	11	0.050	0.030
Forest	12	0.076	0.099
Maize	1	0.097	0.442
Maize	2	0.102	0.480
Maize	3	0.103	0.259
Maize	4	0.045	0.033
Maize	5	0.009	0.028
Maize	6	0.000	0.023
Maize	7	0.000	0.025
Maize	8	0.000	0.027
Maize	9	0.000	0.028
Maize	10	0.020	0.020
Maize	11	0.050	0.040
Maize	12	0.076	0.193
Miscanthus	1	0.097	0.149
Miscanthus	2	0.102	0.155
Miscanthus	3	0.103	0.087
Miscanthus	4	0.045	0.031
Miscanthus	5	0.009	0.019
Miscanthus	6	0.000	0.012
Miscanthus	7	0.000	0.014
Miscanthus	8	0.000	0.019
Miscanthus	9	0.000	0.028
Miscanthus	10	0.020	0.059
Miscanthus	11	0.050	0.087

Miscanthus	12	0.076	0.109
Panicum	1	0.097	0.206
Panicum	2	0.102	0.228
Panicum	3	0.103	0.125
Panicum	4	0.045	0.037
Panicum	5	0.009	0.014
Panicum	6	0.000	0.014
Panicum	7	0.000	0.020
Panicum	8	0.000	0.015
Panicum	9	0.000	0.017
Panicum	10	0.020	0.014
Panicum	11	0.050	0.019
Panicum	12	0.076	0.092
Willow	1	0.097	0.432
Willow	2	0.102	0.482
Willow	3	0.103	0.259
Willow	4	0.045	0.021
Willow	5	0.009	0.026
Willow	6	0.000	0.014
Willow	7	0.000	0.003
Willow	8	0.000	0.022
Willow	9	0.000	0.023
Willow	10	0.020	0.018
Willow	11	0.050	0.039
Willow	12	0.076	NA

Suppl. Ch. 2 Figure 4. The literature convention for atmospheric transmissivity (T_{SW}) was used to calculate the 100-year climate impact of albedo in carbon dioxide equivalents per square meter of maize cropland converted to each of four potential alternative land-uses for Ithaca, NY; (A) annual mean; (B) in January; and (C) in July.

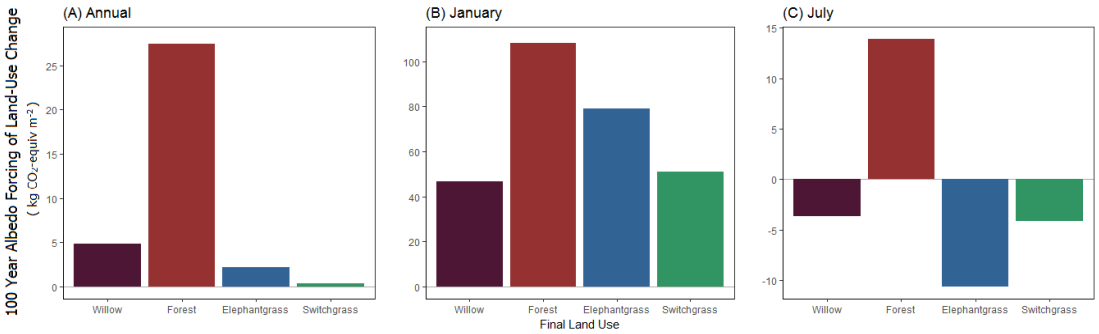

Suppl. Ch. 2 Figure 5. The literature convention for atmospheric transmissivity (T_{SW}) was used to calculate the projected future change in global warming impact of five land-use conversions in relation to changes in snow depth between 0% and 100% loss. Solid lines show the climate forcing of each land cover type as it changes with diminishing snow cover. Vertical, dotted lines reflect the amount of snow cover loss anticipated after 100 years of warming under each climate warming projection. Projections are based on four model ensemble RCP scenarios, an empirical warming scenario, and the extreme, no snow scenario.

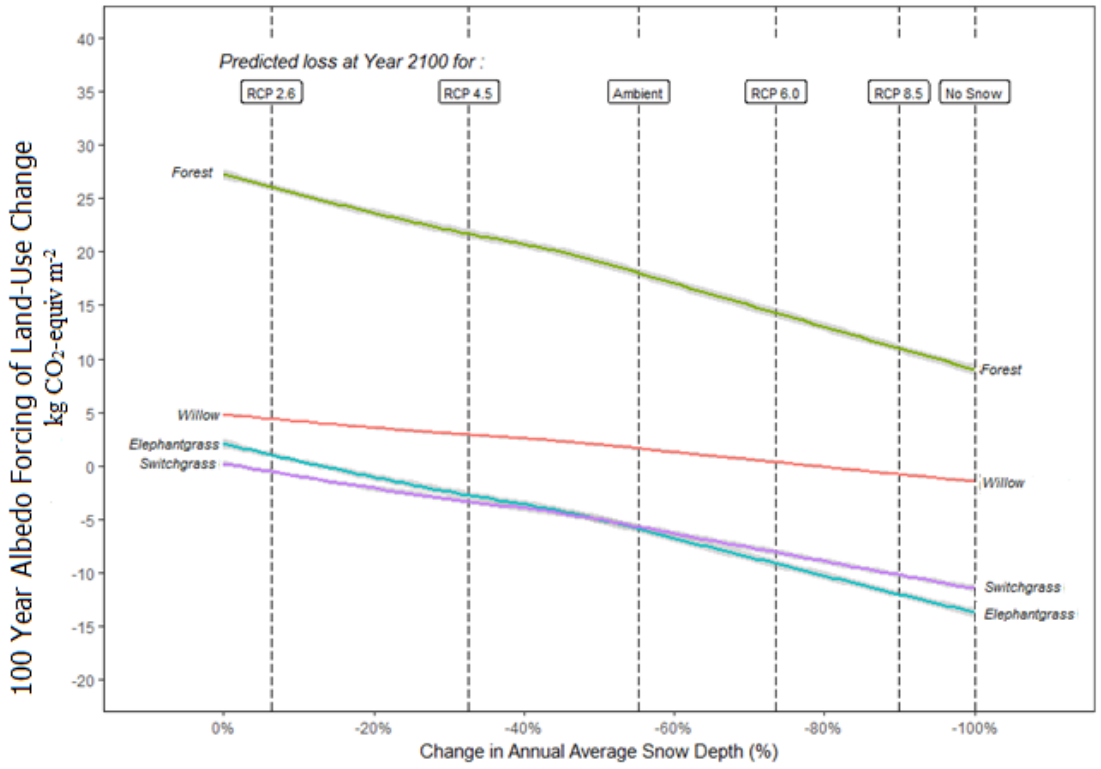

CHAPTER THREE: Net Impacts of Climate Mitigation through Afforestation and Willow Biofuels in Upstate New York

Abstract

In order to strategically implement climate mitigation projects, policy-makers need an accurate accounting of the climate impacts from both biogeochemical and biogeophysical climate forcings. The inclusion of land-use driven biogeophysical effects particularly albedo, and the incorporation of time-integrated carbon sequestration are often neglected in carbon accounting that considers both life-cycle analyses and averted emissions. We assessed the net impact of three forestry and two short-rotation coppiced willow scenarios. We found that willow bioenergy provided the greatest cooling impact (-447 to -796 Mg CO_2-equiv ha^{-1}), but that this effect was controlled substantially by the assumed default mix of power-generation options. Our scenario found afforestation of agricultural land had the potential to a result in a net cooling impact (-156 Mg CO_2-equiv ha^{-1}), but that forest harvest reduced or even reversed this effect depending on harvest intensity. Albedo offset 63 to 79% of greenhouse gas driven emissions in the forest scenarios, and 6 to 11% in the willow scenarios. Such complete accounting of climate forcing is essential for accurate calculations to inform policy, and to identify factors such as averted emissions and harvest frequency that can control the magnitude and direction of climate effects from land-use change.

1. Introduction

A preponderance of evidence for global climate change and its drastic consequences have led to a flurry of international, regional, and local commitments to limit global warming to 2°C or below (UNFCCC, 2015; Rogelj *et al.*, 2018). The most recent Integrated Assessment Models suggest that between 100-1000 Gt of CO_2 will need to be removed from the

atmosphere by 2100, with at least partial implementation within the next 15 years (Rogelj *et al.*, 2018). Within the United States, multi-state commitments such as the Regional Greenhouse Gas Initiative (RGGI) have set emissions caps and established credit markets (Raciti *et al.*, 2012; Regional Greenhouse Gas Initiative, 2018; Massachusetts Department of Environmental Protection, 2019). The nine signatory states are expected to cap carbon emissions at 65 million metric tons in 2020. States, counties, and cities have also set their own local goals. For example, New York State recently committed to a net-zero carbon state economy by 2050, an ambitious goal requiring an 85% reduction in overall emissions and a tripling of current renewable energy generation (New York State Assembly, 2019).

While the overarching goal of these commitments and initiatives is to limit planetary warming to 1.5-2 °C, specific objectives are generally framed in the context of carbon emissions: either their prevention or their retroactive removal from the atmosphere. Such a framework is practical in the context of coordinating and quantifying mitigation efforts, but it can also introduce intrinsic biases. lead to inefficient allocation of resources, or even consequences opposite the intended outcome. Carbon focused mitigation strategies may lead to problematic policy strategies by undervaluing the impact of short-lived greenhouse gases (Fuglestvedt *et al.*, 2000, 2003; Howarth, 2014), the outsized effect of extremes in temperature maximums and rates of change (Sygna, Fuglestvedt and Aaheim, 2002), and the global impact of biogeophysical climate forcings and feedbacks (Bonan, Pollard and Thompson, 1992; Hall, 2004; Naudts *et al.*, 2016). Climate impacts through non-gaseous, radiative mechanisms, as addressed by this study, were particularly neglected until the past decade and are still left out of many analyses (Marland *et al.*, 2003; Betts, 2007; Jackson *et al.*, 2008; Pielke *et al.*, 2011).

Overlooking the radiative impacts of land use change may lead decisionmakers to unintentionally overpredict the benefit of mitigation projects. At best, this may lead to

uneconomical policies and incentive structures; at worst, it could cause systematic underachievement of climate goals or even counteract them. Jones et al (2013) found that when albedo was included in the analysis, policies that incentivized biofuels or reduced global forest cover obtained an additional 0.5 °C global cooling solely from albedo effects (Jones *et al.*, 2013). In bioenergy studies, rotation lengths for growing woody biofuel crops that are optimized solely for carbon sequestration are inexpedient in the context of albedo change (Thompson, Adams and Sessions, 2009; Lutz and Howarth, 2014; Lutz *et al.*, 2016). Moreover, while the choice of crop (deciduous vs coniferous, annual vs perennial) or location (boreal, temperate, tropical) could have little to no climate impact through carbon fluxes, such a choice could have substantial effects through surface reflectivity (Betts, 2000; Jackson *et al.*, 2008; Thompson, Adams and Johnson, 2009; Georgescu, Lobell and Field, 2011).

Climate Mitigation through Land-Use Land-Cover Change

Land-use and land-cover change (LULC) has been identified as an essential tool for reaching the climate mitigation goals set by the international community. The Intergovernmental Panel on Climate Change has found that the majority of scenarios that limit warming to 1.5 °C will require net global emissions from the agricultural, forestry, and land use sector to sequester 2.5 Pg CO_2 per year, by 2050, and to support at least that rate of sequestration through 2100 (Rogelj et al., 2018). Limiting global warming to the goal of 1.5°C from 2010 levels with limited overshoot of greenhouse gas goals will likely require a LULC conversion of as much as six million km^2 of bioenergy crops and almost ten million km^2 of forest by 2050. The importance of LULC is magnified in scenarios that plan for an overshoot of carbon targets – biological carbon sequestration is the only currently viable method for widespread removal of atmospheric carbon dioxide. If such extensive land conversions must be contemplated, it is essential that each LULC project take into account the full climate impact of the land conversion, including the radiative effects of albedo change (as described in

Chapter 2) (Jackson *et al.*, 2008; Thompson, Adams and Sessions, 2009; Georgescu, Lobell and Field, 2011; Lutz and Howarth, 2014; Jones *et al.*, 2015; Kreidenweis *et al.*, 2016; Lutz *et al.*, 2016).

This study examines two potential climate mitigation options – planting of short-rotation willow biofuel crops, and reforestation – in the context of albedo and carbon mediated climate forcing. These two land use options have been considered as candidates for climate mitigation projects due to their high carbon sequestration rates and the potential for use on marginal land (marginally profitable for crop production, often due to rocky, wet, or low nutrient soils). There has been particular interest in the northeastern United States, where agricultural abandonment driven by terrain has left substantial land use more suitable for willow and forest growth than agriculture (Stoof et al., 2015). Willow has been developed and studied extensively both in New York and broader U.S. (Kopp *et al.*, 2001; Heller, Keoleian and Volk, 2003; Keoleian and Volk, 2005; PB *et al.*, 2010). Cultivar breeding and cultivation experiments have improved crop yields and production efficiencies over the past few decades (Volk *et al.*, 2006, 2011; Bacenetti, Pessina and Fiala, 2016). Studies of biofuel adoption in rural and suburban New York state suggest woody biofuels like willow could offset as much as 75,000 Mg of carbon dioxide per year without competing with agricultural or forest land (Raciti *et al.*, 2012). Afforestation/reforestation offers the potential both for carbon sequestration in biomass and, depending on the management scheme, for bioenergy generation as well. The northeastern US was mostly forested prior to European colonization, and many fields naturally revert to forest with little to no direct human interference (Flinn and Vellend, 2005; Cramer, Hobbs and Standish, 2008). Reforestation of all available marginal agricultural land in New York state could sequester an estimated 1-20 Tg CO2 each year, equivalent to 1-10% of state emissions (New York State Research and Development Authority, 2015).

However, the actual sequestration potential will depend on regional land and carbon prices as well as land availability (Raciti *et al.*, 2012). It should be pointed out that both of these land use conversion strategies are considered relatively high cost; in the U.S. estimates suggest that reforestation might cost $16-32 per metric ton of CO_2, including the cost of land purchases (Richards and Stokes, 2004) while selling biofuel from willow fields currently requires three to four (3 year) rotations to break even, in part because of high upfront production costs (Stoof et al., 2015). Nonetheless, these two land uses have some of the best potential for climate mitigation through LULC in the northeastern US.

Accounting for the Complete Climate Impact: GWP_{bio}, Life-Cycle Assessment, and Albedo

Bioenergy fuels are often referred to as "climate-neutral", when in fact these fuels can have substantial impacts on climate throughout the biofuel life cycle. In particular, greenhouse gas emissions are associated with planting, cultivation, and fertilization; harvest, transport, and processing; and combusting in a bioenergy facility. On the other hand, emissions can be averted by replacing fossil fuel energy. Finally, the radiative effect of albedo response to land cover change are not completely understood.

Carbon accounting for biofuels should consider the effects of temporary C sequestration by the crop. That is, during the years to decades between the plant uptake of CO_2 in biomass and its harvest and return to the atmosphere by combustion, the short-term sequestration of carbon exerts a cooling effect on climate. The global warming potential of bioenergy (GWP_{bio}) is a measure of the equivalency between one kg of CO_2 sequestered temporarily in biomass, and one kg of CO_2 sequestered more permanently (i.e. sequestration is maintained for the full time horizon being considered, generally 100 years). If there were no short-term storage (i.e. if biofuels were harvested immediately as they grow) GWP_{bio} would be 1, in the same way as for carbon emitted from conventional fossil fuels. Conversely, if carbon were sequestered for the entire time horizon, GWP_{bio} would be 0. More commonly, biofuels

are harvested at an intermediate point between 0 and 100 years of growth, and GWP_{bio} falls between 1 and 0. As a result, the shorter the rotation period and the slower the growth rate of a bioenergy feedstock, the less valid the common assumption of neutrality (Cherubini, Bright and Strømman, 2012; Holtsmark, 2015). A 2016 review of carbon accounting in forest bioenergy systems found that almost 90% of 101 studies examined made the assumption of neutrality (Røyne *et al.*, 2016). However, a site-specific study of bioenergy crop fields found a 100-year GWP_{bio} scaling factor of 0.82-0.28 for forest sites depending on rotation length and bioenergy production (Cherubini, Strømman and Hertwich, 2011; Bright, Cherubini and Strømman, 2012). Incorporating GWP_{bio} is essential for accurately accounting for the climate impact of bioenergy systems as ignoring this effect can result in inaccuracy in accounting the climate mitigation potential of bioenergy (Cherubini, Bright and Strømman, 2012; Liu *et al.*, 2017).

Life-cycle assessment (LCA) is a tool for accounting for the emissions and inefficiencies introduced either directly or indirectly by a production chain such as bioenergy. Numerous LCA have been conducted on willow, particularly in the context of field to farmgate (from field preparation and planting through harvest) energy costs and carbon emissions. These analyses have largely been conducted in upstate New York, Pennsylvania, and western Europe (Heller, Keoleian and Volk, 2003; Lettens *et al.*, 2003; Heller *et al.*, 2004; Keoleian and Volk, 2005; Goglio and Owende, 2009; Budsberg *et al.*, 2013; Cangiano, 2015). Assessments of the net climate impact of willow biofuels are sensitive to assumptions about crop productivity, drying method, transport distance, and the degree and method of fertilization (Heller, Keoleian and Volk, 2003; Caputo *et al.*, 2011). Emissions per oven dried ton are most sensitive to yield and drying method, while the field to farmgate net energy ratio was most sensitive to transportation distance and fertilization method (Goglio and Owende,

2009; Caputo *et al.*, 2011). In field to biofuel facility analyses, gasification was the largest factor in overall emissions and the net energy ratio; however, the limited number of studies explicitly dealing with this component of LCA does not enable a similar sensitivity analysis (Mann and Spath, 1997; Elsayed, Matthews and Mortimer, 2003; Lettens *et al.*, 2003). Although the need to account for albedo in willow LCA has been indicated in the literature (Cherubini, Bright and Strømman, 2012), the present study is the first to incorporate albedo in a complete assessment of climate impacts.

Numerous forest bioenergy LCA also have been conducted (Lippke et al., 2011; Johnson, Lippke and Oneil, 2013; Røyne et al., 2016) each taking into account various scenarios of forest management. Common management strategies range from clear-cutting to periodic thinning at the level of individual trees, use of mixed species and age forest or plantation monoculture, and a wide range of rotation lengths and frequencies. Emissions and energy use estimates range widely for each of these scenarios, as forestry operations employ different degrees of mechanization depending on the scale of the harvesr and local economics and practices. Nonetheless, international comparisons and meta-analyses of forest biofuels have shown the systematic approaches using LCA produce comparable assessments (Lippke *et al.*, 2011; Røyne *et al.*, 2016). In particular within similar management schemes, forest emissions seem to be most sensitive to drying and storage methods, dry matter losses during processing, and transport distance (Helin *et al.*, 2013; O'Connor, 2013; Röder, Whittaker and Thornley, 2014). Unfortunately, only a handful of forest biofuel LCA have quantitatively addressed the impact of changing albedo from LULC (Helin *et al.*, 2013; Røyne *et al.*, 2016).

Generating electricity from lignocellulosic biomass avoids emissions from electricity generation using fossil fuels (Lippke *et al.*, 2011). The total emissions averted is dependent on the overall energy production and the source of the electricity avoided. Energy generation

from lignocellulosic feedstocks can make use of baled, chipped, pelletized, and torrefied (heated to a coal-like end product) biomass (Forsberg, 2000; Elsayed, Matthews and Mortimer, 2003; Adams, Shirley and McManus, 2015). Electricity is generated from biomass via direct firing and gasification, independently or through cofiring with fossil fuels (Mann and Spath, 1997; Elsayed, Matthews and Mortimer, 2003; Lettens *et al.*, 2003; Heller *et al.*, 2004; Bergman *et al.*, 2005). Woody biofuels can also be utilized for heating and for cogeneration of heat and electric power.

As demonstrated in Chapter 2, a substantial impact on climate can be exerted by local albedo change on the global radiative balance. Carbon sequestration by reforestation in Switzerland was offset 11-109% by reduced local albedo (Schwaab *et al.*, 2015). Modeled carbon sequestration by afforestation in the temperate northern hemisphere was offset 17-35% by satellite-estimated changes in albedo (Betts, 2000). With few exceptions, these offset studies have compared only direct carbon sequestration by unmanaged forestland to carbon equivalents from albedo radiative forcing. Of studies addressing bioenergy, a model of shrub conversion to evergreen needleleaf forest found a 58-64% offset of biogenic carbon sequestration by decreased albedo, and a 48-55% offset by albedo of sequestration and fuel chain emissions (Bright, Cherubini and Strømman, 2012). A study modeling the replacement of annual bioenergy crops with perennial options provided the only complete life-cycle analysis that included albedo (Georgescu, Lobell and Field, 2011); this study used literature reports of sequestration, life cycle emissions, and averted emissions, and found the carbon-equivalent albedo impact was six times greater than the net fossil-fuels emissions.

In this study, we analyzed the climate mitigation potential for both forest and willow bioenergy incorporating four major climate forcings: short and long term biological carbon sequestration; process emissions from biofuel production, processing, and combustion;

averted emissions from fossil fuels not burned, and finally the albedo impact of changing land use. In previous work, we demonstrated that the climate forcing from albedo alone could potentially offset ~50% of biological carbon sequestration from an uncut century-old forest (*Chapter 2*). We predicted that the relative importance of climate forcing from changes in albedo for intensively managed forests and coppiced willow would be greater than for unmanaged forests because of lower C sequestration and high direct emissions. However, we also predicted that management for bioenergy would lead to significant avoided fossil fuel emissions, as electricity generated from biofuels replaced electricity generated by the standard New York fuel mix. We anticipated that incorporation of albedo within bioenergy systems could offset approximately 20-60% of the total climate impact calculated by standard life cycle analyses. This comprehensive look at the climate impact of five land management strategies will help inform goals and expectations for future climate mitigation projects in the northeastern United States and similar cold temperate regions.

2. Methods

Evaluation of Overall Climate Impact

We estimated the climate impact in the setting of New York State for each land use change strategy by calculating emissions from four components: 1. the impact of short and long-term carbon sequestration, 2. emissions generated by the complete production life cycle of biomass production, 3. emissions offset by generating energy through biofuels replacing the standard fuel mix emissions, and finally 4. the impact of land use change on albedo (Figure 1). For each land-use scenario we use a baseline of a maize agricultural field. We calculated emissions for a mixed hardwood forest based on three harvest scenarios, and for willow biofuel for two productivity scenarios (Table 1).

Ch. 3 Table 1. Description of land use scenarios examined in this study, describing the length of a harvest rotation and the proportion harvested at each cut.

Land Use	Management	Rotation Length (years)	Proportion Harvested (%)
Forest	No Harvest	NA	NA
	Low Intensity Harvest	80	40
	High Intensity Harvest	80	60
Willow	Low Productivity	3	100
	High Productivity	3	100

Short- and long-term carbon sequestration (detailed below, *Carbon sequestration in biomass pools*) incorporated both pools with long-term sequestration potential (e.g., soils, forest biomass) and pools with only short-term sequestration (harvested biomass, roots of harvested trees). The impact of pools with regular, periodic losses were estimated using GWP_{bio} (*Global Warning Potential of Biological Carbon Sequestration*) in order to account for the short-term impact of temporarily sequestered carbon on the climate. Other pools we treated using the standard 100-yr GWP of carbon dioxide, and their climate impact was quantified based on the amount of carbon sequestered at the time of calculation. We did not consider natural turnover within pools (e.g., annual tree growth and decay of leaf litter) due to the very short-term nature of the carbon storage and these fluxes were evaluated based only on the accumulated carbon at the time of calculation, as above.

As detailed below, we based the emissions generated over the life-cycle of biofuel production (*Energy Costs and Emissions over the Life Cycle of Lignocellulosic Biofuels*) on cases reported in the literature. The emissions of willow cultivation and use are particularly well-addressed regionally in upstate NY. Emissions for forest management strategies are based on life cycle analyses for site and harvest appropriate machinery and machine hours. Reported emissions factors reflect not only emissions from fuel use during production,

harvest, and transport, but also emissions from indirect sources such as machinery manufacture and off-site nursery emissions.

Offset emissions incorporated net energy ratios (energy produced:energy spent) reported from life cycle analyses for biofuel production, as above (*Energy Costs and Emissions over the Life Cycle of Lignocellulosic Biofuels*). Net energy ratios allowed us to determine the net amount of bioenergy converted into electric power. We then calculated the emissions per MJ of energy for an average fuel mix for NY State and for two low and high emissions scenarios (i.e. high renewables and increased natural gas). Averted emissions are defined as the carbon dioxide equivalents that would have been generated if energy from biofuels had been generated by any of these three alternative power scenarios.

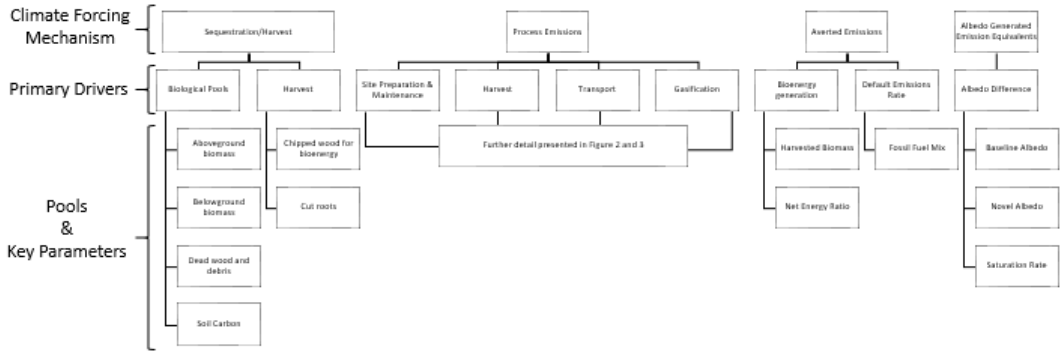

Ch. 3 Figure 1. Conceptual map of study structure, detailing the core mechanisms for climate forcing examined here, the primary drivers of these climate forcings, and the key parameters (i.e. net energy ratio, saturation rate) and subsidiary pools (i.e. aboveground biomass, soil carbon), used to calculate the climate impact. The carbon emissions from bioenergy production, harvest, and gasification are detailed further in Figures 2 and 3.

Carbon sequestration in biomass pools

We considered two scenarios for willow harvest rotation (Figure 2). In the first

scenario, willow fields were planted with the standard mix of willow cultivars currently available to farmers (Low Productivity) (Caputo *et al.*, 2011). In the second scenario, fields were planted with a new mix of willow cultivars, based on recent development of top-yielding clones (High Productivity). Willow was assumed to be replanted every twenty-three years, in accordance with typical stand longevity in the New York State region. Following each year-long planting, willow fields were given an additional year for plugs to set and harvested every three years thereafter. Estimates of annual productivity come from Tully, NY and Geneva, NY and are based on mass following harvest and drying. Belowground biomass was calculated based on a 1:1.75 ratio between roots and shoots (Heller *et al.*, 2004). A ratio of 1.5:1 for coarse and fine roots was estimated from values measured on fertilized short-rotation willow stands (Rytter, 2001; Heinsoo *et al.*, 2009). Roots were assumed to decompose rapidly following harvest (Pacaldo, Volk and Briggs, 2011), and decay parameters for damaged/cut roots were used (Li *et al.*, 2015; Zhang and Wang, 2015) as it was assumed that root decomposition would follow stump removal (Heller, Keoleian and Volk, 2003). Following the stool removal after 23 years, belowground biomass was also assumed to decay, resulting in no net accumulation. However, the short-term effects of biogenic carbon accumulation in root systems was calculated. No coarse woody debris stock was included because although harvests may leave some broken stems behind, this stock is believed to be negligible (Pacaldo, Volk and Briggs, 2011). Net soil carbon sequestration associated with willow biofuel crops is highly uncertain (Djomo, Kasmioui and Ceulemans, 2011), and has generally been reported as non-significant and treated as zero net storage (Grigal and Berguson, 1998; Ulzen-Appiah, 2002; Heller, Keoleian and Volk, 2003; Heller *et al.*, 2004; Caputo, Balogh, Volk, Johnson, Puettmann, Lippke and Oneil, 2014) due to large variability across sites, soil types, and management and to the small magnitude of measured fluxes. Net soil carbon sequestration by

biomass willow is highly uncertain (Djomo, Kasmioui and Ceulemans, 2011), and has generally been reported as non-significant and treated as zero net storage (Grigal and Berguson, 1998; Ulzen-Appiah, 2002; Heller, Keoleian and Volk, 2003; Heller *et al.*, 2004; Caputo, Balogh, Volk, Johnson, Puettmann, Lippke and Oneil, 2014) and we adopt this assumption.

We considered carbon sequestration and bioenergy potential of maple/oak/hickory forest (Figure 3). Three typical management scenarios were considered for forest harvest rotation. In the first, forests were left unharvested following reforestation of an agricultural field (No Harvest). In the second, low-graded forest were selectively harvested, removing the lowest quality trees, resulting in long-term improvement of the stand value at eighty years. In this scenario, 60% of standing live aboveground biomass is removed for bioenergy (High Intensity). In the third case, high graded forest was selectively harvested at eighty years for 40% of living tree aboveground biomass (Low Intensity). We assumed human-assisted reforestation (fencing and planting of original sites) but no fertilizer, herbicides, or other methods were used. We based these assumptions on the natural regenerative trend of northeastern forests; for example, we assumed fencing and planting was necessary due to high herbivory pressures from white-tailed deer in the region (Brown *et al* 2000). No thinning of forest stock was included prior to these selective harvests because of the high costs of such management.

We calculated the total tree biomass using the Carbon Online Estimator (COLE) model of the USDA Forest Service, based on Forest Inventory and Analysis (FIA) data for New York and Pennsylvania (Van Deusen and Heath, 2010). Live tree biomass age class was used to determine the annual growth increment in response to standing stock. We determined the total aboveground and belowground biomass from a regionally appropriate root to shoot ratio (1.0:4.4) (Jackson *et al.*, 1996) (Table 2). We based the fine and coarse root biomass on

ratios seen in an eastern US deciduous hardwood forest (1.0:3.3) (Cairns *et al.*, 1997). We assumed that roots decomposed following harvest in proportion to the aboveground biomass that had been cut. We based decay rate parameters on an exponential decay rate constant for decomposing cut deciduous tree roots in the northeastern US (Li *et al.*, 2015; Zhang and Wang, 2015). We explicitly calculated exponential decay for seven years following harvest, at which point the remaining mass of root detritus was assumed to be negligible. We calculated coarse woody debris and standing dead wood accumulation from COLE and FIA data on standing stocks by age class. We assumed that harvest had no effect on dead wood through either impacts on existing stocks or through addition of slash material. We estimated net soil carbon sequestration by calculating soil carbon accumulation over time from COLE and FIA data on soil stock by age class, and reduced this value by a standard percent difference between forest and agricultural carbon storage (Guo and Gifford, 2002).

Ch. 3 Table 2. Parameters describing growth and harvest of forest and willow biofuels. The use of these parameters is explained in the context of land use growth rate equations.

	Willow (low, high)	**Forest (none, low, high)**	**Units**
Rotation Length	23	80	*years*
Harvests per Rotation	7	1	*Harvests*
Growth Rate			
First harvest	6,10	$0.631 + (0.089\ t) + (-0.001\ t^2) + (0.000\ t^3)$	*ODT* $ha^{-1}\ yr^{-1}$
Subsequent harvests	8.16, 13.6		*ODT* $ha^{-1}\ yr^{-1}$
AGB:BGB	1.75:1.0	4.4:1.0	
Coarse:Fine Roots	1.5:1.0	3.3:1.0	
Root decomposition coefficient (k)	-0.75	-0.75	yr^{-1}
Carbon Content of ODT	50	50	*%*
Mass loss from drying	50	50	*%*

**ODT = Oven dry tonnes of biomass*

Global Warning Potential of Biological Carbon Sequestration

We calculated the global warming potential of biogenic carbon in two parts. First, for a given biofuel carbon emission, we modeled the fraction of the carbon remaining in the atmosphere as the convolution of an impulse response function describing the atmospheric decay of a unit of carbon dioxide due to oceanic and terrestrial uptake (γ_{CO_2}) as shown by Equation 1,

$$\gamma_{CO_2}(t) = A_0 + \sum_{i=1}^{3} A_i e^{-t/\beta_i}$$

(Eq 1)

where: the airborne fraction of CO_2 in the atmosphere is described by the following amplitudes A_0=0.217, A_1=0.259, A_2=0.338, A_3=0.186, and relaxation time scales β_1=172.9, β_2=18.51, β_3=1.186 (Joos *et al.*, 2001, 2013; Forster *et al.*, 2007).

Following harvest at t=τ, the decay function continues to act on the remaining fraction of biomass, less the impact of biological carbon sequestration up until the point of harvest as described by the second half of Equation 2,

$$f_{biological\,Carbon\,dioxide}(t) = \begin{cases} \gamma_{CO_2}(t) - \int_0^t g(tsh)\,\gamma_{CO_2}(t - tsh)\,dtsh \;\forall\, t \le \tau \\ \gamma_{CO_2}(t) - \int_0^\tau g(tsh)\,\gamma_{CO_2}(\tau - tsh)\,dtsh \;\forall\, t > \tau \end{cases}$$

(Eq 2)

where: g(t) represents the growth rate of biomass, normalized to the emissions of a standard harvest cycle. Here, t represents the time increment, tsh represents the time since last harvest, and τ represents t at the time of last harvest. To determine the GWPbio, we multiplied the fraction of carbon in the atmosphere by the radiative efficiency of carbon dioxide to obtain the radiative forcing (RF_{CO2}) and integrated over the time horizon being considered. In this study, we used a 100-year time horizon for our comparisons. To obtain the GWPbio representing the effective units of carbon dioxide per units of harvested carbon dioxide, we divided the time-

integrated radiative forcing by the baseline radiative forcing of typical fossil fuels, integrated over the same time horizon. This is shown by Equation 3,

$$GWP_{bio}(TH) = \frac{\int_0^{TH} \Delta RF_{bio}(t)\,dt}{\int_0^{TH} \Delta RF_{CO_2}(t)\,dt} = \frac{\int_0^{TH} \Re_{CO_2} f_{bio}(t)\,dt}{\int_0^{TH} \Re_{CO_2} y_{CO_2}(t)\,dt}$$

(Eq 3)

where: RE_{CO2} is the radiative efficiency of carbon dioxide, RF represents the radiative forcing, and TH represents the time horizon being considered. This and the preceding equations were developed in previous studies of the GWP of bioenergy (Cherubini, Bright and Strømman, 2012; Guest *et al.*, 2013; Bright *et al.*, 2015).

Energy Costs and Emissions over the Life Cycle of Lignocellulosic Biofuels

Life-cycle analysis of willow bioenergy was based on the energy requirement and carbon emissions of site preparation and management, harvest, transport, and gasification (Table 3; Table 4). We used life-cycle analyses developed in upstate New York to frame our assumptions. Site preparation and management accounted for fertilizer and herbicide production and application, site brush-hogging and rototilling, production of all machinery, nursery production of willow whips, and step planting of willow whips (Caputo, Balogh, Volk, Johnson, Puettmann, Lippke and Oneil, 2014).

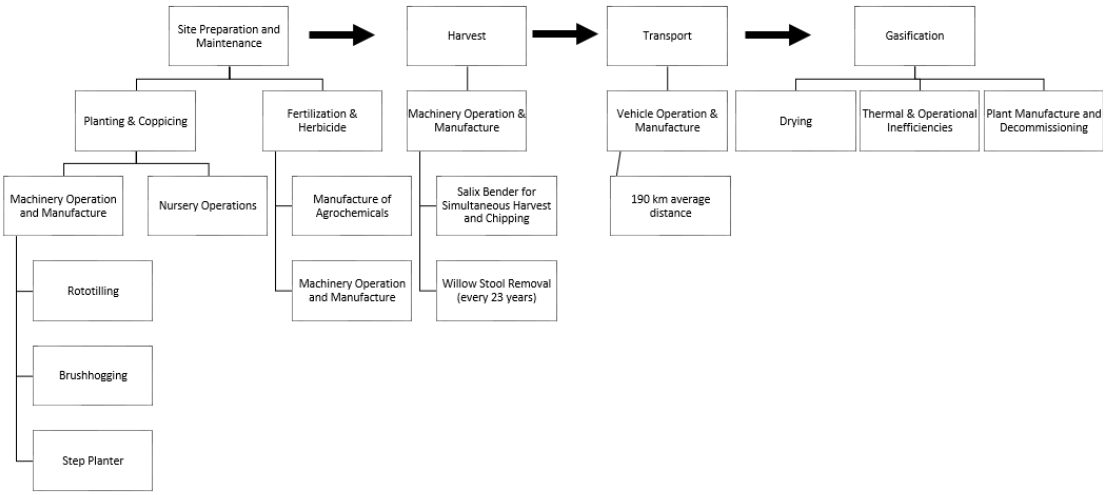

Ch. 3 Figure 2. Conceptual map of the processes included in the life-cycle analysis of short-rotation coppiced willow and its gasification for electric power. Process emissions are the sum of all emissions along the production chain of bioenergy from willow. Averted emissions incorporate energy expenditures throughout the supply chain.

Transport distances and emissions are based on the assumption of a centralized regional biomass plant, rather than several, smaller decentralized plants; the average distances of 195 km are based on NY state road systems, and emissions estimates included the life cycle impacts of transport vehicles.

Finally, we considered the gasification of chipped biomass at the power plant; our calculated energy costs and emissions included plant construction, upstream processes, and eventual decommission as well as thermal & parasitic energy losses of biomass gasification (Lettens *et al.*, 2003). We assumed that all chips were used exclusively for direct-fire biomass gasification and that there was no co-firing.

As explained above, forest harvest followed one of three scenarios: no harvest, high intensity harvest, or low intensity harvest. The high and low intensity scenarios were based on

typical regional harvest regimes. We assumed the use of heavier machinery (feller-buncher, grapple skidder, slasher) for use in this harvest in the higher intensity scenario (Handler *et al.*, 2014) and a less mechanized harvest for the low intensity one, using chainsaws for felling, and a cable skidder for transport (Handler *et al.*, 2014). Biomass chipping took place using an industrial grinder hammer mill at the landing sites in both harvest scenarios. We assumed passive drying, as in the willow case, based on similar studies that used this more energy efficient method over active drying (Matthews, 2001).

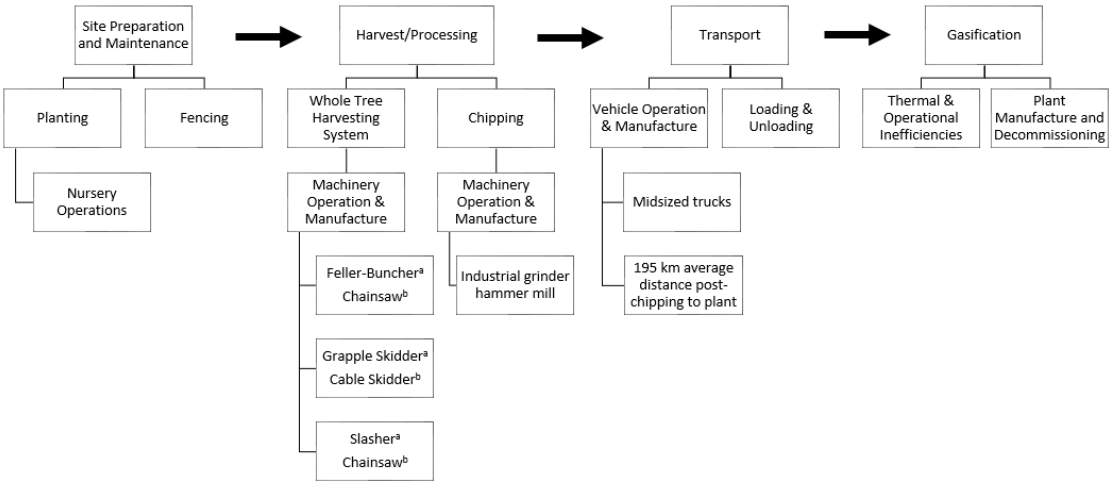

Ch. 3 Figure 3. Conceptual map of the processes included in the life-cycle analysis of a managed mixed-species forest periodically cut for bioenergy and chipped for gasification and electricity generation. Process emissions are the sum of all emissions along the production chain of bioenergy from forest harvest, while the averted emissions incorporate energy use and expenditure throughout production, harvest, transport, and biomass burning.

Our transport scenario assumed that undried chipped wood was shipped by truck from the landing sites to the gasification plants, although chipping at the site of harvest or at the plant itself are occasionally practiced (Johnson, Lippke and Oneil, 2013). The average

transport distance was assumed to be 195 km, identical to the willow scenario (Handler *et al.*, 2014). Transportation emissions and energy costs included loading, unloading, mileage for average load and distance traveled, and the lifetime impact of the trucks themselves.

We calculated the gasification of chipped forest biomass identically as in the chipped willow scenario. Drying and power generation took place at a direct-fire biomass gasification plant. We incorporate the construction, upstream processes, and eventual decommission of the biomass gasification plant, as well as thermal and parasitic energy losses, as energy costs and emissions (Lettens *et al.*, 2003). We assumed that all chips were used exclusively for direct-fire biomass gasification, although current forestry practices make use of a majority of the wood biomass for sawlogs and pulpwood (Munsell and Germain, 2007).

Ch. 3 Table 3. Study parameters for carbon dioxide emissions from forest and willow cultivation, harvest, and burning, as collated from the sources described in the text.

	Forest		**Willow**	
kgCO₂ odt⁻¹	high-intensity	low-intensity	low-productivity	high-productivity
Site Prep, Planting & Maintenance	11.8	11.8	16.3	10.5
Harvesting	47	62	23.8	18.2
Transport	41.2	41.2	47.9	48.9
Gasification	166	166	166	166
Total	266	281	254	244

Averted Emissions from Replacing Conventional Fuels with Biofuels

We calculated the net energy invested in generating each MJ of biofuel energy for each process described above. We used the net energy ratio (energy generated:energy invested, from the field to its final use at the plant) to determine the net amount of energy made available per each hectare of field converted.

Ch. 3 Table 4. Parameters for the energy cost of forest and willow cultivation, harvest, and burning, as collated from the sources detailed above. The energy produced as biofuel energy divided by the energy spent through management processes is the net energy ratio.

	Forest		**Willow**	
***MJ odt*$^{-1}$**	low	high	low	high
Site Prep, Planting & Maintenance	67.1	67.1	129	166
Harvesting	615	792	163	213
Transport	496	496	660	663
Gasification	3,010	3,010	3,010	3,010
Total Energy Inputs	4,188	4,365	3,962	4,052
Total Energy Outputs	20,900	20,900	19,800	19,800
Inputs:Outputs, unitless				
Net Energy Ratio	4.99	4.79	5.00	4.89

Emissions averted were determined based on typical emissions generated for an alternative energy source. Emissions taking into account the entire life cycle of each power source were obtained from the IPCC (Schlömer *et al.*, 2014). A standard fuel mix representative of the 2017 NY State was obtained from ISO New England (*New England Power Grid 2017 – 2018 Profile Sources of Electricity Production*, 2018) (Table 5). By applying the appropriate emissions factor proportional to the fuel mix, we calculated the emissions factor for electricity generation in NY State. Net emissions averted was equal to the emissions that would have been released by conventional practices less the emissions from generating the same amount of energy from biofuels.

Ch. 3 Table 5. The emissions and percent of fuel mix for the primary energy sources in New York. Direct emissions include direct process emissions but excludes albedo, biological sequestration, and averted emissions. It also excludes emissions from the lifetime implementation of the energy product (plant construction, transport). Life-cycle emissions as reported here include these direct emissions as well as emission equivalents from albedo (Schlömer *et al.*, 2014; *New England Power Grid 2017 – 2018 Profile Sources of Electricity Production*, 2018).

	Use in New York State, 2017 ***%***	**Direct Emissions** $g\ CO_2\ MJ^{-1}$	**Life-Cycle Emissions** $g\ CO_2\ MJ^{-1}$
Hydroelectric	21	0	6.67
Natural Gas	43	103	136
Coal	1	211	228
Nuclear	32	0	3.33
Wind	3	0	3.19
New York Fuel Mix	100	46.2	63.4

Radiative impacts from changes to albedo during forest conversion.

Land-use change affects local albedo, and we calculated the radiative impact of this change at the earth surface; we then converted this forcing to its impact at the top of the atmosphere and scaled from a local to a global climate effect. We obtained the monthly albedo averages from sites in Geneva, NY; Urbana and Pana, IL; and Petersham, MA as analyzed and reported in (*Chapter 2*); the baseline case for evaluating land-use change effects on albedo was a maize field. The impact of albedo was calculated using the radiative forcing of changes to surface albedo at the top of the atmosphere ($RF^{TOA}_{\Delta a_s}; W\ m^{-2}$as in Equation 4. The monthly average difference between a baseline and transition albedo ($\Delta\ a_s; unitless$ was multiplied by

the monthly incoming shortwave radiation incident at the land surface ($R_{SW}^{\downarrow}; W\,m^{-2}$) and the upward atmospheric transmittance ($T_{SW}^{\uparrow}; W\,m^{-2}$) for each month of the year (Bright, 2015; Bright *et al.*, 2015).

$$RF_{\Delta a_s}^{TOA}(t)/W\,m^{-2} = \sum_{m=1}^{m=12} \Delta a_s(t,m) R_{SW}^{\downarrow}(t,m) T_{SW}^{\uparrow} \left(\frac{1}{12}\right)\left(\frac{A^{local}}{A^{earth}}\right)$$

(Eq 4)

We obtained the local monthly $R_{SW}^{\downarrow}$ from the NASA Langley Research Center Atmospheric Sciences Data Center NASA/GEWEX SRB Project and from the NASA Langley Research Center Fast Longwave and Shortwave Radiative Fluxes Project. $T_{SW}^{\uparrow}$ is a constant as reported in Bright 2013 (Bright and Kvaleväg, 2013). We normalized these calculations to the local square area converted (A_{local}) out of the total global surface area (A_{global}).

We used the radiative forcing of albedo at the top of the atmosphere to calculate the global warming potential of the transition. An explicit treatment of the normalizing CO_2 forcing was used, as shown below:

$$GWP_{\Delta a_s}(TH) = \frac{\int_0^{TH} RF_{\Delta a_s}^{TOA}(t)\,dt}{\int_0^{TH} \Delta RF_{CO_2}(t)\,dt} = \frac{\int_0^{TH} RF_{\Delta a_s}^{TOA}(t)\,dt}{\int_0^{TH} \Re_{CO_2} y_{CO_2}(t)\,dt}$$

(Eq 5)

where k_{CO_2} is the radiative efficiency (W m^{-2} kg^{-1}) of CO_2 in the atmosphere at 389 ppm (Forster *et al.*, 2007), y_{CO_2} is the impulse-response function (Joos *et al.*, 2013).

However, afforestation is not instantaneous but in fact develops over multiple years as a forest grows; in this case, we must calculate a time evolution of the albedo change $y_{alb}(t)$ that considers the growth dynamics of newly planted vegetation. This decay function measures the

saturation or decay of albedo between the initial and final land-use type (Figure 4). We followed assumptions by Bright et al (2011) that albedo and shortwave radiation scale with each other, and therefore we treat the saturation of albedo by canopy closure as a linear time profile following afforestation or harvest. Again we used monthly shortwave albedo from a maize crop condition as the baseline prior to forestation and for intermittent, desaturated albedo between partial harvests.

$$\gamma_{alb}(t) = \begin{cases} 1 - \left(\frac{t - tsh}{\tau}\right) \forall |t - tsh| < \tau \\ 0 \forall |t| > \tau \end{cases}$$

(Eq 6)

This function should be considered specific to the land-use and management (Bright, Cherubini and Strømman, 2012) as its form is dictated by rates of canopy closure, leaf area index, stem area or height and other properties of vegetative growth (Peterson and Nilson, 2007; Bright, Strømman and Peters, 2011). We used literature estimates to determine the time of canopy closure (albedo saturation) for a mixed hardwood forest (Bright, Cherubini and Strømman, 2012), and used the same linear approach to saturation following subsequent harvest rotations.

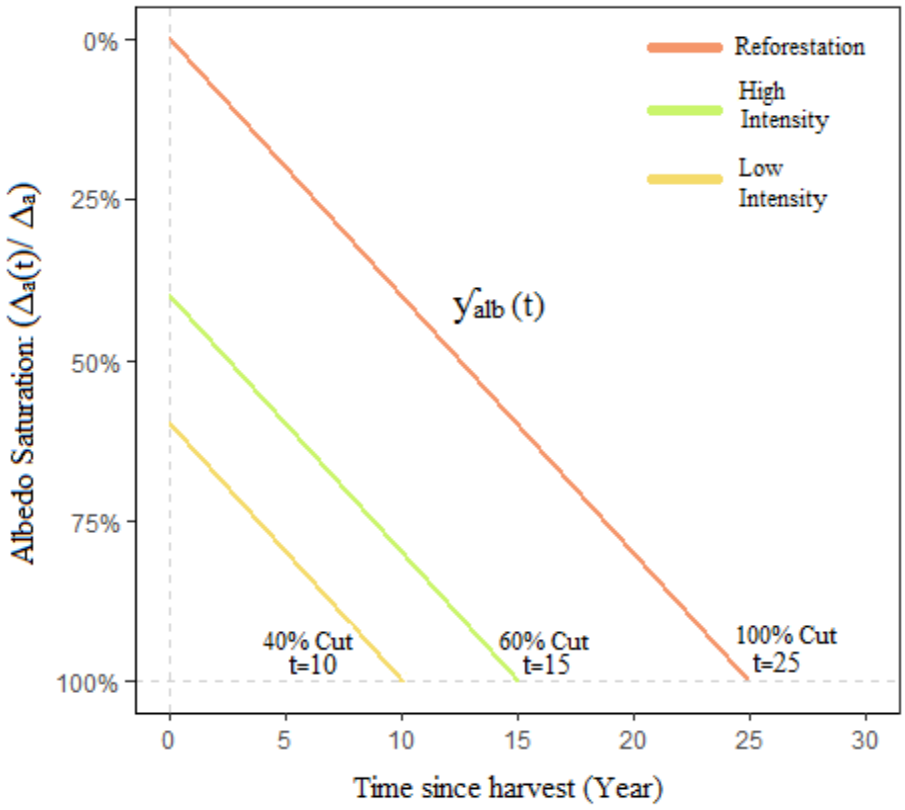

Ch. 3 Figure 4. A conceptual graphic depicting the albedo decay function (γ_{alb}) or re-saturation curve, as it applies to each of the cut percentages dictated by the initial forest growth, where tsh is the time, in years, since the last harvest. Albedo saturation is the percent albedo conversion to the final (forested) case from the initial (baseline) case. We assumed that when regrowth started on completely cleared land, canopy closure and saturation occurred after 25 years of regrowth. Thus, we assumed that 40% and 60% forest cuts would regrow in 10 and 15 years since harvest, respectively.

3. Results

Our study addressed five land-use scenarios, in comparison to a baseline of maize crop field, for both carbon stock and albedo, and in the context of climate in Ithaca, New York. Changes in carbon stock and albedo from the baseline case are used to estimate the

climate impact in carbon-equivalents on a unit area basis over a 100-year time horizon.

Biological Sequestration and Retention of Carbon

Forest and willow land cover, regardless of harvesting practices or bioenergy generation, differed substantially in the long-term fate of carbon (Table 6). Forest scenarios resulted in substantial long-term carbon sequestration. The three-year cycle of total harvests of willow biomass resulted in much lower stocks of carbon both on average and in all but the first few years of forest growth. However, by year 2100, cumulative willow harvests resulted in substantially higher biomass available for biofuel generation than the larger but much less frequent forest harvests.

Ch. 3 Table 6. The fate of biologically fixed carbon after 100 years of growth and harvest under five land management scenarios with two different vegetation types. The non-harvestable carbon pool consists of standing dead wood, coarse and fine roots, and soil carbon (change from cropland). Sequestered harvestable carbon consists of live aboveground biomass not yet harvested. Harvested biomass consists of the total biomass removed over the time period. Shown in parentheses is the amount of carbon in each biomass pool.

Land-Use & Management		**Sequestered Non-Harvestable Biomass** ***Mg CO_2/ha, 2000-2100***	**Sequestered Harvestable Biomass** ***Mg CO_2/ha, 2000-2100***	**Total Harvested Biomass** ***Mg CO_2/ha, 2000-2100***
Forest	None	112 (26%)	311 (74%)	0. (0%)
	Low	102 (22%)	261 (54%)	117 (24%)
	High	98.2 (19%)	230 (46%)	176 (35%)
Willow	Low	14.1 (1%)	29.9 (2%)	1.29×10^3 (97%)
	High	23.5 (1%)	49.8 (2%)	2.14×10^3 (97%)

Forest carbon sequestration was more than 2/3 driven by aboveground carbon storage in live tree biomass, however, there was also substantial belowground storage in coarse and

fine root biomass (Figure 5). Soil carbon accumulation above what had been stored in former agricultural field was negligible, less than one percent of the total stored biomass at 2100. Dead biomass, both in the form of coarse woody debris and standing dead wood, was a little less than half of below-ground biomass. In contrast, the intensively managed coppiced willow field did not store any carbon in dead wood (Figure 5). Aboveground storage was at least 2/3 of total ecosystem carbon storage at most points in the harvest cycle. Note that we assumed negligible net soil carbon accumulation in the willow cases

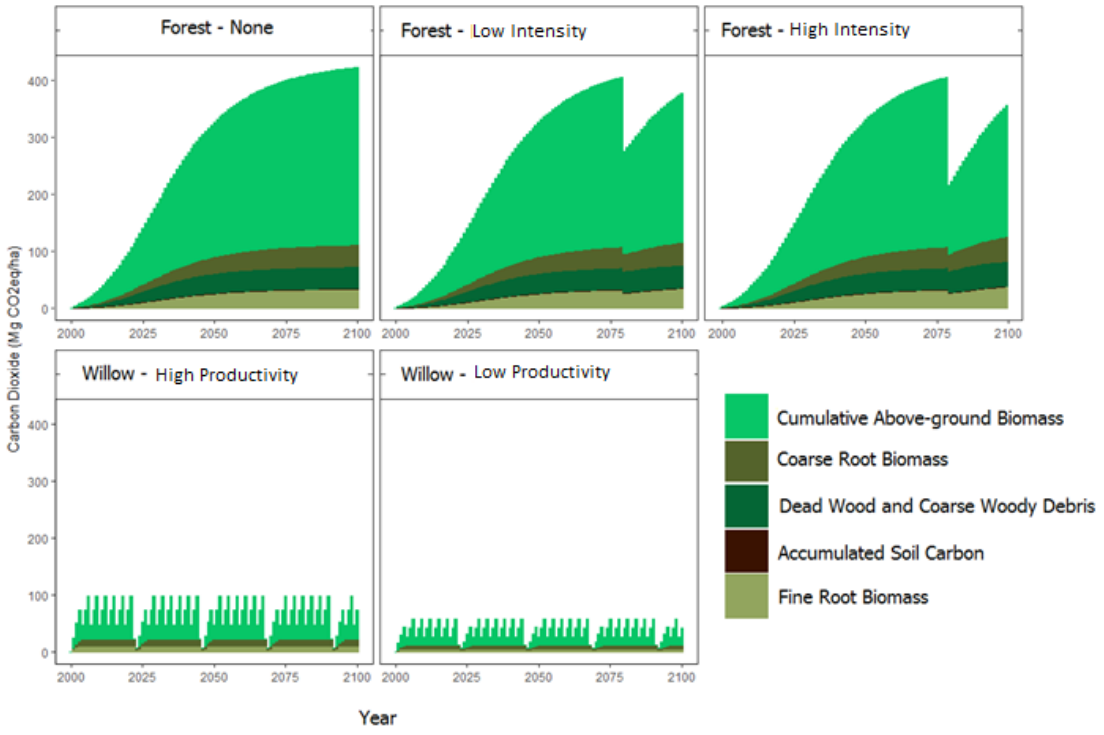

Ch. 3 Figure 5. Accumulated carbon storage by pool for two different land cover types under five different harvest management strategies. Harvested forest is cut every 80 years, removing above-ground biomass and initiating decay of corresponding below-ground biomass. Short-rotation willow is harvested every three years within 23-year rotations; while above-ground biomass is removed at each harvest, and below-ground biomass decays only at the end of each rotation with the removal of willow stool.

The Biogenic Global Warming Potential of Harvested Biomass

Carbon emissions from biomass harvests are removed from the atmosphere at a rate dictated by global ocean and terrestrial uptake (y_{CO2}), as well as by the on-site regrowth of biomass prior to the next harvest (growth rate of biomass). The convolution of these two factors is described by Equation 2, and the net effect on the fraction of carbon dioxide in the atmosphere at any time point following emission is depicted in Figure 6.

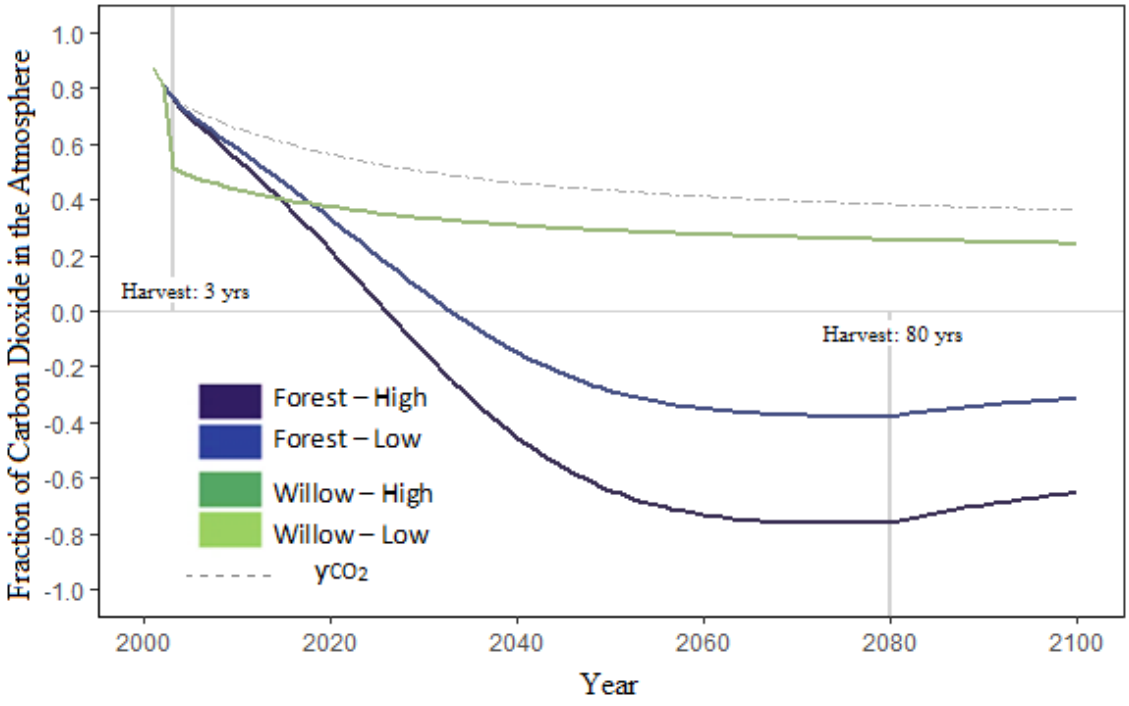

Ch. 3 Figure 6. Atmospheric carbon dioxide decay of biogenic pulse emissions as described in this study, in comparison to a fossil fuel pulse emission, viewed over a 100-year time horizon (TH). Biogenic pulse emissions are colored by source (Willow: Green; Forest: Blue) while the decay of the fossil fuel pulse is shown by the dashed gray line. Inflection points where growth stops can be observed at the point of harvest for willow (3-year rotation) and forest (80-year rotation). These harvest points are marked with a vertical gray line.

The 100-year global-warming potential (GWP) of a pulse of CO_2 emissions with no

intrinsic regrowth (y_{CO_2}, Figure 6, dashed line) is assumed to be 1. Biofuels are often referred to as climate-neutral, implying a GWP of 0. However, in reality the effect of biological carbon sequestration means that the GWP of biofuels (GWP_{bio}) might not be neutral (i.e. if biological sequestration does not remove the full fraction of emitted CO2 prior to reharvest), or may exceed neutrality (if biological sequestration absorbs more CO_2 than was emitted prior to reharvest). GWP_{bio} cannot exceed 1, as there cannot be a higher fraction of atmospheric CO_2 than is removed by background conditions. We calculated the GWP_{bio} for a biogenic pulse from all four of our land-use scenarios, for a time horizon from 1-100 yr. A twenty-year time horizon for GWP has been suggested as more expressive of the short-term effects of methane in the atmosphere. We found that a twenty-year time horizon increased GWP_{bio} of forest from a negative value to nearly 1; in effect, the shorter the time-horizon being considered, the greater the impact of vegetation growth rate. In contrast, for bioenergy sources with very short time horizons, such as the 3-year harvest rotation of willow, time horizon has minimal impact past the rotation year due to the asymptotic nature of the y_{CO_2} function. Where no harvest takes place, the GWP_{bio} is -1, as all sequestered biomass represents CO_2 that has been removed from the atmosphere for the entire time horizon.

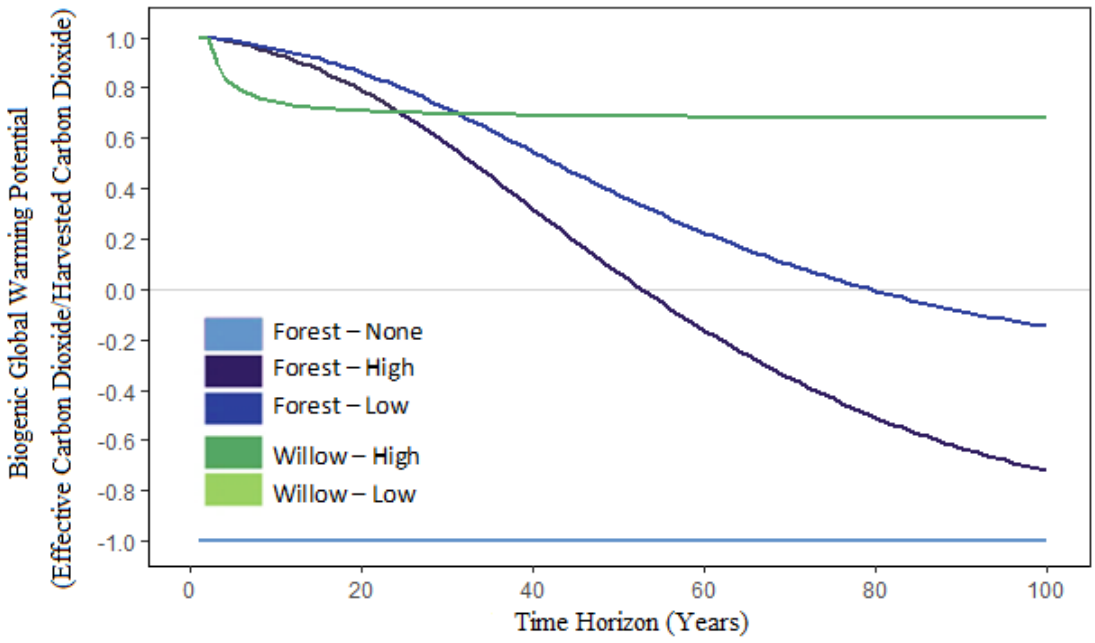

Ch. 3 Figure 7. The global warming potential of five land-use scenarios over a time-horizon from 0-100 yr. Willow, both high and low productivity, is displayed in green; lines overlap as they asymptote at a GWP of 0.68. Dark and medium blue lines represent the high and low harvest forest scenarios. The lightest blue line represents the unharvested forest scenario, where all forest biomass is represented as carbon sequestration.

Biological carbon sequestration at year 2100 was greatest in forest with no and low intensity harvests (Net biological sequestration: -422, -276 Mg CO_2 ha^{-1}) with intermediate sequestration in high-intensity forests (Net biological sequestration: -57.3). In the willow fields, where standing biomass is always quite small, the net effect of fixed carbon was correspondingly small in both low and high productivity cases (Net biological sequestration: 3.77, 5.18 Mg CO_2-equiv ha^{-1}). These carbon values take into account the GWPbio when considering carbon sequestration, except where there was no harvest (Figure 7).

Emissions from Bioenergy Production and Conventional Fuel Replacement

Emissions were also generated by production processes in the field and at the biomass combustion plant. From farm to gate, both high and low productivity willow fields (33.6, 28.1 Mg CO_2-equiv ha^{-1}) emitted 5-7 times the carbon dioxide equivalents as forest harvests. This was driven both by the larger volume of biomass harvested for energy (Table 6), and more emissions-intensive production practices (Table 3). Forest production of farm to gate emissions for both low and high intensity scenarios (4.74, 5.65 Mg CO_2-equiv ha^{-1}) were much smaller. Based on the life cycle analysis, the greatest emissions for both land-uses came from transport and plant inefficiencies; the total emissions from cradle to grave (site preparation to biomass burning) per tonne dried biomass were 285 and 178 Mg CO_2-equiv ha^{-1}, respectively for high and low productivity willow. Forest biomass emissions at the point of burning were 18.0 and 25.6 Mg CO_2-equiv ha^{-1} for low and high intensity cases.

We based averted emissions on a standard NY fuel mix (Table 5), resulting in high averted emissions for both high and low willow (1.17×10^{-3}, 701 Mg CO_2-equiv ha^{-1}) and lower averted emissions for both high-intensity and low-intensity forest (102, 67.1 Mg CO_2-equiv ha^{-1}). We also explored the sensitivity of the averted emissions to a fuel mix consisting of a higher percentage of renewables, or a higher percentage of natural gas (Figure 8); the former fits with a recent statewide policy commitment, and the latter would mimic recent trends of increasing gas and phasing out of coal. The benefit of switching to woody biofuels would decrease steadily as the proportion of non-biofuel renewables increased until at 85% renewables emissions would no longer be averted but rather increased under the willow biofuel scenario. Of course, if natural gas proportion increased the averted emission for willow biofuels would increase considerably (Figure 8).

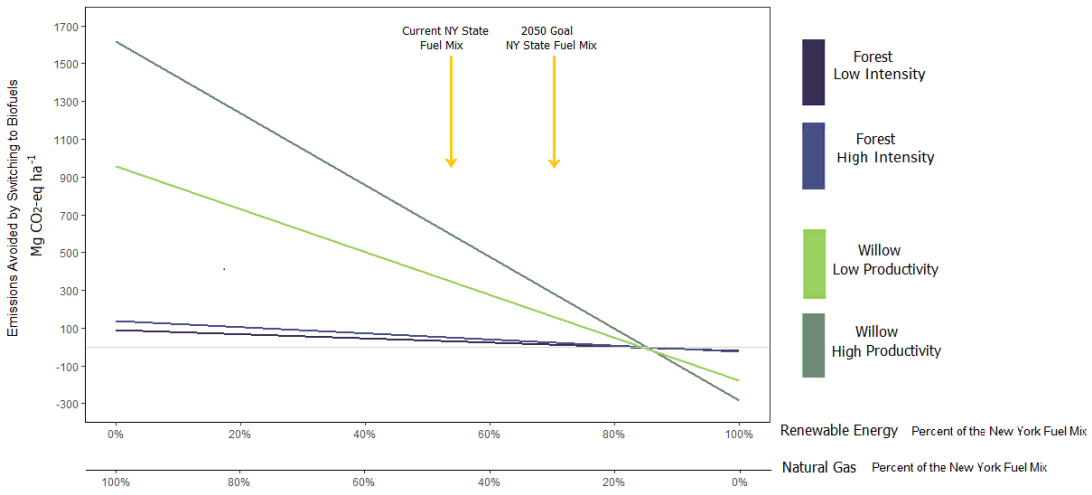

Ch. 3 Figure 8. All emissions calculations presented here are based on direct emissions and are not inclusive of biological sequestration or albedo effects. In this figure, the 1% of the fuel mix represented by coal is attributed equally to renewable energy and natural gas.

Equivalent Emissions from Land-Use Change Effects on Albedo

The change in local albedo from a discrete land-use change can be converted to a global instantaneous radiative forcing as calculated using Eq 4 and 5. The time profile of forest RFa(t) is controlled by the albedo decay function $y'_{alb}(t)$ described in Eq 6. Following initial planting and subsequent harvests, a slow-growing land cover such as the mixed forest will take several years to regrow and re-saturate to a closed-canopy albedo. Thus, as with the carbon-based calculations of GWP, the effect of land-conversion depended on the time-horizon considered (Figure 9). In the afforestation scenarios, longer time-horizons reduce the impact of initial growth, but also allowed the effect of subsequent harvests to slightly reduce the final climate impact.

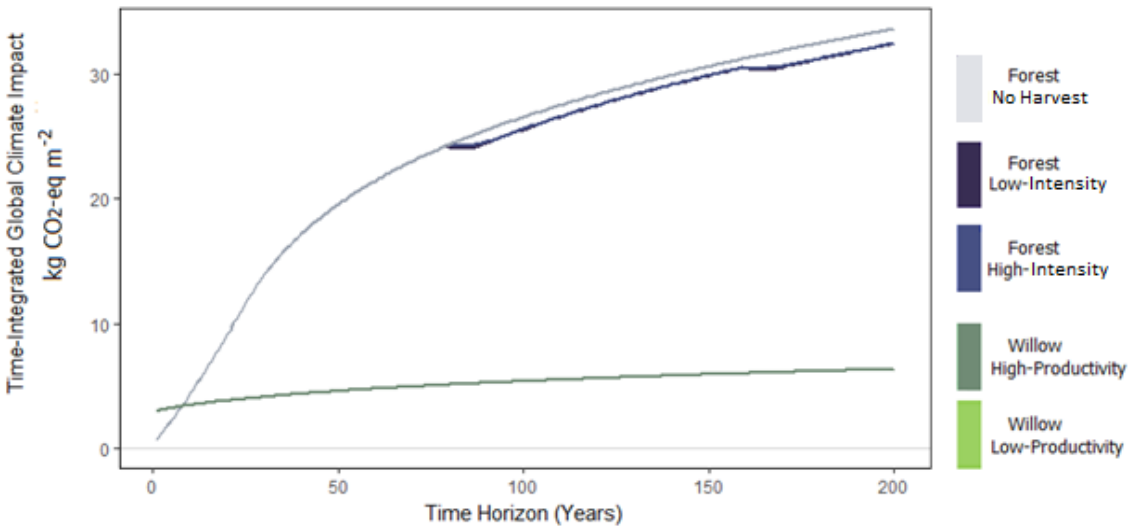

Ch. 3 Figure 9. The climate impact of each land-use conversion for time horizons from 1 to 200 years. Due to the nature of the calculated albedo effect, the impact of albedo is reported here as kg CO_2 m^{-2}.

Net Impact of Land-Use Change on Climate as Mediated by Carbon and Albedo

In the unharvested forest scenario, albedo offset (albedo carbon-equivalents/carbon impact) ~60% of the total biological carbon sequestration relative to the baseline land use of a maize field (Unharvested Forest: 266 vs -422 Mg CO_2 ha^{-1}). However, for harvested forest, the impact of albedo equaled or exceeded the total impact of carbon sequestration and harvest (Low-intensity Forest: 256 vs -276 Mg CO_2 ha^{-1}; High-intensity Forest: 256 vs -57.3 Mg CO_2 ha^{-1}). Due to the relatively low total harvest volumes (i.e. compared with willow), both averted and process emissions were relatively small parts of the total climate impact (Low-intensity Forest: -67.1 and 18.0 Mg CO_2 ha^{-1}; High-intensity Forest -102 and 25.6 Mg CO_2 ha^{-1}).

In the willow biofuel scenario, albedo exerted a relatively smaller positive forcing (53.5 Mg CO_2 ha^{-1}) than for forest harvest while on-site carbon sequestration was negligible due to high harvest frequency (High Productivity: 39.3 Mg CO_2 ha^{-1}; Low Productivity: 22.1

Mg CO_2 ha^{-1}). However, the cumulative impact of biomass harvests included both higher process emission and much higher averted emissions. The averted emissions based on the NY fuel mix baseline (High Productivity: -1.17×10^{-3} Mg CO_2 ha^{-1}; Low Productivity: -701 Mg CO_2 ha^{-1}) offset almost 70% of the process emissions (High Productivity: 285 Mg CO_2 ha^{-1}; Low Productivity: 178 Mg CO_2 ha^{-1}).

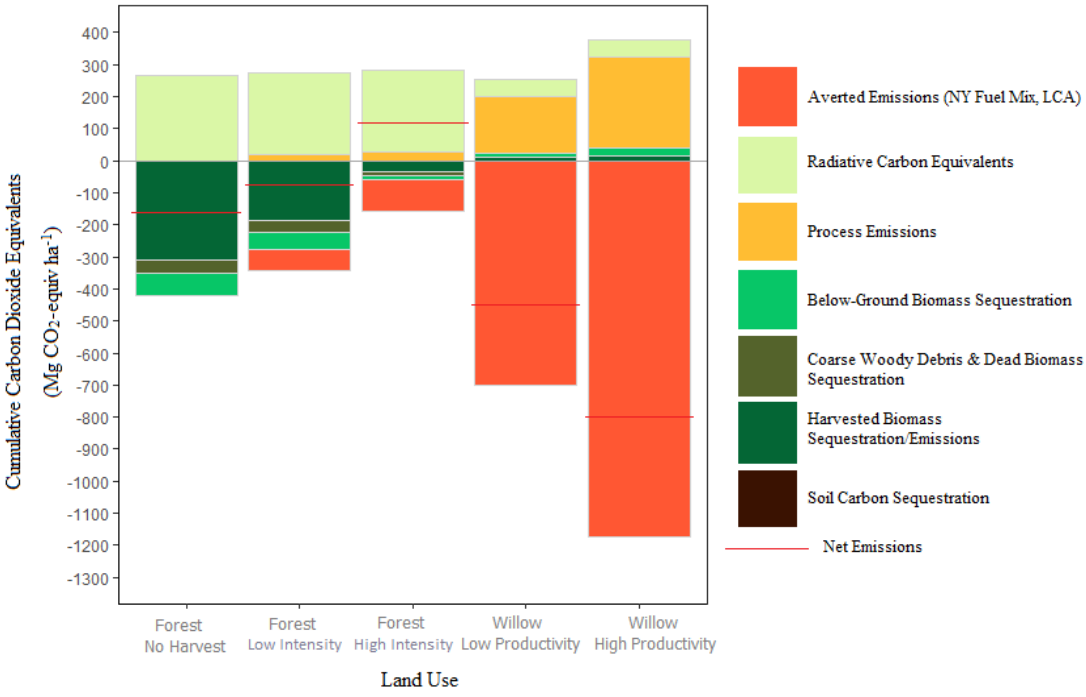

Ch. 3 Figure 10. Comparison of emissions and sequestration for the given biofuels scenarios from four major climate forcings: biomass sequestration and emissions (green to dark brown), process emissions (yellow), averted emissions (orange), and equivalent radiative emissions from albedo (light green). The net impact (the sum of positive and negative climate forcings) is shown as a red horizontal line.

Of the five land-use and management scenarios, only high-productivity forest had a climate warming impact, driven by the large change in albedo but small time-integrated carbon sequestration (123 Mg CO_2 ha^{-1}) (Figure 10). Unharvested and low-productivity forest

were found to have a small net cooling impact on climate (-156 and -69 Mg CO_2 ha^{-1}), driven by the large carbon sequestration relative to the baseline but offset by a substantial warming impact from albedo. Both high and low productivity willow management scenarios had large cooling impacts driven by the large averted emissions which exceeded all other climate forcings (-447 and -796 Mg CO_2 ha^{-1}).

4. Discussion

We hope this study will serve as a decision support tool for climate mitigation policy in the northeastern United States. Here we draw several conclusions regarding best practices for land conversion. Firstly, we identified that when converting land from agriculture to forest biofuels, the rotation length and cut intensity controlled the potential benefit to climate mitigation, with longer rotations and less intensive cuts being more beneficial largely because of greater time integrated carbon sequestration in biomass. Second, we identified that the potential benefit of a bioenergy intensive crop, specifically willow, depended on the mix of fuels being replaced such that an increase in other renewable energy options could reverse the climate benefit of conversion. Finally, we have been able to highlight sources of uncertainty and critical areas of research as detailed below. We found that when all the climate forcings from biological carbon sequestration, life-cycle greenhouse gas emissions, averted fossil fuel emissions, and changes in albedo (relative to a baseline of a maize field) are considered, unharvested and low-intensity harvest forest resulted in substantial net cooling of the climate. High-intensity forest and willow grown for bioenergy resulted in almost the same or greater net warming of climate.

Sources of Uncertainty and Sensitivity in the Analysis

Our study used the best existing data on standard management practices for both forest and willow; however, these practices are site and region specific, and the conclusions of this study may not be universally applicable where different management practices are

employed. Previous studies have suggested that estimates of emissions and energy usage are sensitive to transport distance, fertilizer methods and amounts, and biofuel drying practices (Heller, Keoleian and Volk, 2003; Caputo *et al.*, 2011). We examined some of these key assumptions (Suppl. Table 2), and we found that changing the assumed biofuel transport distance or using active rather than passive drying methods did not substantially increase net carbon emissions. Fertilization methods introduce additional complexities, as both indirect emissions during manufacture and emissions of the potent greenhouse gas, N_2O, must be taken into account. Previous work has specifically investigated a wide range of nitrogen fertilization practices appropriate to upstate NY; these suggest that switching from a standard ammonium sulfate fertilizer to sulfur-coated urea or regionally sourced biosolids would raise net emissions by ~0.6 or lower them by ~1.5 to 2.5 Mg CO_2-eq ha^{-1} yr^{-1} respectively (Heller, Keoleian and Volk, 2003). Growing willow without fertilizer would lower emissions by only ~0.023 Mg CO_2 ha^{-1} yr^{-1} (Caputo *et al.*, 2014). Fertilization, and other site preparations (mounding, herbicides), are very uncommon in northeastern US forestry, and so were not examined in-depth by this study; literature from European countries suggest that more substantial site cultivation (mounding) would result in an additional emission of 0.60 kg CO_2 odt^{-1} yr^{-1} and spraying herbicides would increase emissions by 1.2 kg CO_2 odt^{-1} yr^{-1} (Matthews and Mortimer, 2000). Conversely, we assumed high herbivore pressure on newly abandoned fields, and so included both fencing to exclude deer and ensure seedling survival, and planting and nursery emissions. Many parts of Europe and New England experience lower herbivore pressures than in New York State, and will be less likely to fence properties, as fencing is expensive both to build and maintain. Similarly, forests with fewer deer would have more opportunities for natural regeneration reducing the need for planting. If neither fencing nor planting of saplings was required, we would expect to reduce emissions by about 9 kg CO_2-equiv odt^{-1} (Matthews and Mortimer, 2000).

A significant source of uncertainty for the forest cases is the temporal changes in albedo with forest development following harvest or new forest planting. We assumed a linear re-saturation of albedo with forest age, and that the revealed understory resembled the maize agriculture baseline. While these assumptions are not realistic reflections of a probable real-world case (e.g., canopy closure may be expected to follow a more complex, site-specific decay curve (Bright, Cherubini and Strømman, 2012; Otto *et al.*, 2014), while recently cleared forest is likely darker than a maize field (Bright *et al.*, 2015)); nevertheless, this result likely provides a maximum estimate of the effect of forest harvest on albedo. It should also be noted that the assumed baseline (here an open maize cropfield) is critical in determining the final albedo impact, and must be clearly defined in all such experiments.

A further source of uncertainty that will be essential to address is the assumption of a mixed deciduous broadleaf forest in all our forest carbon calculations; this forest type was chosen because it is common in the region and was available as an option in the COLE forest growth simulator that we used. We note that our empirical albedo values were obtained from a mixed stand with about 30% conifer (*Pinus strobus, Tsuga canadensis*). A brief look at the growth rates of white pine suggested that a 30% pine forest would sequester 6, 5, or 1% more live tree carbon by 2100 depending on whether a high, low, or no harvest management strategy was used. Further work should make use of these more representative growth rates in order to ensure that carbon and albedo values are directly comparable, and in order to ensure that the divergence across harvest methods is not being under-represented.

However, assumptions of biomass yield and rotation times exerted a substantial impact on the net climate forcing. Yield and rotation were found to exert the greatest impact on GWP_{bio}, as higher growth rates and longer rotation periods resulted in lower net emissions, or even net sequestration. This effect has also been reported in the literature, demonstrating across sites and species that longer rotations lead to low emissions and higher sequestration

(Cherubini *et al.*, 2011; Cherubini, Strømman and Hertwich, 2011; Bright, Cherubini and Strømman, 2012). In all land-use scenarios, the carbon forcing from process emissions exceeded the fossil fuel emissions avoided by replacing the New York standard energy mix with bioenergy. Thus, higher bioenergy production only slightly increased the net emissions for both forest and willow scenarios. Rotation length affected forest albedo by increasing the effect of intermediate albedo following harvests. However, this effect was small in comparison to the total albedo forcing from land-use change. Consequently, long rotation lengths and low biomass harvests resulted in the greatest climate cooling. Future studies might identify the combinations of small harvests and rotation lengths that would result in substantial cooling impacts from managed forestry.

The intrinsic assumption of GWP_{bio}

The metric GWP_{bio} was first introduced to combat the harmful assumption of carbon-neutrality in bioenergy evaluations. In our study, assuming no net emissions from carbon sequestered and then harvested for bioenergy would have overpredicted forest emissions by as much as 200 Mg CO_2-equiv ha^{-1} and underpredicted willow emissions by as much as 30 Mg CO_2-equiv ha^{-1}. However, this methodology introduces its own assumptions and biases, which should be considered. First, the impulse response function on which $\gamma_{CO_2}(t)$ is based assumes global uptake by natural forests distributed across the planet. In the scenario described here, our small, managed afforestation is examined in isolation against the backdrop of an unchanged global biosphere. However, a broader application of this methodology might encompass either new management regimes for previously natural forest, or wide-scale reforestation of the much greater magnitude that may be required to combat climate change. In this case, the impulse response function itself would be affected by the forest growth rate and by later harvest.

Additionally, when GWP_{bio} is used in isolation, it is easy to miss the cost in lost

carbon sequestration of not permitting the forest to grow and sequester carbon across the entire 100-year time horizon. In this work, we characterize this lost carbon by comparing sequestration of unmanaged forest to sequestration from each of the two harvest scenarios, quantifying the opportunity cost of the harvest strategy. However, the willow scenario does not incorporate such an estimate, as willow is almost always grown in a three-year growth-harvest rotation. The opportunity cost of harvested carbon is worth considering explicitly where it may influence management decisions such as harvest rotation and magnitude.

The importance of the albedo offset to carbon emissions and sequestration

Forest carbon sequestration in the unharvested case was comparable to literature values, as was the offset by albedo change associated with reforestation of agricultural land. We had anticipated an offset of greenhouse gas forcings by albedo of 20-60%. Although reported offsets ranged from 11-109% depending on snow cover and species composition (Bird *et al.*, 2008; Schwaab *et al.*, 2015), offsets for temperate, deciduous forest suggested a lower range of 17-35% (Betts, 2000). Our estimate of a 60% offset by albedo change is comparatively high, likely driven by the high albedo baseline condition of a maize cropfield. This assertion is supported by a study of the albedo offset comparing grassland and coniferous forest which also found about a 60% offset (Schwaiger and Bird, 2010).While the effect of the albedo offset on willow biofuels was less substantial, the total albedo forcing is still a significant impact; without inclusion of albedo, climate cooling by willow would be overestimated by about ten percent. The magnitude of this offset supports that the value of climate mitigation projects can be highly inaccurate if the radiative effects of an albedo change are ignored.

Conclusions from net impacts

Determining the net impact of climate mitigation projects such as reforestation and bioenergy production has been the purpose of research both within and beyond our study

region. In large part, these studies have focused on only a subset of the factors addressed in this paper, resulting in a wide range of expected climate outcomes. Our results demonstrate the value of accounting for all significant impacts on climate, and especially the importance of the often overlooked biogeophysical impacts, such as albedo.

Forest carbon sequestration in the unharvested case was comparable to literature values, as was the offset by albedo change from the baseline maize field. Harvested carbon sequestration values and predicted GWP_{bio} are much lower than estimates typically made for complete biomass harvests as we had assumed partial rather than clear-cut harvests (Cherubini, Strømman and Hertwich, 2011; Bright, Cherubini and Strømman, 2012). The resulting net sequestration describes the carbon sunk by forest growth less the biomass harvested by cuts. In harvested forest, lower carbon sequestration and relatively low averted and process emissions increase the importance of the biogeophysical impact as albedo was found to be only minimally impacted by partial harvests over a 100-year time horizon. The relative intensity of these cuts, and the rotation length, will dictate the net impact of climate mitigation through forestry, and inclusion of albedo will be essential to determining this precise cut-off.

The net impact of willow bioenergy base on a life-cycle analysis of process emissions, was estimated to be 10.8 to 11.2 g CO_2-equiv MJ^{-1} (Heller *et al.*, 2004). We calculated a slightly higher emissions rate of 12.3 and 12.8 g CO_2-equiv MJ^{-1} (high and low productivity respectively). Heller et al. (2004) also indicated that willow might lead to averted emissions between 275 g CO_2-equiv MJ^{-1} (based on the typical US energy grid) and 2.69 g CO_2-equiv MJ^{-1} (for 100% renewable, non-biofuel energy). In comparison, our study using the current New York energy grid and suggested an averted emissions of 63 g CO_2-equiv MJ^{-1}; if 100% renewables were assumed, averted emissions would be only 3.2 g CO_2-equiv MJ^{-1}. This difference is due to the relatively high percentage of renewables already represented in the

NYS fuel mix (Table 5) and led to a lower estimate of averted emissions than previous work. Carbon sequestration by willow, both with and without the context of $GWP_{bio,}$ has been previously characterized in the literature. Heller et al. (2004) accounted for carbon sequestration as a mass balance amounting to only 3.7 Mg CO_2-equiv MJ^{-1} per 23-year planting cycle, or ~53 Mg CO_2-equiv MJ^{-1} over 100 years, about half the estimate made by our study. Another study suggested a higher range of cumulative carbon sequestration of (van Bussel, 2006). Our conclusion of a substantial net climate cooling from conversion to willow biomass is robust to assumptions regarding process emissions, but sensitive to the base fuel mix; under a high renewables fuel mix, conversion to willow could become a net warming impact on climate.

5. Conclusions

Inclusion of land-use driven biogeophysical effects is essential to determining the net climatic impact of mitigation projects. Here we assessed the net impact of three forestry and two short-rotation coppiced willow projects. We identified conditions under which these projects might be net carbon sinks and sources and determined that quantifying albedo as a carbon-equivalent forcing would be integral to any policy decision. Overall, we determined that willow bioenergy provided the greatest cooling impact, but that this was controlled substantially by the background fuel mix. Afforestation had a net cooling impact, but forest harvest reduced or even reversed this effect.

Acknowledgments

Solar insolation data obtained from the NASA Langley Research Center Atmospheric Sciences Data Center NASA/GEWEX SRB Project and the NASA Langley Research Center (LaRC) POWER Project, funded through the NASA Earth Science/Applied Science Program.

References

Abbas, D. and Handler, R. M. (2018) 'Life-cycle assessment of forest harvesting and transportation operations in Tennessee', *Journal of Cleaner Production*. Elsevier Ltd, 176, pp. 512–520. doi: 10.1016/j.jclepro.2017.11.238.

Adams, P. W. R., Shirley, J. E. J. and McManus, M. C. (2015) 'Comparative cradle-to-gate life cycle assessment of wood pellet production with torrefaction', *Applied Energy*. Elsevier Ltd, 138, pp. 367–380. doi: 10.1016/j.apenergy.2014.11.002.

Bacenetti, J., Pessina, D. and Fiala, M. (2016) 'Environmental assessment of different harvesting solutions for Short Rotation Coppice plantations', *Science of the Total Environment*. Elsevier B.V., 541, pp. 210–217. doi: 10.1016/j.scitotenv.2015.09.095.

Bergman, P. *et al.* (2005) 'Torrefaction for biomass co-firing in existing coal-fired power stations', *Energy Research Centre of the Netherlands (ECN)*, (July), p. 71.

Betts, R. (2000) 'Offset of the potential carbon sink from boreal forestation by decreases in surface albedo.', *Letters to Nature*, 408, pp. 187–190. doi: 10.1038/35041545.

Betts, R. (2007) 'Implications of land ecosystem-atmosphere interactions for strategies for climate change adaptation and mitigation', *Tellus, Series B: Chemical and Physical Meteorology*, 59(3), pp. 602–615. doi: 10.1111/j.1600-0889.2007.00284.x.

Bird, D. N. *et al.* (2008) 'Incorporating changes in albedo in estimating the climate mitigation benefits of land use change projects', *Biogeosciences Discussions*, 5(2), pp. 1511–1543. doi: 10.5194/bgd-5-1511-2008.

Bonan, G. B., Pollard, D. and Thompson, S. L. (1992) 'Effects of Boreal Forest Vegetation on Global Climate', *Nature*, 359(6397), pp. 716–718. doi: Doi 10.1038/359716a0.

Bright, R. M. (2015) 'Metrics for biogeophysical climate forcings from land use and land cover changes and their inclusion in life cycle assessment: A critical review', *Environmental*

Science and Technology, 49(6), pp. 3291–3303. doi: 10.1021/es505465t.

Bright, R. M. *et al.* (2015) 'Quantifying surface albedo and other direct biogeophysical climate forcings of forestry activities', *Global Change Biology*, 21(9), pp. 3246–3266. doi: 10.1111/gcb.12951.

Bright, R. M., Cherubini, F. and Strømman, A. H. (2012) 'Climate impacts of bioenergy: Inclusion of carbon cycle and albedo dynamics in life cycle impact assessment', *Environmental Impact Assessment Review*. Elsevier Inc., 37, pp. 2–11. doi: 10.1016/j.eiar.2012.01.002.

Bright, R. M. and Kvaleväg, M. M. (2013) 'Technical Note: Evaluating a simple parameterization of radiative shortwave forcing from surface albedo change', *Atmospheric Chemistry and Physics*, 13, pp. 11169–11174. doi: 10.5194/acp-13-11169-2013.

Bright, R. M., Strømman, A. H. and Peters, G. P. (2011) 'Radiative forcing impacts of boreal forest biofuels: A scenario study for Norway in light of albedo', *Environmental Science and Technology*, 45(17), pp. 7570–7580. doi: 10.1021/es201746b.

Budsberg, E. *et al.* (2013) 'Life-Cycle Assessment for the Production of Bioethanol from Willow Biomass Crops via Biochemical Conversion*', *Forest Products Journal*, 62(4), pp. 305–313. doi: 10.13073/fpj-d-12-00022.1.

van Bussel, L. (2006) *The potential contribution of a short- rotation willow plantation to mitigate climate change.*

Cairns, M. A. *et al.* (1997) 'Root biomass allocation in the world's upland forests', *Oecologia*, 111(1), pp. 1–11. doi: 10.1007/s004420050201.

Cangiano, M. L. (2015) *Carbon Budget of Maize and Shrub Willow for Bioenergy*, *Pennsylvania State Universit*. Pennsylvania State University, Graduate School, College of Engineering.

Caputo, J. *et al.* (2011) 'Incorporating Uncertainty into Life-Cycle Analysis (LCA) of Short-

Rotation Willow (SALIX SPP .) Crops'.

Caputo, J., Balogh, S. B., Volk, T. A., Johnson, L., Puettmann, M., Lippke, B. and Oneil, E. (2014) 'Incorporating Uncertainty into a Life Cycle Assessment (LCA) Model of Short-Rotation Willow Biomass (Salix spp.) Crops', *Bioenergy Research*, 7(1), pp. 48–59. doi: 10.1007/s12155-013-9347-y.

Caputo, J., Balogh, S. B., Volk, T. A., Johnson, L., Puettmann, M., Lippke, B., Oneil, E., *et al.* (2014) 'Incorporating Uncertainty into Life-Cycle Analysis (LCA) of Short- Rotation Willow (SALIX SPP .) Crops', *Bioenergy Research*, 7(1), pp. 48–59. doi: 10.1007/s12155-013-9347-y.

Cherubini, F. *et al.* (2011) 'Carbon dioxide emissions from biomass combustion for bioenergy: Atmospheric decay and contribution to global warming', *GCB Bioenergy*, 3(5), pp. 413–426. doi: 10.1111/j.1757-1707.2011.01102.x.

Cherubini, F., Bright, R. M. and Strømman, A. H. (2012) 'Site-specific global warming potentials of biogenic carbon dioxide for bioenergy: contributions from carbon fluxes and albedo dynamics', *Environmental Research Letters*, 7, pp. 1–11. doi: 10.1088/1748-9326/7/4/045902.

Cherubini, F., Strømman, A. H. and Hertwich, E. (2011) 'Effects of boreal forest management practices on the climate impact of CO2 emissions from bioenergy', *Ecological Modelling*. Elsevier B.V., 223(1), pp. 59–66. doi: 10.1016/j.ecolmodel.2011.06.021.

Cramer, V. A., Hobbs, R. J. and Standish, R. J. (2008) 'What's new about old fields? Land abandonment and ecosystem assembly', *Trends in Ecology and Evolution*, 23(2), pp. 104–112. doi: 10.1016/j.tree.2007.10.005.

Djomo, S. N., Kasmioui, O. El and Ceulemans, R. (2011) 'Energy and greenhouse gas balance of bioenergy production from poplar and willow: A review', *GCB Bioenergy*, 3(3), pp. 181–197. doi: 10.1111/j.1757-1707.2010.01073.x.

Elsayed, M. . A. ., Matthews, R. . and Mortimer, N. . D. . (2003) *Carbon and Energy Balances for a Range of Biofuels Options*, *Resources Research Unit Sheffield Hallam University Prepared*.

Flinn, K. M. and Vellend, M. (2005) 'Recovery of forest plant communities in post-agricultural landscapes', *Frontiers in Ecology and the Environment*, 3(5), pp. 243–250. doi: 10.1890/1540-9295(2005)003[0243:ROFPCI]2.0.CO;2.

Forsberg, G. (2000) 'Biomass energy transport: Analysis of bioenergy transport chains using life cycle inventory method', *Biomass and Bioenergy*, 19(1), pp. 17–30. doi: 10.1016/S0961-9534(00)00020-9.

Forster, P. *et al.* (2007) 'Changes in atmospheric constituents and in radiative forcing.', *Climate Change 2007: The Physical Science Basis. Contribution of Working Group I to the Fourth Assessment Report of the Intergovernmental Panel on Climate Change*, pp. 129–234. doi: 10.1103/PhysRevB.77.220407.

Fuglestvedt, J. S. *et al.* (2000) 'Climate implications of GWP-based reductions in greenhouse gas emissions', *Geophysical Research Letters*, 27(3), pp. 409–412. doi: 10.1029/1999GL010939.

Fuglestvedt, J. S. *et al.* (2003) 'Metrics of Climate Change: Assessing Radiative Forcing and Emission Indices', *Climatic Change*, 58, pp. 267–331.

Georgescu, M., Lobell, D. B. and Field, C. B. (2011) 'Direct climate effects of perennial bioenergy crops in the United States', *Proceedings of the National Academy of Sciences*, 108(11), pp. 4307–4312. doi: 10.1073/pnas.1008779108.

Goglio, P. and Owende, P. M. O. (2009) 'A screening LCA of short rotation coppice willow (Salix sp.) feedstock production system for small-scale electricity generation', *Biosystems Engineering*. IAgrE, 103(3), pp. 389–394. doi: 10.1016/j.biosystemseng.2009.03.003.

Grigal, D. F. and Berguson, W. E. (1998) 'Soil carbon changes associated with short-rotation

systems', *Biomass and Bioenergy*, 14(4), pp. 371–377. doi: 10.1016/S0961-9534(97)10073-3.

Guest, G. *et al.* (2013) 'Consistent quantification of climate impacts due to biogenic carbon storage across a range of bio-product systems', *Environmental Impact Assessment Review*. Elsevier B.V., 43, pp. 21–30. doi: 10.1016/j.eiar.2013.05.002.

Guo, L. B. and Gifford, R. M. (2002) 'Soil carbon stocks and land use change: A meta analysis', *Global Change Biology*, 8(4), pp. 345–360. doi: 10.1046/j.1354-1013.2002.00486.x.

Hall, A. (2004) 'The role of surface albedo feedback in climate', *Journal of Climate*, 17(7), pp. 1550–1568. doi: 10.1175/1520-0442(2004)017<1550:TROSAF>2.0.CO;2.

Handler, R. M. *et al.* (2014) 'Environmental impacts of roundwood supply chain options in Michigan : life-cycle assessment of harvest and transport stages', *Journal of Cleaner Production*. Elsevier Ltd, 76, pp. 64–73. doi: 10.1016/j.jclepro.2014.04.040.

Heinsoo, K. *et al.* (2009) 'Fine root biomass and production in a Salix viminalis and Salix dasyclados plantation', *Estonian Journal of Ecology*, 58(1), pp. 27–37. doi: 10.3176/eco.2009.1.03.

Helin, T. *et al.* (2013) 'Approaches for inclusion of forest carbon cycle in life cycle assessment - A review', *GCB Bioenergy*, 5(5), pp. 475–486. doi: 10.1111/gcbb.12016.

Heller, M. C., Keoleian, G. A. and Volk, T. A. (2003) 'Life cycle assessment of a willow bioenergy cropping system', *Biomass and Bioenergy*, 25(2), pp. 147–165. doi: 10.1016/S0961-9534(02)00190-3.

Heller, M. C. M. *et al.* (2004) 'Life cycle energy and environmental benefits of generating electricity from willow biomass', *Renewable Energy*, 29(7), pp. 1023–1042. doi: 10.1016/j.renene.2003.11.018.

Holtsmark, B. (2015) 'Quantifying the global warming potential of CO_2 emissions from wood fuels', *GCB Bioenergy*, 7(2), pp. 195–206. doi: 10.1111/gcbb.12110.

Howarth, R. W. (2014) 'A bridge to nowhere: Methane emissions and the greenhouse gas

footprint of natural gas', *Energy Science and Engineering*, 2(2), pp. 47–60. doi: 10.1002/ese3.35.

Jackson, R. B. *et al.* (1996) 'A Global Analysis of Root Distributions for Terrestrial Biomes', *Oecologia*, 108(3), pp. 389–411.

Jackson, R. B. *et al.* (2008) 'Protecting climate with forests', *Environmental Research Letters*, 3(4), pp. 1–5. doi: 10.1088/1748-9326/3/4/044006.

Johnson, L., Lippke, B. and Oneil, E. (2013) 'Modeling Biomass Collection and Woods Processing Life-Cycle Analysis*', *Forest Products Journal*, 62(4), pp. 258–272. doi: 10.13073/fpj-d-12-00019.1.

Jones, A. D. *et al.* (2013) 'Greenhouse gas policy influences climate via direct effects of land-use change', *Journal of Climate*, 26(11), pp. 3657–3670. doi: 10.1175/JCLI-D-12-00377.1.

Jones, A. D. *et al.* (2015) 'Accounting for radiative forcing from albedo change in future global land-use scenarios', *Climatic Change*, pp. 691–703. doi: 10.1007/s10584-015-1411-5.

Joos, F. *et al.* (2001) 'Global warming feedbacks on terrestrial carbon uptake under the intergovernmental Panel on Climate Change (IPCC) emission scenarios', *Global Biogeochemical Cycles*, 15(4), pp. 891–907. doi: 10.1029/2000GB001375.

Joos, F. *et al.* (2013) 'Carbon dioxide and climate impulse response functions for the computation of greenhouse gas metrics: A multi-model analysis', *Atmospheric Chemistry and Physics*, 13(5), pp. 2793–2825. doi: 10.5194/acp-13-2793-2013.

Keoleian, G. A. and Volk, T. A. (2005) 'Renewable energy from willow biomass crops: Life cycle energy, environmental and economic performance', *Critical Reviews in Plant Sciences*, 24(5–6), pp. 385–406. doi: 10.1080/07352680500316334.

Kirschbaum, M. U. F. *et al.* (2011) 'Implications of albedo changes following afforestation on the benefits of forests as carbon sinks', *Biogeosciences*, 8(12), pp. 3687–3696. doi: 10.5194/bg-8-3687-2011.

Kopp, R. F. *et al.* (2001) 'Willow biomass production during ten successive annual harvests', *Biomass and Bioenergy*, 20(1), pp. 1–7. doi: 10.1016/S0961-9534(00)00063-5.

Kreidenweis, U. *et al.* (2016) 'Afforestation to mitigate climate change: impacts on food prices under consideration of albedo effects', *Environmental Research Letters*, 11(8), p. 085001. doi: 10.1088/1748-9326/11/8/085001.

de la Fuente, T. *et al.* (2017) 'Fuel consumption and GHG emissions of forest biomass supply chains in Northern Sweden: a comparison analysis between integrated and conventional supply chains', *Scandinavian Journal of Forest Research*. Taylor & Francis, 32(7), pp. 568–581. doi: 10.1080/02827581.2016.1259424.

Lettens, S. *et al.* (2003) 'Energy budget and greenhouse gas balance evaluation of sustainable coppice systems for electricity production', *Biomass and Bioenergy*, 24(3), pp. 179–197. doi: 10.1016/S0961-9534(02)00104-6.

Li, A. *et al.* (2015) 'Fine root decomposition , nutrient mobilization and fungal communities in a pine forest ecosystem', *Soil Biology and Biochemistry*. Elsevier Ltd, 83(January), pp. 76–83. doi: 10.1016/j.soilbio.2015.01.019.

Lippke, B. *et al.* (2011) 'Life cycle impacts of forest management and wood utilization on carbon mitigation: Knowns and unknowns', *Carbon Management*, 2(3), pp. 303–333. doi: 10.4155/cmt.11.24.

Liu, W. *et al.* (2017) 'Analysis of the Global Warming Potential of Biogenic CO2 Emission in Life Cycle Assessments', *Scientific Reports*. Nature Publishing Group, 7(July 2016), p. 39857. doi: 10.1038/srep39857.

Lutz, D. A. *et al.* (2016) 'Tradeoffs between three forest ecosystem services across the state of New Hampshire, USA: timber, carbon, and albedo', *Ecological Applications*, 26(1), pp. 146–161.

Lutz, D. A. and Howarth, R. B. (2014) 'Valuing albedo as an ecosystem service: Implications

for forest management', *Climatic Change*, 124(1–2), pp. 53–63. doi: 10.1007/s10584-014-1109-0.

Mann, M. K. and Spath, P. L. (1997) *Life cycle assessment of a biomass gasification combined-cycle power system*. doi: 10.2172/567454.

Marland, G. *et al.* (2003) 'The climatic impacts of land surface change and carbon management, and the implications for climate-change mitigation policy', *Climate Policy*, 3(2), pp. 149–157. doi: 10.1016/S1469-3062(03)00028-7.

Massachusetts Department of Environmental Protection (2019) *310 CMR 7 Air Pollution Control*.

Matthews, R. W. (2001) 'Modelling of energy and carbon budgets of wood fuel coppice systems', *Biomass and Bioenergy*, 21(1), pp. 1–19. doi: 10.1016/S0961-9534(01)00016-2.

Matthews, R. W. and Mortimer, N. D. (2000) 'Estimation of carbon dioxide and energy budgets of woodfired electricity generation systems in Britain', *Bioenergy for mitigation of CO2 emissions: the power, transportation and industrial sectors. Proceedings of a Workshop organised by IEA Bioenergy Task 25, 27-30 September 1999, Gatlinburg, USA*, pp. 45–58.

McKechnie, J. *et al.* (2011) 'Forest bioenergy or forest carbon? Assessing trade-offs in greenhouse gas mitigation with wood-based fuels', *Environmental Science and Technology*, 45(2), pp. 789–795. doi: 10.1021/es1024004.

Morse, J. L., Duran, J. and Groffman, P. M. (2015) 'Soil Denitrification Fluxes in a Northern Hardwood Forest: The Importance of Snowmelt and Implications for Ecosystem N Budgets', *Ecosystems*, 18(3), pp. 520–532. doi: 10.1007/s10021-015-9844-2.

Munsell, J. F. and Germain, R. H. (2007) 'Woody biomass energy: An opportunity for silviculture on nonindustrial private forestlands in New York', *Journal of Forestry*, 105(8), pp. 398–402. doi: 10.1093/jof/105.8.398.

Naudts, K. *et al.* (2016) 'Biophysical Climate Impacts of Recent Changes in Global Forest

Cover', *Science*, 351(6273), pp. 597–601. doi: 10.1126/science.aac9976.

New England Power Grid 2017 – 2018 Profile Sources of Electricity Production (2018).

New York State Assembly (2019) *The New York State Climate Leadership and Community Protection Act*. United States.

New York State Research and Development Authority (2015) 'New York State Greenhouse Gas Inventory and Forecast : Inventory 1990-2014. Final Report.', (April 2014), pp. 1990–2014.

O'Connor, D. (2013) *Literature Review and Sensitivity Analysis of Biopower Life-Cycle Assessments and Greenhouse Gas Emission*. Golden Colorado.

Otto, J. *et al.* (2014) 'Forest summer albedo is sensitive to species and thinning: How should we account for this in Earth system models?', *Biogeosciences*, 11(8), pp. 2411–2427. doi: 10.5194/bg-11-2411-2014.

Pacaldo, R. S., Volk, T. A. and Briggs, R. D. (2011) 'Carbon balance in short rotation willow (Salix dasyclados) biomass crop across a 20-year chronosequence as affected by continuous production and tear-out treatments', *Aspects of Applied Biology: Biomass and Energy Crops IV*, 112(Biomass and Energy Crops IV), pp. 131–138. doi: 10.13140/2.1.3767.1364.

PB, W. *et al.* (2010) 'New York State Energy Research and Development Authority Report', in Z, W. (ed.) *Renewable fuels roadmap and sustainable biomass feedstock supply for New York*, p. Ei-E103.

Peterson, U. and Nilson, T. (2007) 'Successional reflectance trajectories in northern temperate forests', 1161. doi: 10.1080/01431169308904361.

Pielke, R. A. *et al.* (2011) 'Land use/land cover changes and climate: Modeling analysis and observational evidence', *Wiley Interdisciplinary Reviews: Climate Change*, 2(6), pp. 828–850. doi: 10.1002/wcc.144.

Raciti, S. M. *et al.* (2012) 'Local-Scale Carbon Budgets and Mitigation Opportunities for the

Northeastern United States', *BioScience*, 62(1), pp. 23–38. doi: 10.1525/bio.2012.62.1.7.

Regional Greenhouse Gas Initiative (2018) *Model Rule: Carbon Dioxide Budget Trading Program*. doi: 10.2307/j.ctvjsf42m.5.

Richards, K. R. and Stokes, C. (2004) 'A review of forest carbon sequestration cost studies: A dozen years of research', *Climate change*, 63, pp. 1–48.

Röder, M., Whittaker, C. and Thornley, P. (2014) 'How certain are greenhouse gas reductions from bioenergy? Life cycle assessment and uncertainty analysis of wood pellet-to-electricity supply chains from forest residues', *Biomass and Bioenergy*, 79, pp. 50–63. doi: 10.1016/j.biombioe.2015.03.030.

Rogelj, J. *et al.* (2018) 'Mitigation Pathways Compatible With 1.5°C in the Context of Sustainable Development', *Global warming of 1.5°C. An IPCC Special Report on the impacts of global warming of 1.5C above pre-industrial levels and related global greenhouse gas emission pathways in the context of strengthening the global response to the threat of climate change, s*, p. 82pp. Available at: https://www.ipcc.ch/site/assets/uploads/sites/2/2019/02/SR15_Chapter2_Low_Res.pdf.

Røyne, F. *et al.* (2016) 'Climate impact assessment in life cycle assessments of forest products: Implications of method choice for results and decision-making', *Journal of Cleaner Production*, 116(January), pp. 90–99. doi: 10.1016/j.jclepro.2016.01.009.

Rytter, R. M. (2001) 'Biomass production and allocation, including fine-root turnover, and annual N uptake in lysimeter-grown basket willows', *Forest Ecology and Management*, 140(2–3), pp. 177–192. doi: 10.1016/S0378-1127(00)00319-4.

Schlömer, S. *et al.* (2014) 'Annex III: Technology-specific cost and performance parameters.', in Edenhofer, O., R. Pichs-Madruga, Y. Sokona, E. Farahani, S. Kadner, K. Seyboth, A. Adler, I. Baum, S. Brunner, P. Eickemeier, B. Kriemann, J. Savolainen, S. Schlömer, C. von Stechow, T. Z. and J. C. M. (ed.) *Climate Change 2014: Mitigation of Climate Change.*

Contribution of Working Group III to the Fifth Assessment Report of the Intergovernmental Panel on Climate Change. Cambridge, United Kingdom; New York, NY: Cambridge University Press, pp. 1329–1356.

Schwaab, J. *et al.* (2015) 'Carbon storage versus albedo change: Radiative forcing of forest expansion in temperate mountainous regions of Switzerland', *Biogeosciences*, 12(2), pp. 467–487. doi: 10.5194/bg-12-467-2015.

Schwaiger, H. P. and Bird, D. N. (2010) 'Integration of albedo effects caused by land use change into the climate balance: Should we still account in greenhouse gas units?', *Forest Ecology and Management*. Elsevier B.V., 260(3), pp. 278–286. doi: 10.1016/j.foreco.2009.12.002.

Stoof, C. R. *et al.* (2015) 'Untapped Potential: Opportunities and Challenges for Sustainable Bioenergy Production from Marginal Lands in the Northeast USA', *Bioenergy Research*, 8(2), pp. 482–501. doi: 10.1007/s12155-014-9515-8.

Sygna, L., Fuglestvedt, J. S. and Aaheim, H. A. (2002) 'The adequacy of GWPs as indicators of damage costs incurred by global warming', *Mitigation and Adaptation Strategies for Global Change*, 7(1), pp. 45–62. doi: 10.1023/A:1015879109042.

Thompson, J. D., Rummer, B. and Schweitzer, C. (2011) 'Harvesting Productivity and Disturbance Estimates of Three Silvicultural Prescriptions on the Daniel Boone National Forest, Kentucky', *Proceedings of the 17th Central Hardwood Forest Conference*, 78(334), pp. 398–408.

Thompson, M., Adams, D. and Johnson, K. N. (2009) 'The Albedo Effect and Forest Carbon Offset Design', *Journal of Forestry*, 107(8), pp. 425–431.

Thompson, M. P., Adams, D. and Sessions, J. (2009) 'Radiative forcing and the optimal rotation age', *Ecological Economics*. Elsevier B.V., 68(10), pp. 2713–2720. doi: 10.1016/j.ecolecon.2009.05.009.

Ulzen-Appiah, F. (2002) *Soil Organic Matter In Experimental Short-Rotation Intensive Culture (Sric) Systems: Effects Of Cultural Factors, Season And Age*, *State University of New York College of Environmental Science & Forestry*.

UNFCCC (2015) 'Paris Agreement, United Nations Framework Convention on Climate Change.', in *21st Conference of the Parties*. Paris, France. doi: FCCC/CP/2015/L.9.

Van Deusen P and Heath, L (2010). "Weighted analysis methods for mapped plot forest inventory data: Tables, regressions, maps and graphs". *Forest Ecology and Management*. 260, pp. 1607-1612.

Volk, T. A. *et al.* (2006) 'The development of short-rotation willow in the northeastern United States for bioenergy and bioproducts, agroforestry and phytoremediation', *Biomass and Bioenergy*, 30, pp. 715–727. doi: 10.1016/j.biombioe.2006.03.001.

Volk, T. A. *et al.* (2011) 'Yields of willow biomass crops across a range of sites in North America', *Aspects of Applied Biology*, 112, pp. 67–74.

Zhang, X. and Wang, W. (2015) 'The decomposition of fine and coarse roots: Their global patterns and controlling factors', *Scientific Reports*. Nature Publishing Group, 5, pp. 1–10. doi: 10.1038/srep09940.

Supplementary Information

The high intensity scenario was based on low-grading as a harvest strategy for the long-term sustainability and profitability of a forest. In this practice, low-grade trees are selectively removed in order to promote a diverse forest stock and ensure future high value harvests. These harvests generally cut back 50-70 % of standing biomass; in our study we assumed 60% harvest (Thompson, Rummer and Schweitzer, 2011; Handler *et al.*, 2014; Abbas and Handler, 2018). In the low intensity scenario, we assumed a style of harvest called high-grading in which foresters selectively cut only the most valuable trees, resulting in high

short-term economic returns but the gradual loss of diversity and forest biomass of value for later harvests. This harvest practice results in a minimal loss of biomass, with harvests ranging between 30 and just over 50% removals of standing live biomass (Thompson, Rummer and Schweitzer, 2011; Handler *et al.*, 2014; Abbas and Handler, 2018). Our study assumed a high-grading cut remove 40% of the biomass.

Harvests incorporated the manufacture and use of a bender multi-harvester and chipper; we assumed no loss of biomass during harvest (Lettens *et al.*, 2003) (Suppl. Table 1). We assumed passive drying was used; while active drying is not uncommon in energy production from willow, it is less common than passive air drying and was not included in previous New York based life-cycle assessments (Heller, Keoleian and Volk, 2003; Caputo, Balogh, Volk, Johnson, Puettmann, Lippke, Oneil, *et al.*, 2014). The method of chip drying results in substantially different life cycle estimates (Matthews, 2001; Heller, Keoleian and Volk, 2003; Caputo, Balogh, Volk, Johnson, Puettmann, Lippke, Oneil, *et al.*, 2014).

Suppl. Table 1. Original sources of emissions and energy use parameters used in the life cycle analysis and for calculation of averted emissions.

Land Use	Primary Process	Sub Process	kg CO_2 odt^{-1}	MJ odt^{-1}	As reported in:
Willow	Prep, Planting, Maintenance		10.5 to 16.3	129 to 166	(Caputo, Balogh, Volk, Johnson, Puettmann, Lippke and Oneil, 2014)
	Harvest		18.2 to 23.8	163 to 213	(Caputo, Balogh, Volk, Johnson, Puettmann, Lippke and Oneil, 2014)
	Transport		47.9 to 48.9	663 to 666	(Caputo, Balogh, Volk, Johnson, Puettmann, Lippke and Oneil, 2014)
	Gasification		156	2830	(Lettens *et al.*, 2003)
Forest	Prep, Planting, Maintenance	Planting & Nursery	1.33	1.77	(Matthews and Mortimer, 2000)
		Fencing	10.5	16.9	(Matthews and Mortimer, 2000)
	Harvest	Feller-Buncher/ Grapple Skidder/Slasher	38.3 to 52.6	496 to 674	(Handler *et al.*, 2014)
		Felling Cable Skidder Bucking	46.6 to 48.6	584 to 609	(Handler *et al.*, 2014)
		Chipping	9.15	118	(de la Fuente *et al.*, 2017)
	Transport*		41.2	496	(Handler *et al.*, 2014)
	Gasification		166	3007	(Lettens *et al.*, 2003)

* Oven-dried tonnes of harvested biomass

**Originally reported for 200 km, adjusted to 195 km of transport

Suppl. Table 2. Sensitivity of emissions profile to initial assumptions. In the active biomass drying case, we examined how powered, rather than passive, drying would affect the emissions generated by management of each land-use case. Values were based on literature measurements (Lettens *et al.*, 2003) or best approximations (McKechnie *et al.*, 2011) for willow and forest respectively. In the efficient gasification case, we used literature emissions estimates that ignored thermal inefficiencies and parasitic energy losses, as their inclusion or exclusion was a major source of discrepancies in cradle to grave emissions estimates in the literature (Mann and Spath, 1997; Elsayed, Matthews and Mortimer, 2003; Lettens *et al.*, 2003). The distributed plants case was based on scenario building for biomass transport in New York; in this study, we followed Caputo *et al*'s assumption of a single, centralized biomass plant in New York, resulting in an average transport distance of 190 km. However, they also proposed a distributed biomass plant scenario, with an average transport distance of 80 km, with proportionally lower emissions as described here (Caputo, Balogh, Volk, Johnson, Puettmann, Lippke and Oneil, 2014). Finally, nitrous oxide and methane emissions from forest and willow were not considered by the main study, as emissions are highly variable based on site conditions and can be difficult to quantify precisely, both in the new land-uses and in the original maize cropland (Morse, Duran and Groffman, 2015). However, we do provide an approximation of nitrous oxide emissions from a fertilized willow field without reference to the emissions that might have been expected under the previous maize regime (Heller *et al.*, 2004). This will be an important area for future research, as methane and nitrous oxide fluxes from land-use change can be substantial (Kirschbaum *et al.*, 2011).

Mg CO_2e ha^{-1} 100 $years^{-1}$	Forest (High)	Forest (Low)	Willow (Low)	Willow (High)
Active Biomass Drying	23.136	19.412	1.898	3.164
Efficient Gasification	-0.015	-0.010	-23.067	-43.392
Distributed Plants	-0.003	-0.002	9.373	15.948
N_2O Emissions	---	---	2.635	4.391